



Project No. 037005

CECILIA



Central and Eastern Europe Climate Change Impact and Vulnerability Assessment

Specific targeted research project

1.1.6.3.I.3.2: Climate change impacts in central-eastern Europe

D 6.6: Report about the sensitivity analysis of the selected agriculture crops and the most vulnerable forest stands to climate change impacts

Due date of deliverable: Month 36

Actual submission date: Month 43

Start date of project: 1st June 2006

Duration: 43 months

Lead contractor for this deliverable: National Forest Centre – Forest Research Institute Zvolen (FRI)

Project co-funded by the European Commission within the Sixth Framework Programme (2002-2006)		
Dissemination Level		
PU	Public	X
PP	Restricted to other programme participants (including the Commission Services)	
RE	Restricted to a group specified by the consortium (including the Commission Services)	
CO	Confidential, only for members of the consortium (including the Commission Services)	

CONTENTS

1	AGRICULTURE – THE MARCHFEL REGION (AUSTRIA)	3
1.1	INTRODUCTION: HEAT STRESS ON PLANTS	3
1.2	ANALYSES: CLIMATE CHANGE IMPACTS ON SELECTED CROPS IN THE INVESTIGATION AREA MARCHFELD....	4
1.3	DISCUSSION.....	7
2	AGRICULTURE - THE CZECH REPUBLIC	9
2.1	SENSITIVITY OF WINTER WHEAT PHENOLOGY UNDER EXPECTED CLIMATE	9
2.1.1	<i>Sensitivity of the winter wheat production to climate change at different altitudes</i>	9
2.1.2	<i>Sensitivity of the winter wheat production under future climate according to the soil conditions</i>	13
2.1.3	<i>Sensitivity of spring barley phenology under expected climate</i>	15
2.1.4	<i>Sensitivity of the spring barley production to climate change at different altitudes</i>	18
2.1.5	<i>Sensitivity of the spring barley production under future climate according to the soil conditions</i>	19
3	FOREST ECOSYSTEMS – SLOVAKIA	22
3.1	INTRODUCTION	22
3.2	MODELLING APPROACH	23
3.2.1	<i>Model calibration</i>	28
3.2.2	<i>Model outputs</i>	29
3.2.3	<i>Methodology</i>	29
3.3	RESULTS	34
3.3.1	<i>Spruce (Picea abies) sensitivity to climate change</i>	36
3.3.2	<i>Fir (Abies alba) sensitivity to climate change</i>	40
3.3.3	<i>Beech (Fagus sylvatica) sensitivity to climate change</i>	43
3.3.4	<i>Oak (Quercus sp.) sensitivity to climate change</i>	47
3.4	CONCLUSIONS.....	50
4	AGRICULTURE – THE SLOVAK REPUBLIC	51
4.1	INTRODUCTION	51
4.1.1	<i>Sensitivity of field crop yields with respect to agro-climatic conditions</i>	52
4.1.2	<i>Sensitivity of field crop yields with respect to meteorological datasets</i>	54
4.1.3	<i>Sensitivity of field crop yields with respect to climate change impacts</i>	57
4.2	CONCLUSIONS.....	58
5	FOREST ECOSYSTEMS – POLAND	64
5.1	INTRODUCTION.....	64
5.2	RESULTS.....	67
5.2.1	<i>Critical load function of acidity</i>	67
5.2.2	<i>Critical load of nutrient nitrogen</i>	69
5.2.3	<i>Current critical load exceedances</i>	70
5.2.4	<i>Defining critical loads parameters sensitive to climate</i>	73
5.2.5	<i>Climate data from Regional Climate Model</i>	73
5.2.6	<i>Deposition data from Regional Climate Model-Air Quality Modelling System</i>	76
5.2.7	<i>Impacts of climate changes on critical loads</i>	78
5.2.8	<i>Exceedances of critical loads induced by climate changes</i>	80
5.3	CONCLUSIONS.....	85
6.	REFERENCES	87

1 AGRICULTURE – THE MARCHFEL REGION (AUSTRIA)

A sensitivity analysis with the crop simulation model DSSAT can be done by modifying one or more weather, soil, genotype or management inputs, followed by re-running the simulation. Changes in the simulated results reflect the sensitivity of the system to the particular input(s) (Shrestha 2004). To study heat stress during vegetative growth, sensitivity tests were performed for changes up to +2°C maximum or minimum temperature as well as both temperatures together on the climate change scenarios with middle climate sensitivity.

1.1 Introduction: Heat stress on plants

In semi-arid and arid environments water stress is connected with temperature stress and leaf temperatures usually increase above air temperature as a result of stomata closure and reduced transpiration (Hatfield 1979). The leaf temperatures under these conditions can limit dry matter accumulation because of increased respiration, reduced photosynthesis and cellular damage (Basra 1993). Consequently heat stress, in particular during vegetative and reproductive stages, causes severe yield reductions in different crops (Pessarakli 1999).

Table 1.1 *Examples of annual crop species adapted to cool and warm seasons (Hall 2001)*

Cool-Season Annuals	Warm-Season Annuals
Barley, brassicas, canola, fava bean, flax, garbanzo bean, Irish potato, lentil, lettuce, lupine, mustard, oat, pea, radish, rye, spinach, triticale, turnip, vetch, wheat	Common bean, cotton, cowpea, cucurbits, finger millet, grain amaranth, lima bean, maize, mung bean, pearl millet, pepper, pigeon pea, rice, sesames, sorghum, soybean, sunflower, sweet potato, tobacco, tomato

Plants have an optimal temperature range for growth as well as for reproduction. In table 1.2 the temperature ranges for adaptation of cool-season and warm-season annual crop plants are provided. These estimates are very approximate, since these two groups contain many different species (table 1.1), and extreme temperature limits depend on the duration of exposure and extend of hardening (Hall 2001).

Table 1.2 *Temperature ranges of adaptation of cool-season and warm-season crop plants (Hall 2001)*

	Night Temperatures °C		Day Temperatures °C	
	Minimum	Maximum	Optimum	Maximum
	<i>Freezing</i>	<i>Heat stress</i>		<i>Heat stress</i>
Cool-season annuals	-30 to -1	> 16 to 24	18 to 28	> 28 to 40
	<i>Chilling</i>	<i>Heat stress</i>		<i>Heat stress</i>
Warm-season annuals	<6 to 18	>20 to 30	26 to 36	>30 to 50

Since plants are unable of maintaining a temperature optimal for their growth, a slight increase in temperature can affect physiological and biochemical process crucial for plant growth. Plants are able to tolerate temperatures of 5-10°C above the optimal temperature without being stressed. At temperatures of 12-15°C above the optimal temperature, plants begin to suffer from heat stress. An unexpected increase in temperatures of 15°C or more above the optimal range can affect seriously the plant growth and development, depending upon duration of the heat stress. Lethality results from a combination of cellular changes that the heat induces and the incapability to restore normal cellular function afterwards. Heat stress events cause irreversible damage during vegetative and reproductive stages in many crop plants. Some reasons are low photosynthetic activity, poor floral development, pollen sterility, which affect seed and fruit set as well as quality. High temperature affects numerous

physiological activities associated with seeding growth and vigour, root growth, nutrient uptake, water relations of cells, solute transport, photosynthesis, respiration, general metabolisms, fertilization as well as maturation of fruits. The rate of photosynthesis in most species decreases at about 35°C which is attributed to protein denaturation, loss of membrane integrity, photoinhibition and ion imbalance. High temperature has also an effect on chloroplast biogenesis and senescence, causes disintegration of chloroplast grana, brings about disruption of the structure of membrane protein, influences protein-lipid interactions, affects electron transport activity and substantially decreases the activity of Rubisco enzyme (Di Toppi and Pawlik-Skowrońska 2003).

However, plants have the possibility to resist high temperature stress by avoidance or by tolerance mechanisms (Levitt 1980). So, heat stress does not mean immediately lethality. Examples of heat avoidance mechanisms are insulation, decreased respiration, decreased absorption of radiant energy through reflectance or decreased chromophore content, transpirational cooling (Levitt 1980). Potential mechanisms of heat tolerance are the synthesis of protectants (Levitt 1980), increased thermostability of enzymes (Weber et al. 1977), and increased saturation of fatty acid (Basra 1993). So during the period of heat acclimation, a set of novel proteins is synthesized; they so called heat-shock proteins (HSPs) (Vierling 1991). These proteins are thought to enable cells to survive the harmful effects of heat by two general types of mechanisms: as molecular chaperones and by targeting proteins for degradation (Hall 2001).

1.2 Analyses: Climate change impacts on selected crops in the investigation area Marchfeld

The DSSAT model 4.02 was applied to winter wheat, spring barley and maize to assess different analysis under climate scenarios for NE Austria. For this deliverable the climate scenarios were performed with the global circulation models (GCMs) ECHAM 5, HadCM 3 and NCAR PCM. Synthetic daily weather series of 100 consecutive years (input to crop growth models) were produced with stochastic weather generator (Met&Roll) (Dubrovsky 1997) for present conditions (1961-1990) and 2021-2050 (2035). To account for the uncertainties nine (3x3) scenario sets were defined (Dubrovsky et al. 2005):

- uncertainty in scenario pattern: 3 sets of GCMs
- uncertainty in the scaling factor: function of emission scenario and climate sensitivity.

Hereby three versions of scaling factor for a given period were used:

- high climate sensitivity +4.5 K per doubling ambient CO₂
- middle climate sensitivity +2.6 K per doubling ambient CO₂
- low climate sensitivity +1.5 K per doubling ambient CO₂

A CO₂ concentration in the atmosphere of 360 ppm was assumed according the emission scenario A1B for present conditions and 452 ppm for the year 2035. 5 soil classes were analyzed in the investigation area (see D6.1 and 6.2). The simulated values of the climate scenarios contain the CO₂ fertilizing effect, adapted sowing date, rainfed agriculture and contemporary crops without consideration of potential profit cuts caused by pest or diseases.

The next tree figures should give an overview of the relative yield change of the tree selected crops to the present changes for the different GCM's.

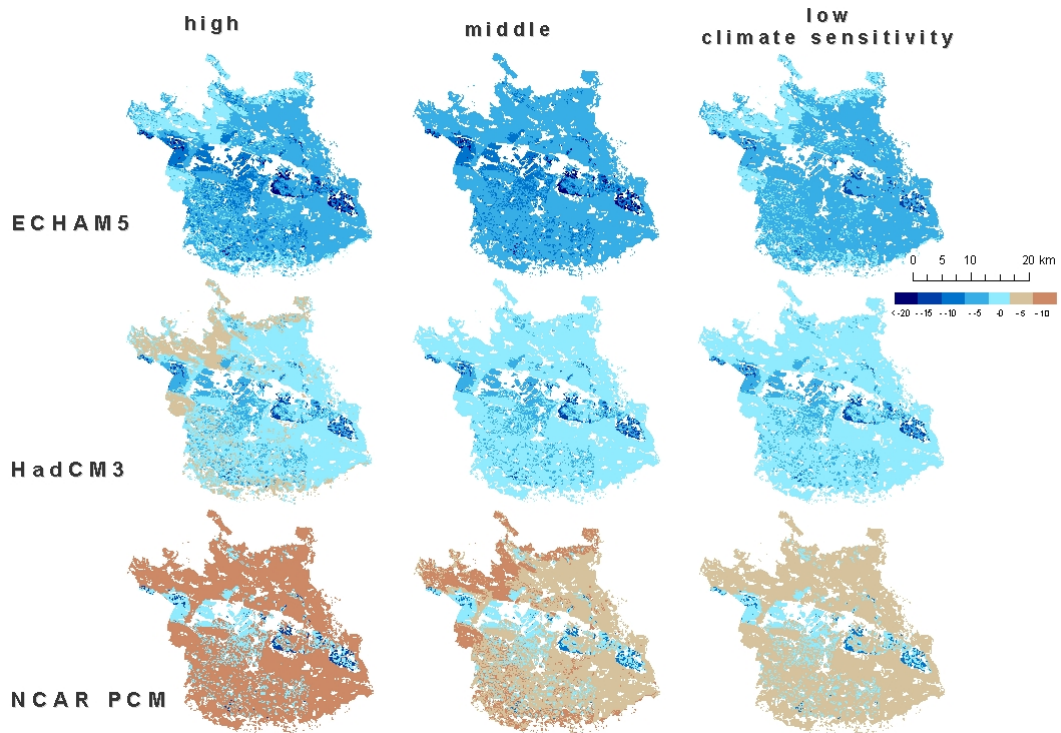


Figure 1.1 *Relative change of the winter wheat yield to the present conditions for different GCMs in the investigation area Marchfeld – 2035 – ploughed soil*

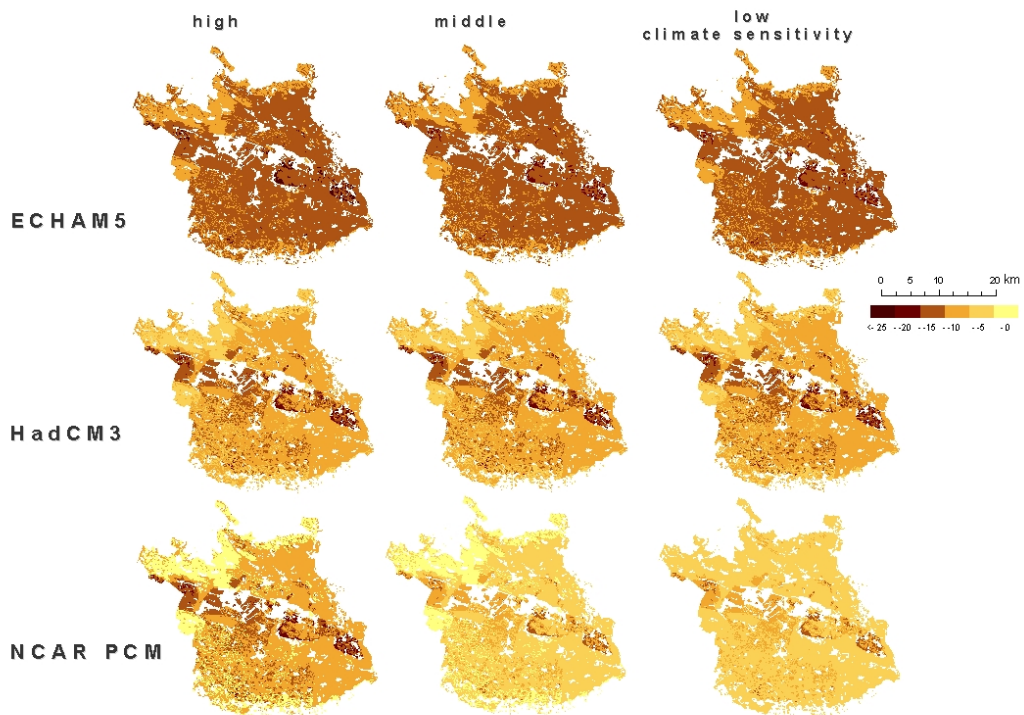


Figure 1.2 *Relative change of the spring barley yield to the present conditions for different GCMs in the investigation area Marchfeld – 2035 – ploughed soil*

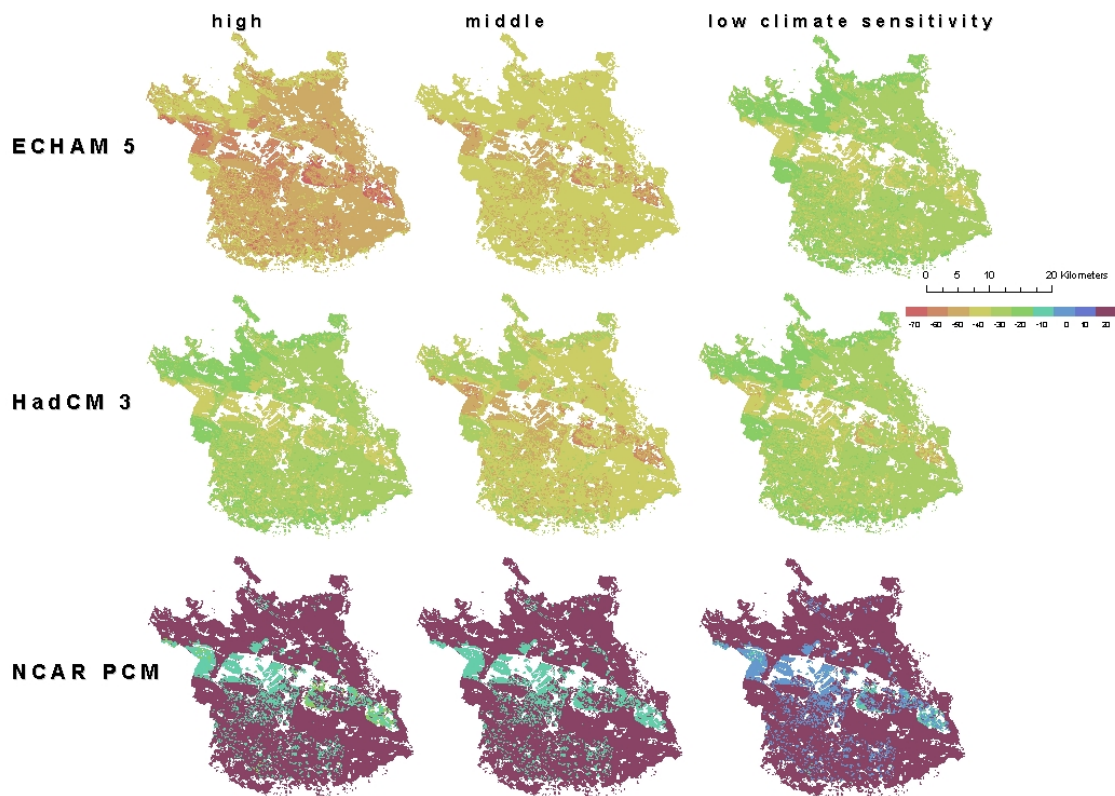


Figure 1.3. *Relative change of the maize yield to the present conditions for different GCMs in the investigation area Marchfeld – 2035 – ploughed soil*

Sensitivity analysis of selected agriculture crops to climate change impacts

In a next step heat stress for the tree different crops through sensitivity analysis was studied. Heat stress is a complex function of the height of temperature, duration as well as rate of increase of the temperature. The thresholds of the temperatures for the different crops differ very much and they vary also according to the plant development stage (Eitzinger et al 2008). The 3 GCM's with middle climate sensitivity were used as basis of the sensitivity analysis. Increases of their maximum temperature as well as an increase of their maximum and minimum temperatures together up to 2°C were hereby applied. Sensitivity analysis was calculated with a sandy, shallow (Parachernozem, soil class 2) as well as a medium soil (Chernozem/Fluvisol, soil class 3).

A threshold of the heat stress refers usually to daily mean temperature above that a traceable reduction of growth or damages in plant starts. The Hungarian Meteorological Service, for example, provides a heat index forecast, defined as a daily average temperature above 25°C (Eitzinger et. al. 2008). The average number of days during one year reaching this threshold is summarized in table 1.3. The calculations are based on the tree different climate change scenarios (middle climate sensitivity) for 2035 as well as their increase of maximum and minimum temperatures up to 2°C.

Table 1.3 Number of days during one year with an average temperature above 25°C for the different climate change scenarios (middle climate sensitivity) as well as their increase of maximum and minimum temperatures up to 2°C

GCM's		Tmean	Tmean (Tmax+1°C)	Tmean (Tmax +2°C)	Tmean (Tmax +2 Tmin +1°C)	Tmean (Tmax +2°C Tmin +2°C)
ECHAM 5	days Tmean>25°C	10	13	16	21	26
	at least 3 successive days with a Tmean>25°C	3	4	6	8	11
HadCM 3	days Tmean>25°C	13	17	21	26	31
	at least 3 successive days with a Tmean>25°C	4	6	9	12	16
NCAR PCM	days Tmean>25°C	9	12	16	20	24
	at least 3 successive days with a Tmean>25°C	3	4	6	8	11

1.3 Discussion

A yield decrease for winter wheat until 2035 can be expected by the scenarios ECHAM 5 and HadCM 3 (fig 1.3). The simulated positive effect of enhanced CO₂ concentrations in the atmosphere on photosynthesis rate can neither recoup the lower precipitation in spring and summer nor the higher temperature. A yield increase was only predicted by NCAR PCM on medium soils (up to 10%). An additional temperature increase from these scenarios would mean a further yield loss until 12% (fig 1.4). All tree GCMs demonstrate similar reactions in the sensitivity analysis.

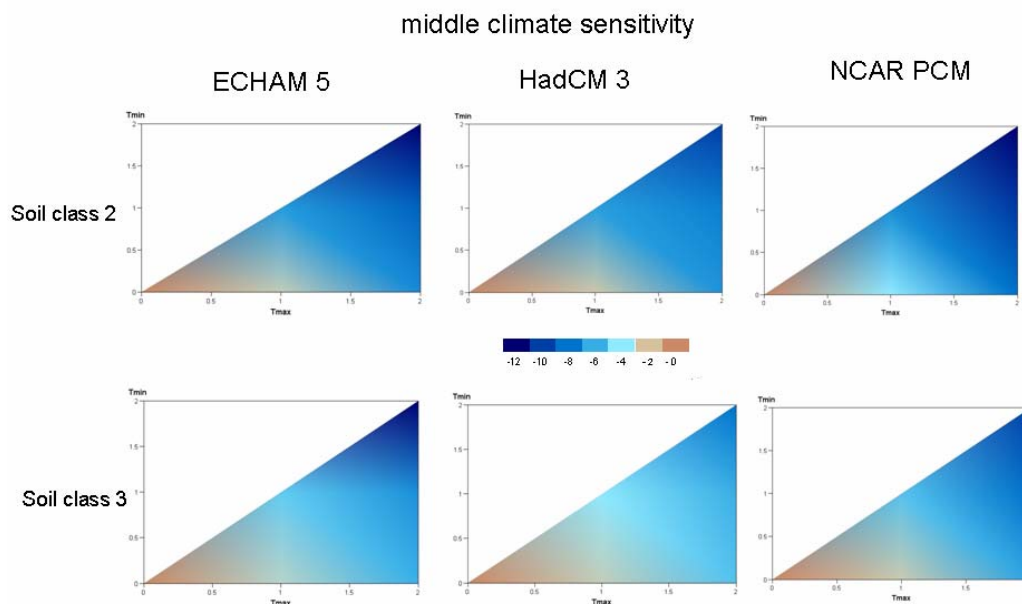


Figure 1.4. Sensitivity of winter wheat to maximum and minimum temperature changes (basis: ECHAM 5, HadCM 3, NCAR PCM: 2035; middle climate sensitivity)

Until 2035 a yield decrements up to 25% was predicted for spring barely by the different GCM's (fig 1.2). The highest loss was hereby simulated by ECHAM 5. Further temperature raise from these scenarios would result in additional yield decrements, which are just up to 0.5% in respect to the 2035 scenarios with middle climate sensitivity (fig 1.5).

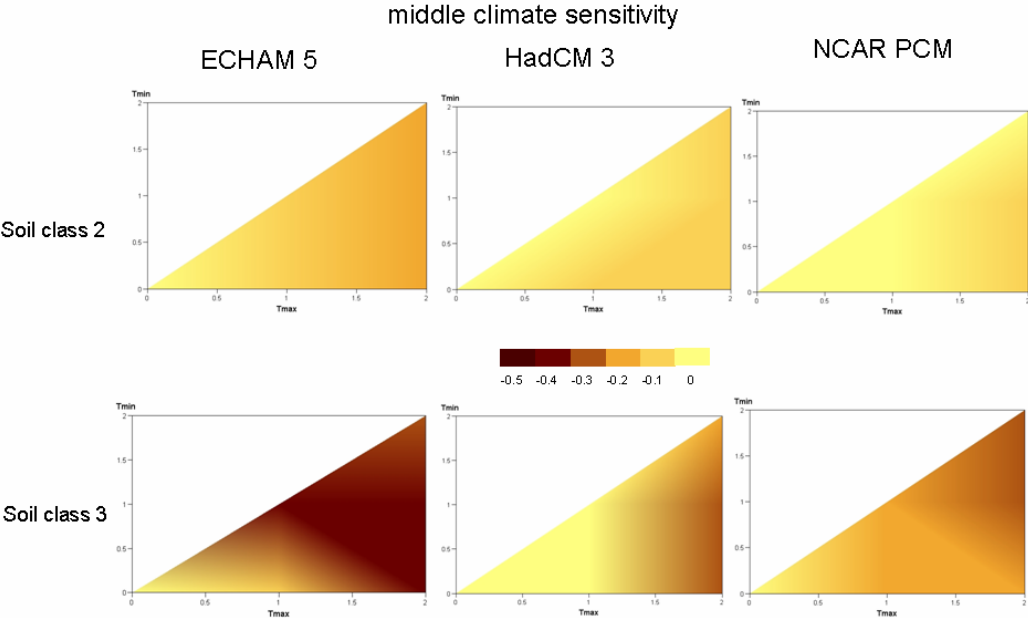


Figure 1.5 *Sensitivity of spring barley to maximum and minimum temperature changes (basis: ECHAM 5, HadCM 3, NCAR PCM: 2035; middle climate sensitivity)*

In case of maize, there is also a high decrease of yield until 2035 by ECHAM 5 and HadCM3 (up to -70%) (fig 1.3). Only NCAR PCM predicts for the medium soils a yield increase up to 20%. Higher temperature in ECHAM 5 and NCAR PCM 2035 would mean yield loss; but in HadCM 3 slightly yield increase, especially for the Parachernozem (fig 1.6).

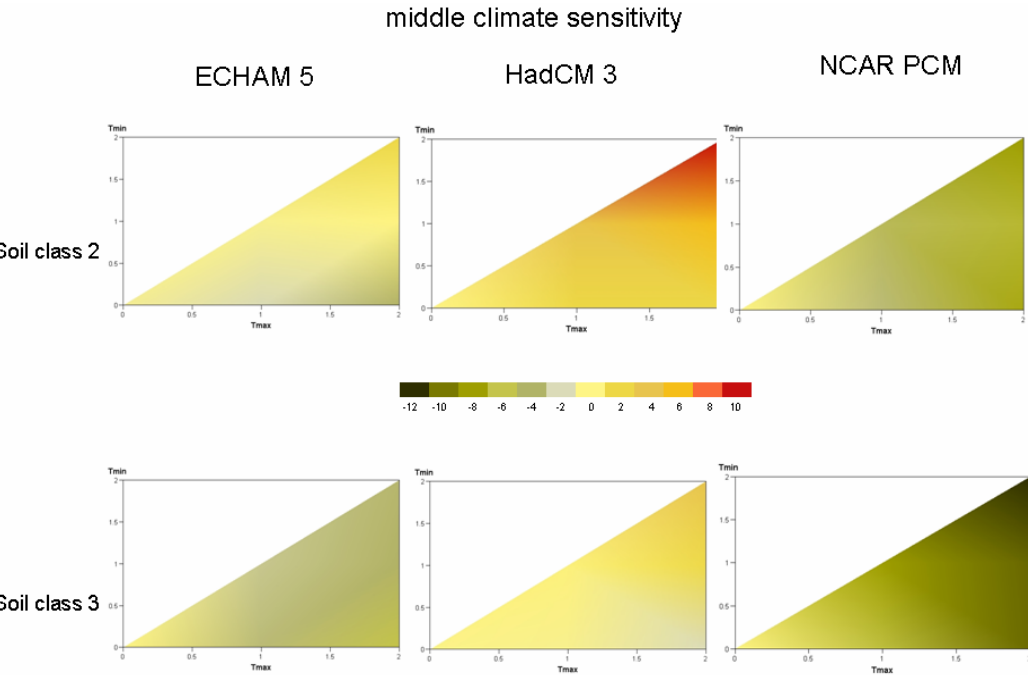


Figure 1.6 *Sensitivity of maize to maximum and minimum temperature changes (basis: ECHAM 5, HadCM 3, NCAR PCM: 2035; middle climate sensitivity)*

2 AGRICULTURE - THE CZECH REPUBLIC

Within the presented study the IAP and CHMI teams focused on sensitivity of developmental stages of two key cereals (winter wheat and spring barley) to expected changes in climate over the whole Czech Republic and in detail analyzed vulnerability of cereal production over individual soil types. This analysis is meant to complement analysis carried out by the Austrian team.

2.1 Sensitivity of winter wheat phenology under expected climate

Basic step for assessing phenology is the sowing day, from which derives the onset of phenological phases. Therefore, the optimal sowing date must be specified for the current climate. Fig. 2.1 and 2.2 offer the phenological stage “flowering“ which are only based on model simulations. The sowing date is primarily determined by soil moisture. Under climate change scenarios sowing date will shift mainly due to increased drought (e.g. TRNKA et al., 2004a) especially in lowlands (maize production areas). The study indicates shift of suitable conditions up to three days in the case of the ECHAM model, or almost ten days for the situation simulated by the model NCAR and HadCM. Anthesis date (Fig. 2.1) shows the largest difference with the current state model HadCM, and in South Moravia the onset occurs 25 days earlier for year 2050. In two other scenarios, the anthesis shift is smaller (e.g. for ECHAM model it is in the range 7 to 8 days). However, it is important to mention that this is a flowering date determining, and not growth duration. This will be reduced because according of all models to sowing date will be enabled significantly later than in the current climatic conditions.

A similar conclusion could be done for the physiological maturity (Fig. 2.2), according to the HadCM scenario it will start at the warmest locations of CR between 23 and 36 days earlier. This is in line with the work of OLESEN et al., (2000), that the increase in temperature by 1 °C during the phase of the grain filling reduces the length of this phase of 5%. The total duration of growth (sowing date-physiological maturity) may be reduced under SRES - A2 2050 by up to six weeks. It should be noted that this is a the most severe emission scenario considered and other combinations as SRES-B1 2020, SRES-A2 2020 a SRES-B1 2050 will lead to less dramatic changes in the onset of tested phenological phases.

2.1.1 Sensitivity of the winter wheat production to climate change at different altitudes

Territory of the CR was divided into 8 categories altitude identified in Fig. 2.3, where are presented results for three scenarios of climate change and the SRES-A2 emission scenario. According to the model ECHAM (Fig. 2.3) there is likely yield increase in all altitudes, and the higher benefit would be in areas of lower altitude. On the other hand significantly drier HadCM scenario and as well as NCAR scenario will benefit more medium and high altitudes. There are positive effects of warming in conjunction with the rise of CO₂ concentrations up to yield increase about 2 t.ha⁻¹ while lower altitudes will profit lower. Spatial analysis carried out for the winter wheat yield concerning altitude suggests that yield should increase especially in highlands, where increasing temperature will provide favorable conditions, rainfall will remain sufficient and soil conditions are still relatively good.

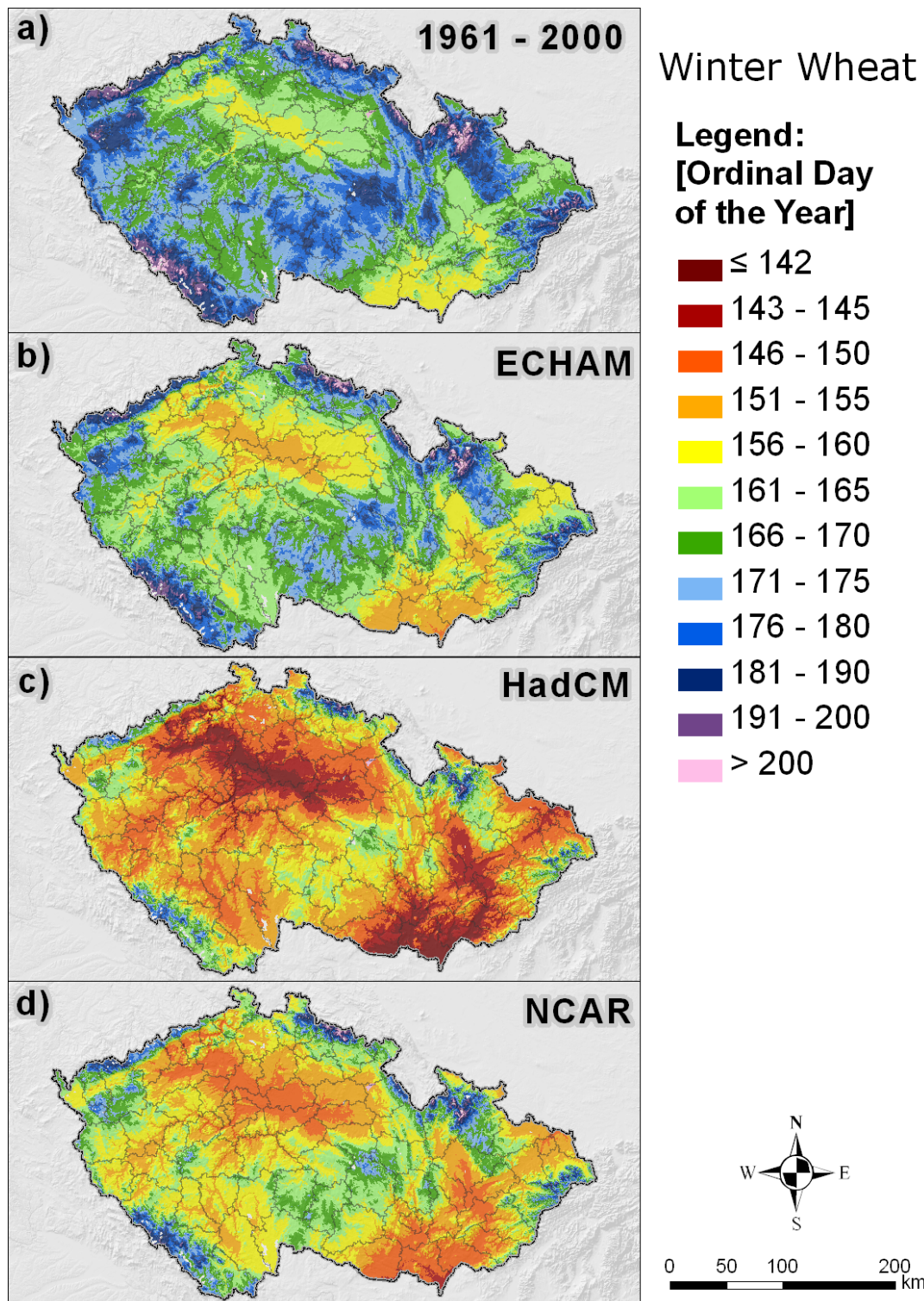


Figure 2.1 Flowering of winter wheat for a) the current climatic conditions (1961 - 2000) b, c, d) for the year 2050 under SRES - A2 emission scenarios and three GCM in the CR (a median of simulations for each grid cell network with a resolution of 500 x 500m).

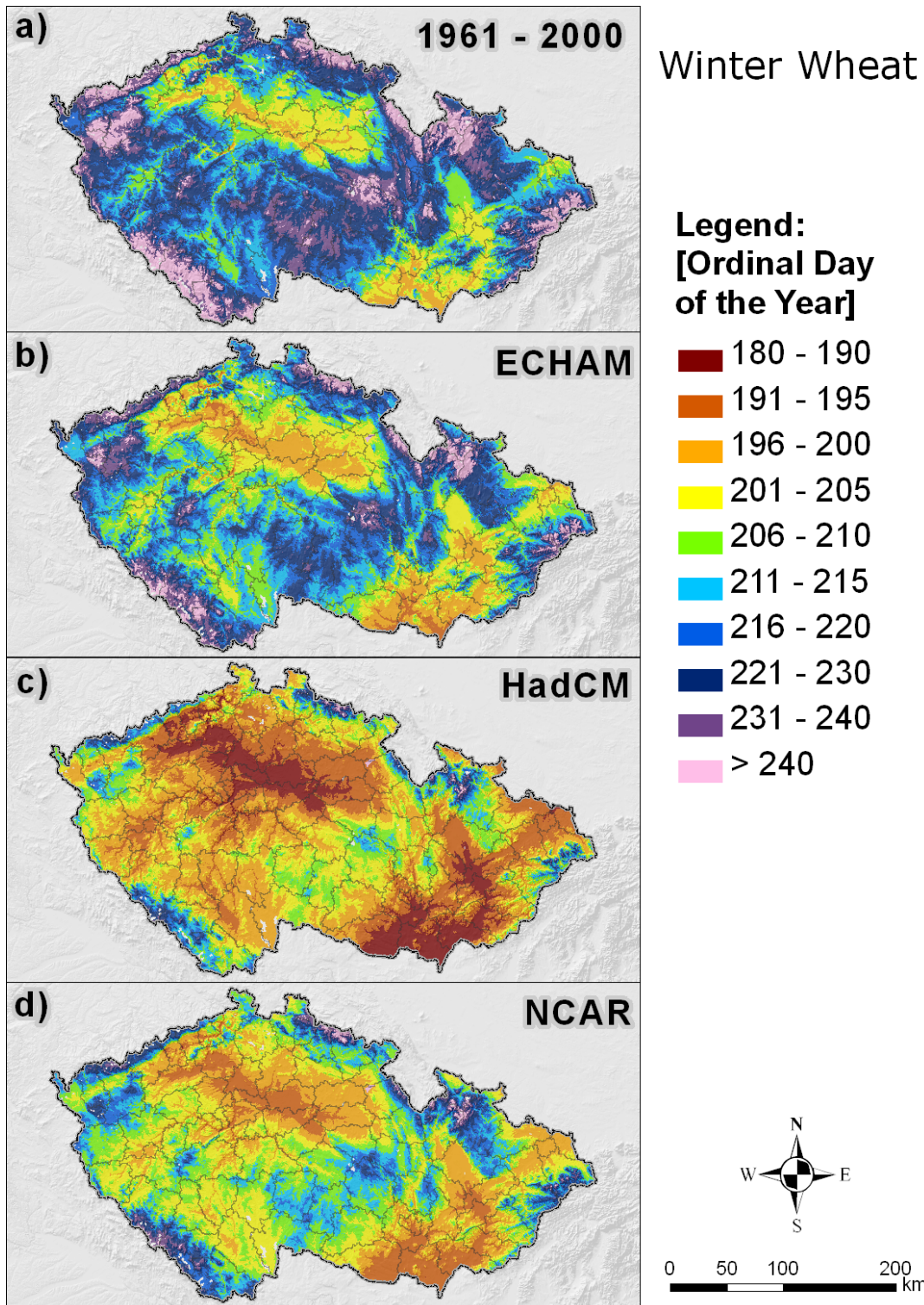
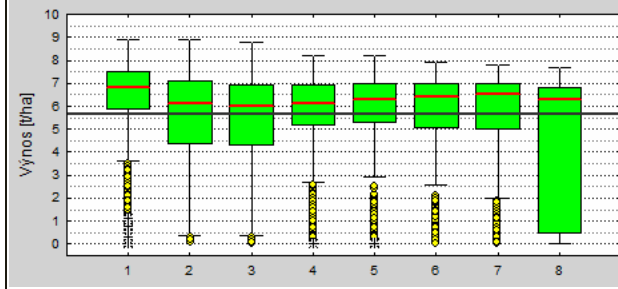


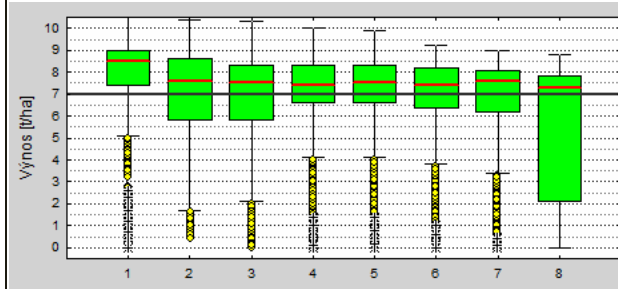
Figure 2.2 *Physiological maturity dates of winter wheat a) for the current climatic conditions (1961 - 2000) b, c, d) for the year 2050 under SRES - A2 emission scenarios and three GCM in the CR (a median of 99 simulations for each grid cell network with a resolution 500 x 500m).*

Winter Wheat – (1961-2000) – altitude

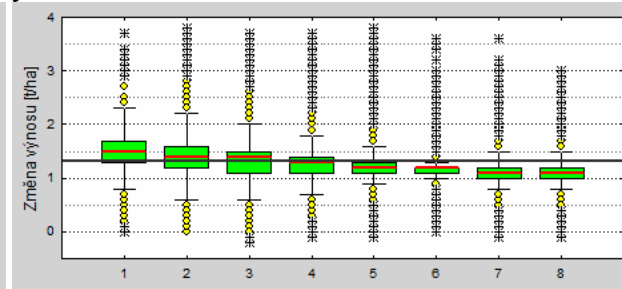


1	2	3	4	5	6	7	8
< 250	250-300	300-400	400-450	450-500	500-550	550-600	≥ 600
average yield [t.ha⁻¹]							
6.5	5.5	5.3	5.6	5.7	5.6	5.5	4.5
coefficient of variation [%]							
24.9	40.5	42.0	34.9	34.8	36.5	42.1	63.9

ECHAM

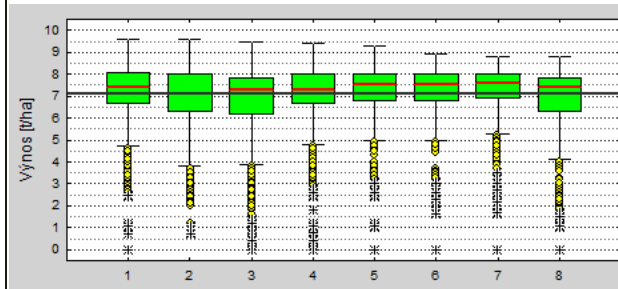


yield difference

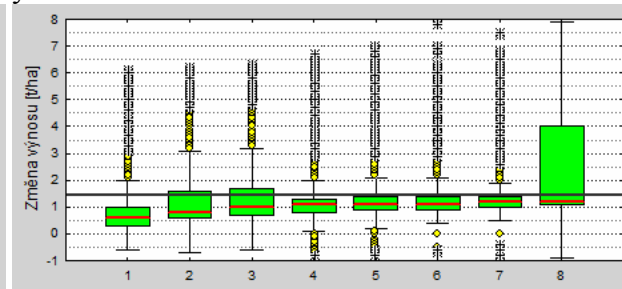


1	2	3	4	5	6	7	8	1	2	3	4	5	6	7	8
average yield [t.ha⁻¹]								average yield difference [t.ha⁻¹]							
8.0	6.9	6.6	6.9	6.9	6.8	6.6	5.6	1.5	1.4	1.3	1.3	1.2	1.1	1.1	1.0
coefficient of variation [%]								coefficient of variation [%]							
20.5	33.9	36.0	30.4	30.8	31.9	34.6	53.0	22.5	37.9	40.9	34.6	35.4	33.6	35.9	40.2

HadCM

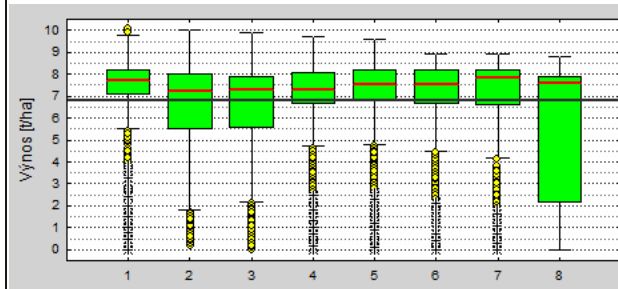


yield difference

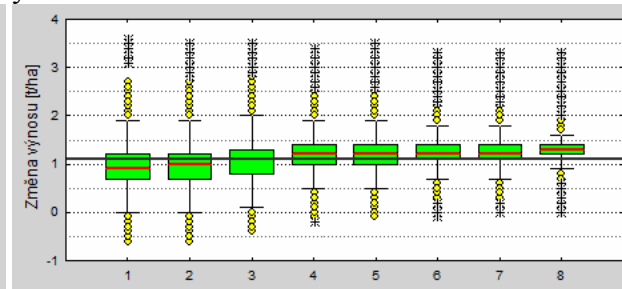


1	2	3	4	5	6	7	8	1	2	3	4	5	6	7	8
average yield [t.ha⁻¹]								average yield difference [t.ha⁻¹]							
7.3	7.0	6.9	7.1	7.2	7.2	7.3	7.0	0.8	1.5	1.6	1.5	1.5	1.6	1.8	2.4
coefficient of variation [%]								coefficient of variation [%]							
15.4	18.6	19.8	17.8	17.5	15.9	15.0	19.9	119.	111.	95.2	85.1	84.2	84.1	89.1	83.6

NCAR



yield difference



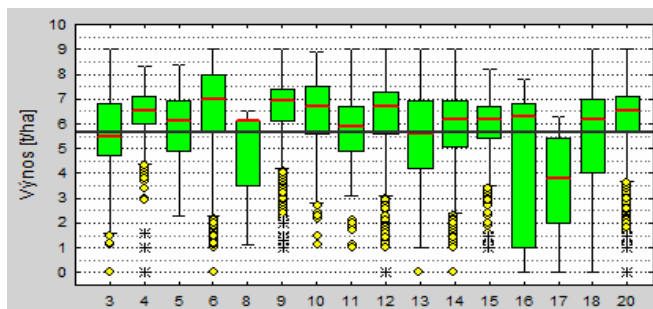
1	2	3	4	5	6	7	8	1	2	3	4	5	6	7	8
average yield [t.ha⁻¹]								average yield difference [t.ha⁻¹]							

7.4	6.5	6.4	6.9	6.9	6.9	6.7	5.8	0.9	1.0	1.1	1.2	1.2	1.2	1.3	1.3
coefficient of variation [%]								coefficient of variation [%]							
19.9	31.1	32.5	27.9	28.1	29.2	31.2	42.6	64.1	62.4	49.3	35.9	35.6	34.2	35.0	34.5

Figure 2.3 Summarizing yields of winter wheat following categories of the altitude for the current climatic conditions (1961-2000) and impacts of climate change under the three GCM scenarios and SRES-A2. The green graph is interquartile (IQR) range ($x_{75}-x_{25}$) for each category of altitude, the red line in the box is the median category, bearded boxes ($1.5 \times IQR$) = adjacent values, the yellow points = outliers, stars = extreme values. Black continuous line is delivered the national average yield, respectively yield changes on arable land.

2.1.2 Sensitivity of the winter wheat production under future climate according to the soil conditions

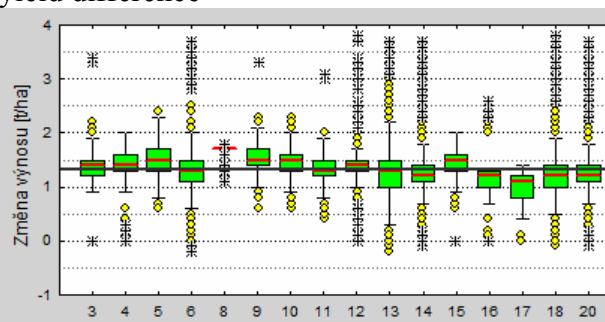
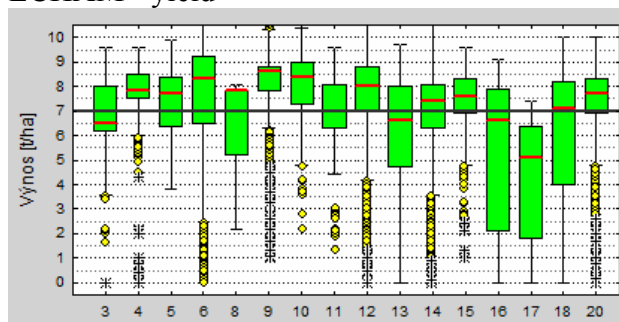
Soil fertility and its response to climate change conditions a function of the soil type, which reflects the particular physical properties of the soil profile. The stability of these characteristics is the basis for the use of growth models or other dynamic calculations for example in precision agriculture (e.g., KHOSLA et al., 2007). Within the territory of CR the grid cells network containing the same soil type were analyzed, regardless of the location within the region, altitude and production areas. Based on data from the Czech Geological Survey we selected 20 soil types (Fig. 2.4), for which climate change impacts were processed in terms of winter wheat yield.



3	4	5	6	8	9	10	11	12	13	14	15	16	17	18	20
rendzic Leptosols calic Leptosols Regosols			Fluvisols	Vertisols	Chernozem	Phaeozems	greyic Phaeozems	haplic Luvisols	Albeluvisols	Cambisols	Pelosols	entic Podzols	haplic Podzols	Stagnosols	Gleysols
average yield [t.ha⁻¹]															
5.3	6.3	5.9	6.1	4.7	6.7	6.6	5.7	6.2	4.7	5.4	5.9	3.7	3.5	4.8	5.9
coefficient of variation [%]															
33.4	19.3	19.7	37.8	37.0	19.5	19.9	26.6	27.0	50.2	40.8	19.9	87.9	64.3	55.9	30.6

ECHAM - yield

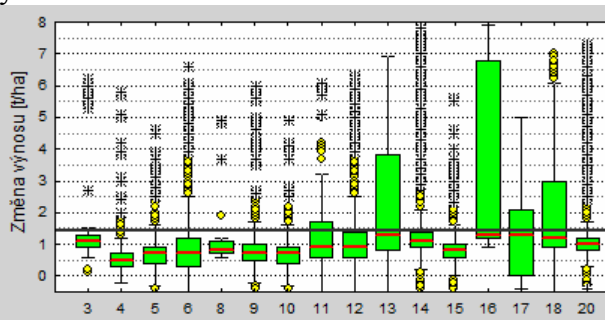
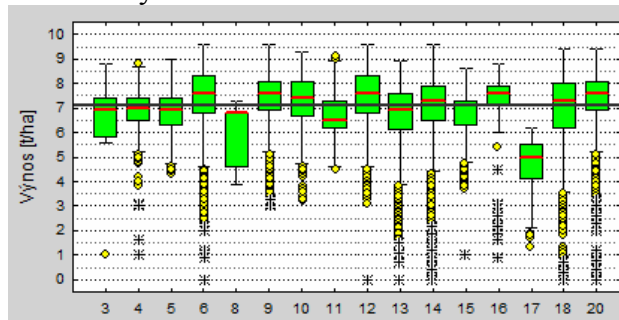
yield difference



3	4	5	6	8	9	10	11	12	13	14	15	16	17	18	20
average yield [t.ha⁻¹]															
6.7	7.7	7.4	7.4	6.4	8.2	8.1	7.0	7.6	6.0	6.6	7.4	4.9	4.4	6.0	7.2
VK [%]															
23.7	17.1	17.1	32.7	29.0	15.2	15.6	21.1	22.2	41.9	35.3	16.9	67.2	55.7	47.0	25.8
average yield difference[t.ha⁻¹]															
1.4	1.4	1.4	1.3	1.6	1.5	1.5	1.3	1.4	1.3	1.2	1.4	1.2	1.0	1.2	1.3
VK [%]															
26.4	19.3	19.6	36.3	9.4	14.0	15.2	25.3	27.1	44.6	39.5	17.6	64.7	42.1	51.1	32.0

HadCM - yield

yield difference

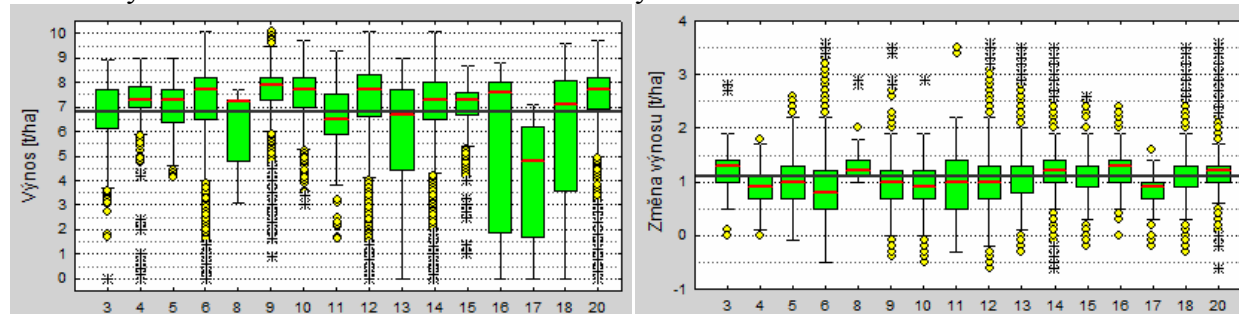


3	4	5	6	8	9	10	11	12	13	14	15	16	17	18	20
average yield [t.ha⁻¹]															
6.8	6.9	6.8	7.3	6.1	7.5	7.3	6.8	7.5	6.8	7.0	6.8	7.0	4.6	6.9	7.3

VK [%]	14.1	14.1	13.8	18.6	17.4	14.0	14.6	15.0	14.4	18.4	17.9	13.6	26.4	27.2	23.5	14.7
	average yield difference[t.ha⁻¹]															
	1.6	0.6	0.8	1.2	1.4	0.8	0.7	1.1	1.2	2.1	1.6	0.9	3.2	1.2	2.1	1.4
VK [%]	98.5	102.1	92.6	127.6	99.4	77.1	76.6	118.1	96.9	88.2	90.2	72.7	82.6	111.9	90.4	91.3

NCAR - yield

yield difference



	3	4	5	6	8	9	10	11	12	13	14	15	16	17	18	20
	average yield [t.ha⁻¹]															
	6.5	7.2	7.0	6.9	6.1	7.7	7.5	6.5	7.3	5.8	6.6	7.0	5.0	4.3	5.9	7.1
VK [%]	24.1	16.3	15.0	30.9	21.5	14.6	13.9	21.4	21.9	42.0	34.0	15.6	67.9	53.4	46.2	25.0
	average yield difference[t.ha⁻¹]															
	1.2	0.9	1.0	0.8	1.4	1.0	0.9	0.8	1.0	1.1	1.2	1.1	1.2	0.8	1.2	1.2
VK [%]	26.9	33.3	39.8	80.6	38.7	37.7	50.6	97.4	53.2	63.3	38.1	31.0	50.2	54.2	59.5	43.0

Figure 2.4 Summarizing yields of winter wheat following categories of the soil types for the current climatic conditions (1961-2000) and impacts of climate change under the three GCM scenarios and SRES-A2. The green graph is interquartile (IQR) range ($x_{75}-x_{25}$) for each category of soil types, the red line in the box is the median category, bearded boxes ($1.5 \times IQR$) = adjacent values, the yellow points = outliers, stars = extreme values. Black continuous line is delivered the national average yield, respectively yield changes on arable land.

Analysis of average yields for the current climate (1961-2000) shows that the yields in most soil types vary in logical terms. Above-average yield level is achieved on the best soils. Some soil types (11, 3, 8, 16, 17) are in the area of arable land represented less than one percent and the analysis of its fertility regarding climate change has rather theoretical importance.

2.1.3 Sensitivity of spring barley phenology under expected climate

Similar methodology as for winter wheat was applied for spring barley (variety Akcent). Model CERES - Barley has been validated at three locations (TRNKA et al., 2004b). Fig. 2.5 and Fig. 2.6 are shown changes of two selected phenological phases for 2050 under SRES-A2 and the three scenarios of climate change. Analogous to winter wheat there is a significant reduction in its duration especially for drier scenarios based on the model HadCM.

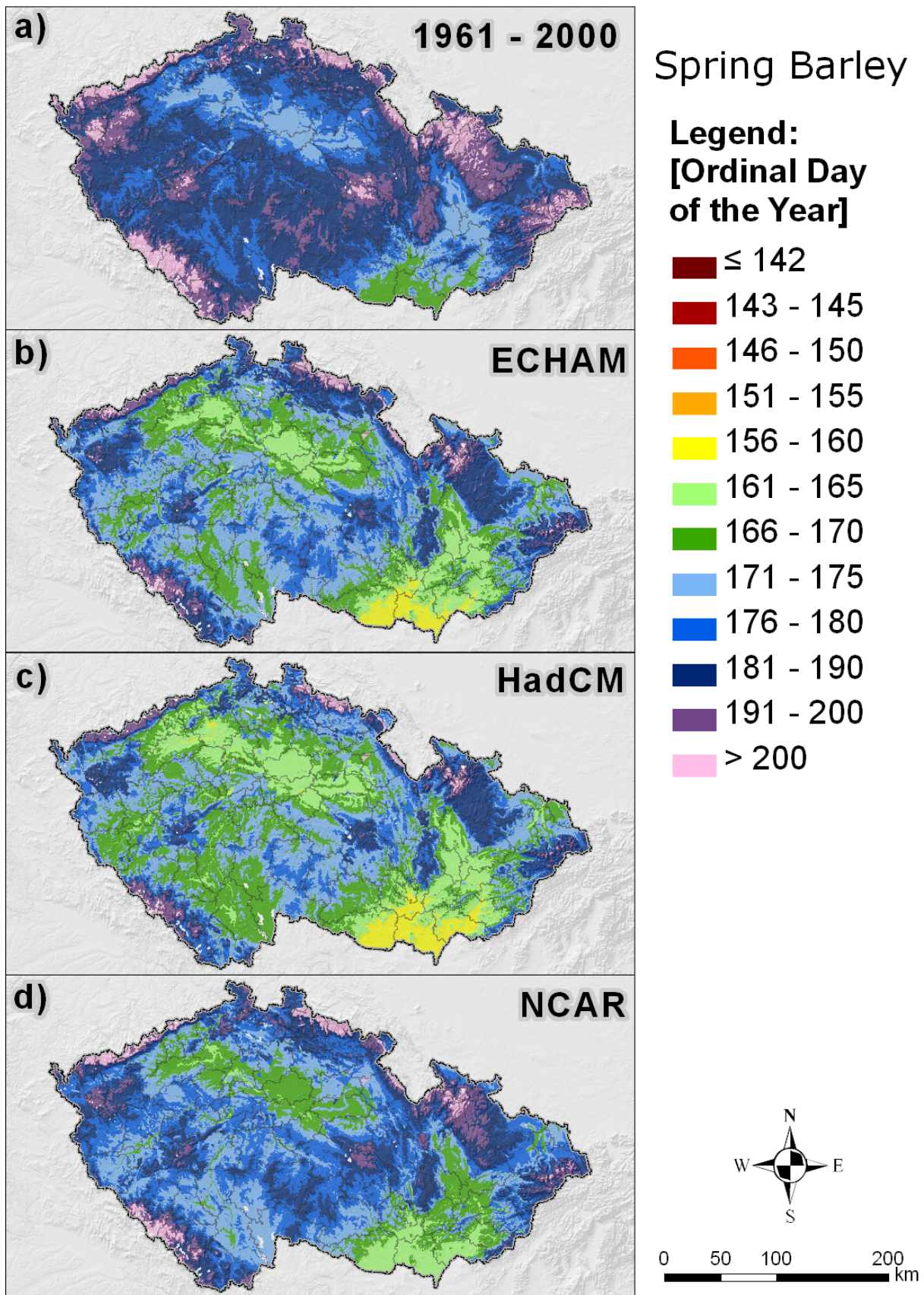


Figure 2.5 Dates of spring barley flowering a) for the current climatic conditions (1961 - 2000) b, c, d) for the year 2050 under emission scenarios SRES - A2 and three GCM in the CR (a median of 99 simulations for each grid cell network with a resolution of 500 x 500m).

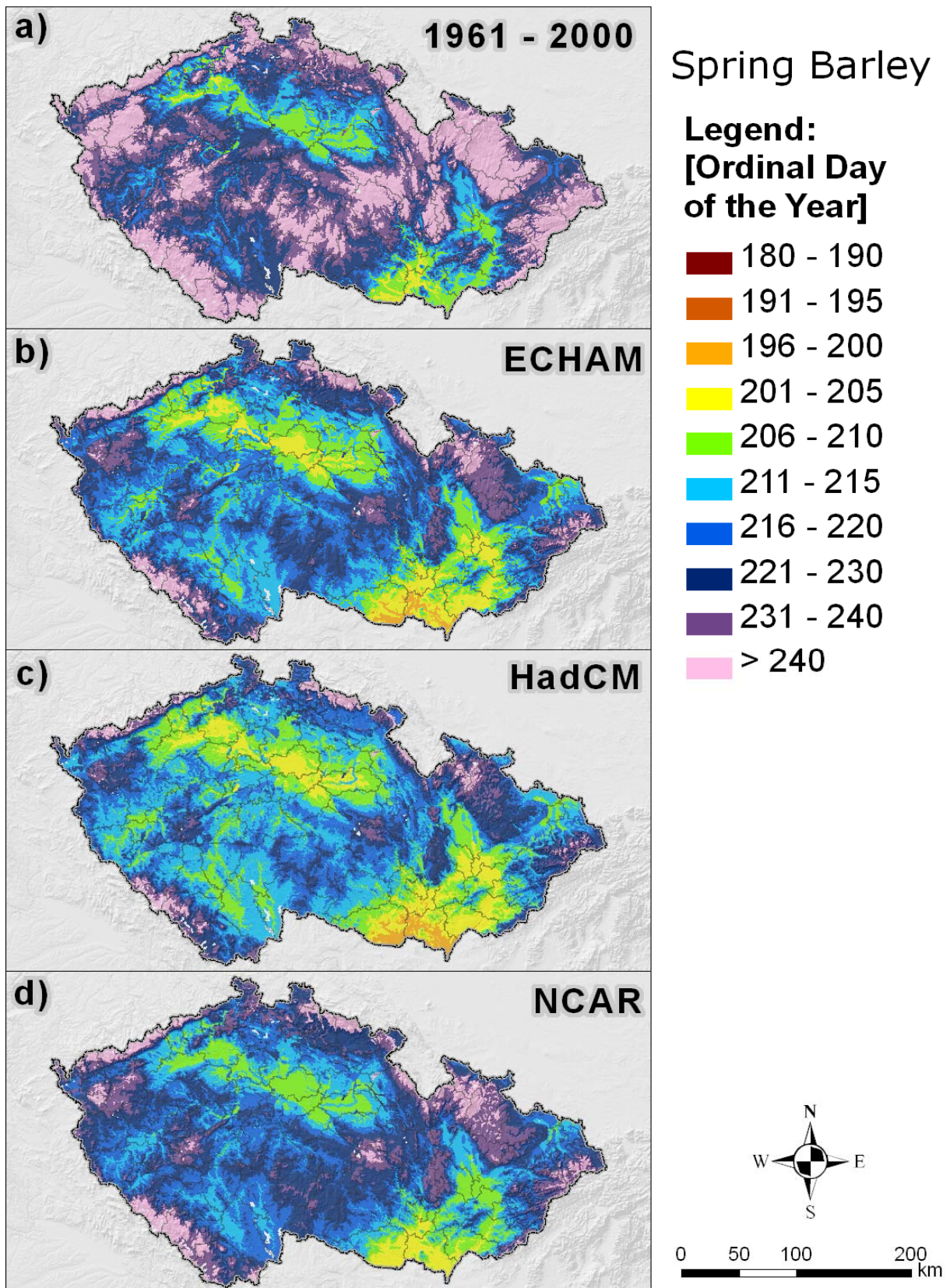
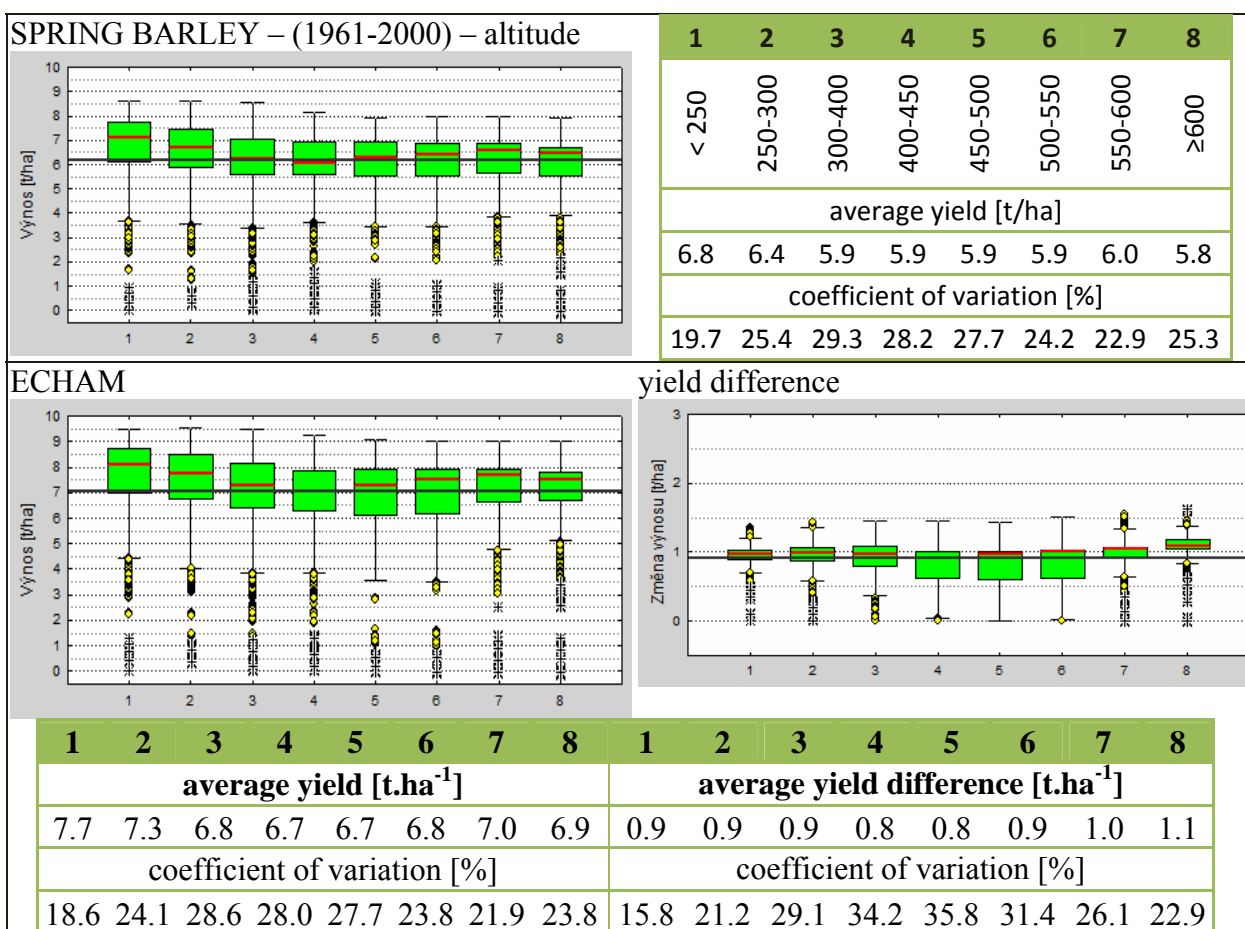


Figure 2.6 Dates of spring barley physiological maturity a) for the current climatic conditions (1961 - 2000) b, c, d) for the year 2050 under emission scenarios SRES - A2 and three GCM in the CR (a median of 99 simulations for each grid cell network with a resolution of 500 x 500m).

2.1.4 Sensitivity of the spring barley production to climate change at different altitudes

The highest yields in the current climate models are simulated by CERES - Barley model at lower altitude with the lowest variability (note the coefficient of variation is the proportion of standard deviation and average percentage). Significant impact has the fact that this is the best soil area in altitude level around 250 m, where arable land is composed from chernozem 43%, fluvisols 16%, phaeozems 10%, haplic Luvisols 7%, cambisols 6%, regosols 6%.

In the changed climate conditions is a very similar spatial pattern of yield distribution in all scenarios, all categories of altitude. It might be concluded that unlike in case of winter wheat no particularly vulnerable or resilient altitude class can be found in case of spring barley. Driest scenario HadCM shows the lowest yield increase with its higher variability, suggesting possible negative consequences of extreme climate years.



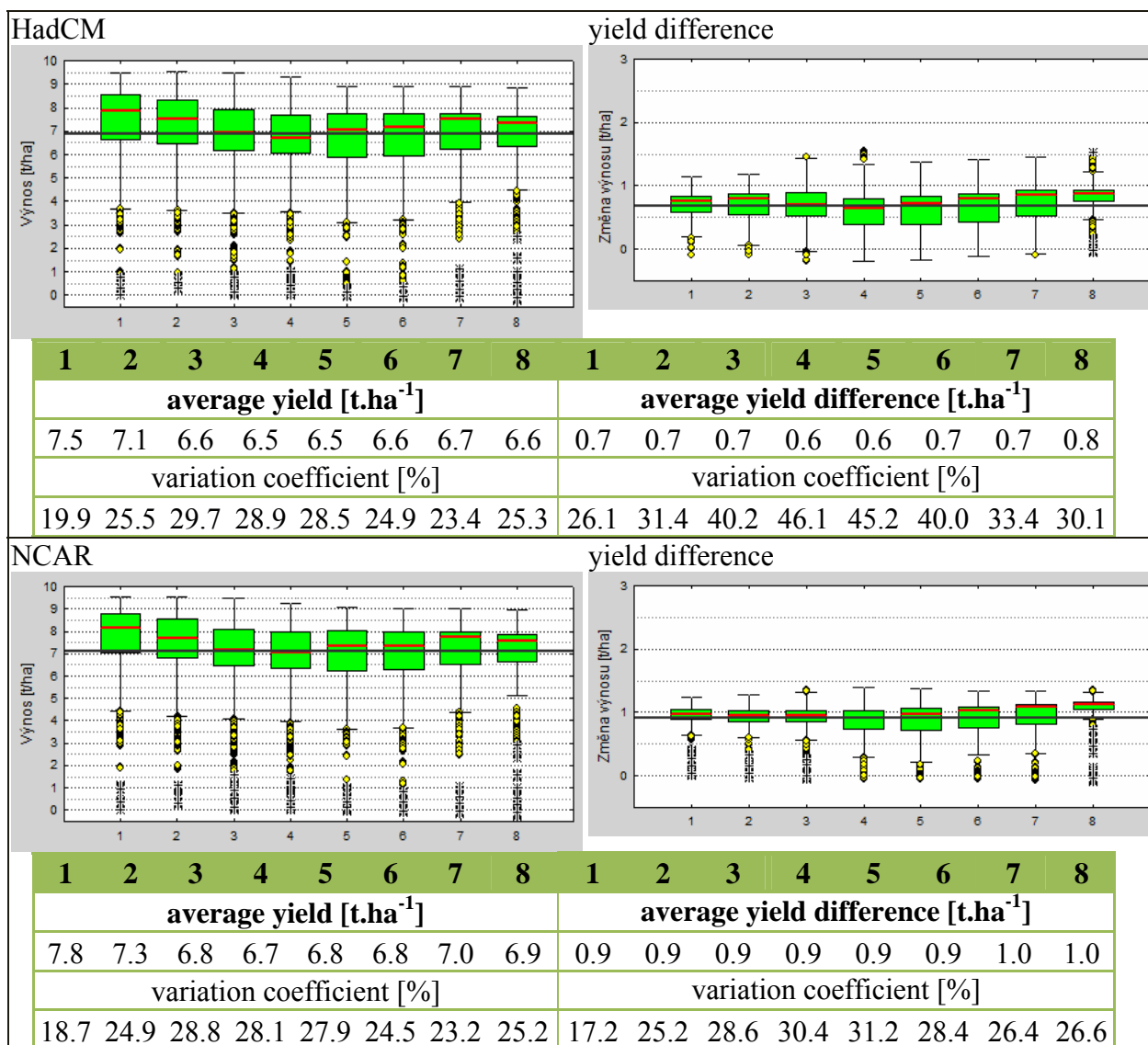
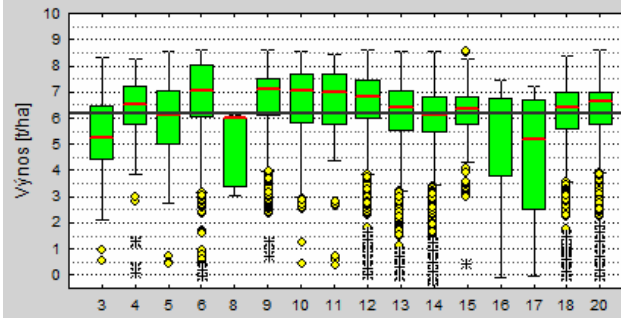


Figure 2.7 Summarizing yields of spring barley following categories of the altitude for the current climatic conditions (1961-2000) and impacts of climate change under the three GCM scenarios and SRES-A2. The green graph is interquartile (IQR) range ($x_{75}-x_{25}$) for each category of altitude, the red line in the box is the median category, bearded boxes ($1.5 \times IQR$) = adjacent values, the yellow points = outliers, stars = extreme values. Black continuous line is delivered the national average yield, respectively yield changes on arable land.

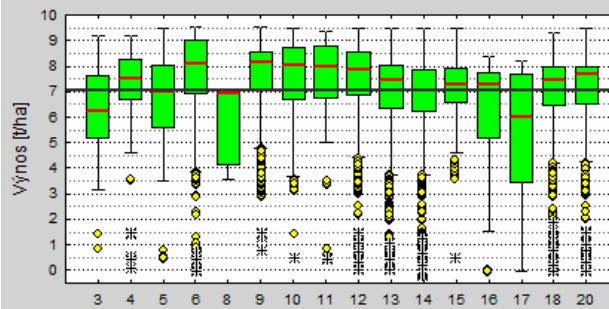
2.1.5 Sensitivity of the spring barley production under future climate according to the soil conditions

In contrast to winter wheat there is no significant influence of soil type in the changed climate, which means, and it is likely that climate change in terms of yields of spring barley will be not significantly reflected by any particular soil type (Fig. 2.8). The smallest yield increase can be described according to scenario based on the HadCM model while variability increased in the same way as for altitude analysis.

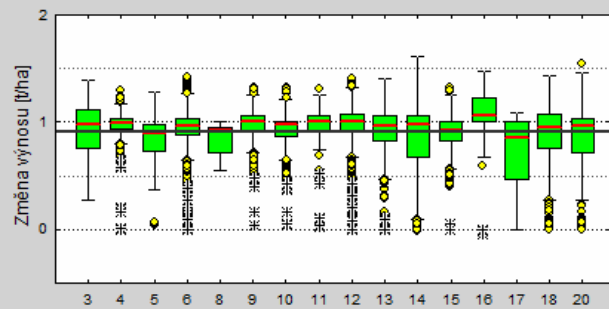


3	4	5	6	8	9	10	11	12	13	14	15	16	17	18	20
rendzic Leptosols calcic Leptosols Regosols			Fluvisols	Vertisols	Chernozem	Phaeozems	greyic Phaeozems	haplic Luvisols	Albeluvisols	Cambisols	Pelosols	entic Podzols	haplic Podzols	Stagnosols	Gleysols
average yield [t/ha]															
5,4	6,3	6,0	6,8	5,2	6,8	6,8	6,6	6,6	6,0	5,8	6,2	4,8	4,3	5,9	6,2
coefficient of variation [%]															
24,0	20,7	22,5	24,5	23,1	18,7	20,2	24,1	20,2	28,2	27,9	16,6	50,7	61,4	31,0	21,3

ECHAM - yield

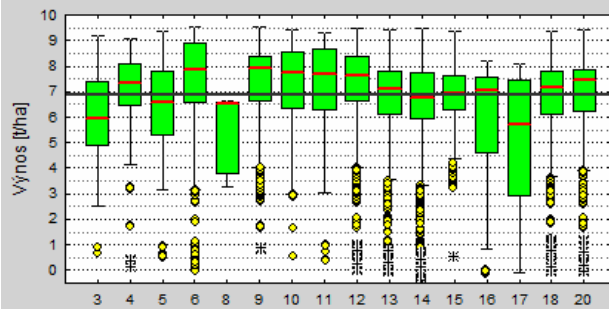


yield difference

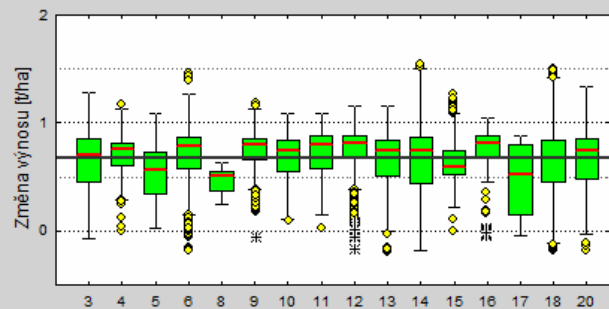


	3	4	5	6	8	9	10	11	12	13	14	15	16	17	18	20
average yield [$t \cdot ha^{-1}$]																
	6.3	7.3	6.8	7.7	6.0	7.7	7.7	7.6	7.6	6.9	6.7	7.1	5.8	5.0	6.7	7.1
VK [%]	22.1	19.7	22.5	23.5	21.7	17.5	19.0	23.1	19.2	27.1	27.5	16.3	46.1	59.9	30.2	21.2
average yield difference [$t \cdot ha^{-1}$]																
	0.9	1.0	0.8	0.9	0.9	1.0	0.9	1.0	1.0	0.9	0.9	0.9	1.0	0.7	0.9	0.9
VK [%]	21.7	16.8	26.5	23.4	14.7	13.1	14.9	21.4	18.3	27.5	32.8	18.0	38.9	56.1	34.1	27.8

HadCM - yield



yield difference



	3	4	5	6	8	9	10	11	12	13	14	15	16	17	18	20
average yield [$t \cdot ha^{-1}$]																
	6.0	7.0	6.5	7.5	5.6	7.5	7.5	7.4	7.4	6.6	6.5	6.9	5.5	4.7	6.5	6.9

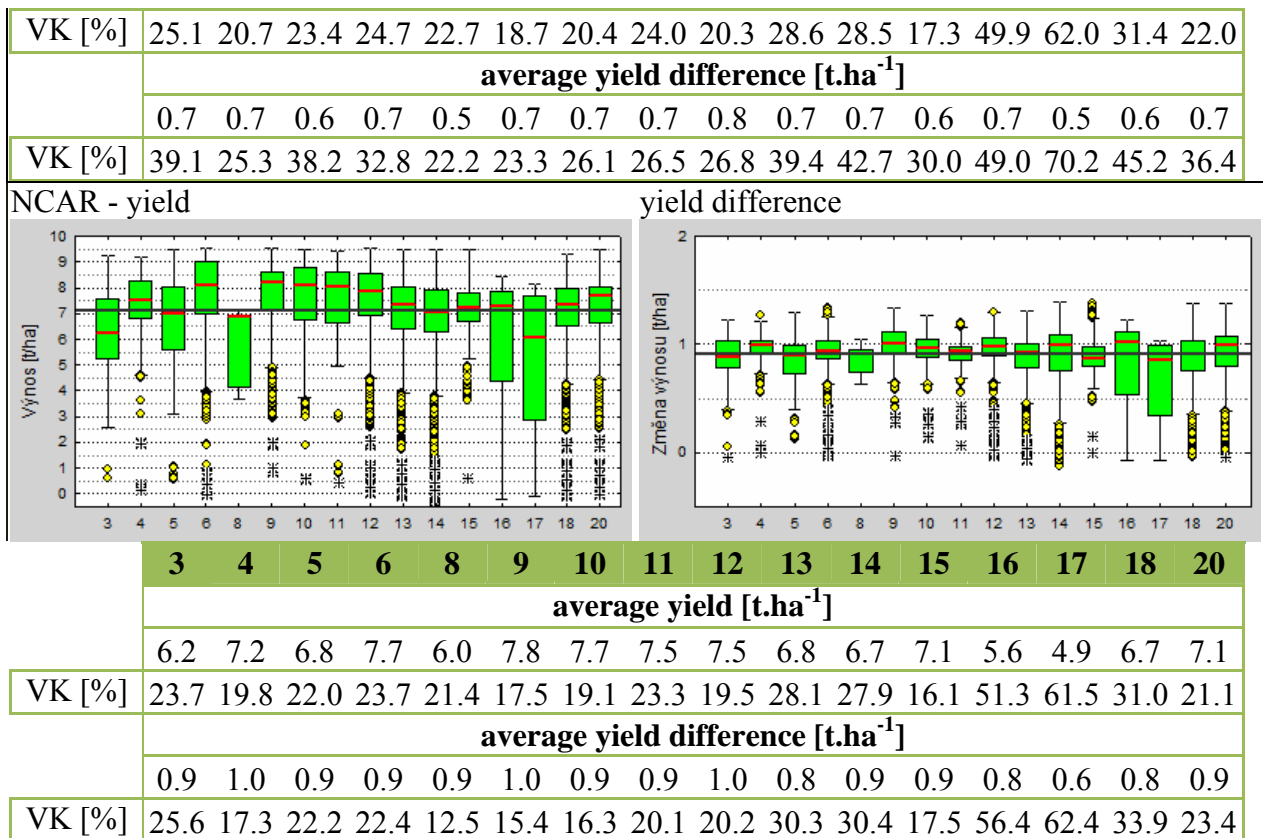


Figure 2.8 Summarizing yields of spring barley following categories of the soil types for the current climatic conditions (1961-2000) and impacts of climate change under the three GCM scenarios and SRES-A2. The green graph is interquartile (IQR) range ($x_{75}-x_{25}$) for each category of soil types, the red line in the box is the median category, bearded boxes ($1.5 \times IQR$) = adjacent values, the yellow points = outliers, stars = extreme values. Black continuous line is delivered the national average yield, respectively yield changes on arable land.

3 FOREST ECOSYSTEMS – SLOVAKIA

3.1 Introduction

In forestry well-developed European countries the transition from stand models based on mean and area characteristics to tree models has appeared. The models are taking into account competition relations, mortality processes and different thinning concepts and they are closely knitted with site quality and climate. The models work at more detail modelling level and they are more flexible and versatile. They offer modelling even-aged single species stands for static thinning concepts and site quality assessment, but they are also highly applicable for mixed uneven-aged stands with dynamic thinning concepts and site quality description. The models include wide range of output values covering production, ecological and economical parameters of forest stands. Rich tradition, powerful modelling background and sophisticated single tree growth simulators (SILVA, MOSES, PROGNAUS, BWIN, STAND) have been evident in German speaking countries and Scandinavian countries (PRETZSCH 1992, HASENAUER 1994, STERBA 1995, NAGEL 1996, PUKKALA-MIINA 1997, SLOBODA-PFREUNDT 1989).

The system of mathematical equations for modelling of tree values increments (diameter, height and eventually crown parameters) is fundamental component of individual tree growth models. Many of them are based on site quality definition directly through climate and soil factors (**ecological site classification**). The approach has a great importance for increment sensitivity to different site factors. The current stand growth models like yield tables are not able to satisfy such modelling requirements.

Objective of this work is to carry out the sensitivity analysis of most vulnerable forest stands to climate change impacts using growth model SIBYLA. The model was developed on the basis of research project of 5th framework programme of European Union: „Implementing Tree Growth Models as Forest Management Tools“ (FABRIKA and DURSKY 2006). One of the project objectives has been the development of algorithms and software solutions of growth simulator fully adapted to Slovak production and economical conditions. First necessary assumption is system of ecological site classification for main Slovak tree species (spruce, fir, pine, beech and oak).

SIBYLA parameterisation was based on wide range of foreign and Slovak data:

1. The net of long-term Bavarian experimental plots of the Chair of Forest Yield Sciences in Munich is primary material for the derivation of functions describing the impact of climate and soil factors on tree increment. In addition, Rhein-Pfalz and Lower Saxony experimental plots have been used for the model. The model is based on 404 experimental plots with 578 measuring time points and more than 150000 trees. These data sets are composed of information of breast height diameters, tree heights, heights of crown onsets, crown diameters regarding to different site conditions, growth position and tree vitality.
2. Yield tables (HALAJ et al. 1987), mainly height and diameter growth curves, were used as the basis for ecological site classification according to KAHN (1994) and were used for deriving height and diameter increments. The yield tables were based on data from experimental plots established in 1964 –1973. Additional data comes from permanent plots established in the past for various scientific purposes. Most of the plots were under the third or fourth cycle of measurement. The total number of measurements was 2199 for spruce, 436 for fir, 724 for pine, 1239 for beech and 746 for oak. Description of experimental data is published in (HALAJ and ŘEHÁK 1979).

3. The next important source for the development of the SIBYLA model was data from the inventory on the diameter and height structures of Slovak forests (HALAJ 1957, 1978). This data was used for determining relations between maximal stand height (or maximal diameter) and dominant stand height (or mean diameter) in order to construct a model of ecological site classification. The diameter inventory was carried out on 740 spruce stands, 370 fir stands, 380 pine stands, 420 beech stands and 370 oak stands. The height structure was based on 85 permanent plots of spruce, 57 plots of fir, 55 plots of oak and 75 plots of beech.

3.2 Modelling approach

The model SIBYLA is sensitive to nine site values:

s_1 ... content of NO_x in air (ppb)

s_2 ... content of CO_2 in air (ppm)

s_3 ... content of nutriment in soil (relative value within interval 0 - 1)

s_4 ... number of vegetation days (days with mean daily temperature bigger than 10°C)

s_5 ... annual temperature amplitude (difference between minimal and maximal temperature during year in $^\circ\text{C}$)

s_6 ... mean daily temperature in vegetation season in $^\circ\text{C}$

s_7 ... soil moisture (relative value within interval 0 - 1)

s_8 ... summary of rainfalls in vegetation season in mm

s_9 ... index of aridity by DE MARTONE in $\text{mm}\cdot^\circ\text{C}^{-1}$ derived by: $s_9 = \frac{s_8}{s_6 + 10}$

Transformation of site values s_i to relative values of their influence r_i is performed by transformation functions. The functions have been created on analytical principles and they are based on *fuzzy sets* algorithms (Fig. 3.1). Ecological amplitude of a value s is presented on the x -axis, it means range between minimal and maximal value for tree survival (for example range of mean temperatures in $^\circ\text{C}$ or precipitation total in mm). Transformed value r is presented on y -axis ranging from 0 to 1. If site value s influences the species in range from 0.9 to 1.0 the species is under *optimal* conditions. Interval from 0.5 to 0.9 means *sub-optimal* conditions and interval from 0 to 0.5 means *minimal (pessimal)* conditions. The mentioned principle was applied for all tree species (spruce, fir, pine, beech and oak) and for all site values. The breakpoints (c_j) have been identified in each function and linear vectors have been created by:

$$r_T = \left(\prod_{i=4}^6 r_i \right)^{1-\gamma_4} \cdot \left(1 - \prod_{i=4}^6 (1-r_i) \right)^{\gamma_4} \quad (3)$$

$$r_H = \left(\prod_{i=7}^9 r_i \right)^{1-\gamma_5} \cdot \left(1 - \prod_{i=7}^9 (1-r_i) \right)^{\gamma_5} \quad (4)$$

The nutriment effect combines content of N₂O and CO₂ in air and content of nutriments in soil. The thermal effect combines number of days of vegetation season, temperature amplitude and mean temperature in vegetation season. The humidity effect combines soil moisture, total precipitation and aridity index. The effects are aggregated into effect of asymptote reduction (r_A) and culmination age reduction (r_{tkulm}) to produce the curve of tree height potential and reduction effect of increment of basal area (r_g):

$$r_A = (r_N \cdot r_T \cdot r_H)^{1-\gamma_1} \cdot (1 - (1-r_N)(1-r_T)(1-r_H))^{\gamma_1} \quad (5)$$

$$r_{tkulm} = (r_N \cdot r_T \cdot r_H)^{1-\gamma_2} \cdot (1 - (1-r_N)(1-r_T)(1-r_H))^{\gamma_2} \quad (6)$$

$$r_g = (r_N \cdot r_6 \cdot r_8)^{1-\gamma} \cdot (1 - (1-r_N)(1-r_6)(1-r_8))^{\gamma} \quad (7)$$

In term of non-significant influence, only mean temperature in vegetation season (r_6) as thermal effect and total precipitation (r_8) as humidity effect is applied for calculation of r_g . The parameters γ have been derived by regression analysis from experimental data of research plots (KAHN 1994) and are published by PRETZSCH and KAHN (1998).

New production ranges were derived for diameter and height **growth potential** by methodology of KAHN (1994) using the data from Slovak yield tables. Produced upper and lower height curves are modelled by minimal and maximal asymptote and by minimal and maximal culmination age. The Korf function has been adapted for this:

$$h_{\max} = c \cdot A \cdot e^{\frac{k}{(1-p) \cdot t^{p-1}}} \quad (8)$$

The function describes development of height potential (h_{\max}) in dependence on age (t). The coefficients of the model (A , k , p) were derived from yield tables (HALAJ ET AL. 1987) and coefficient c , which is describing relation between maximal and dominant height is derived from research of height structure of Slovak stands by HALAJ (1978) on basis of analysis of height distribution functions. Potential of diameter increment ($i_{d\max}$) is second output of the model. Such potential depends on tree diameter ($d_{1.3}$), what is given by function:

$$i_{d\max} = d_{1.3} \cdot \frac{k}{\left(\frac{-k}{\ln\left(\frac{d_{1.3}}{c \cdot A}\right) \cdot (p-1)} \right)^{\frac{p}{p-1}}} \quad (9)$$

The coefficients of the model (A , k , p) were derived from yield tables (HALAJ ET AL. 1987) and coefficient c , which is describing relation between maximal and mean diameter is derived from research of diameter structure of Slovak stands by (HALAJ 1957) on basis of

analysis of diameter distribution functions. Derived functions comparing to functions of SILVA model are presented in Figures 3.2 and 3.3.

Ecological parameters influence except for growth process, also the **mortality processes**. The mortality model of SIBYLA growth simulator is sensitive to climatic and soil parameters. The model of natural tree mortality was adopted from the growth simulator SILVA 2.2 (ĎURSKÝ 1997, ĎURSKÝ et al. 1996). The model is activated at the beginning of 5-year simulation interval, and consists of two parts: a model simulating the probability of tree survival, and a model simulating the threshold stand density. The model of tree survival probability is based on the logistic regression, which is a function of survival probability (function F -logit):

$$F(x) = \frac{1}{1 + e^{-L(x)}} \quad (10)$$

where $L(x)$ is the logical value calculated for a particular tree:

$$L(x) = a_0 + a_1 \cdot d_{1.3} + a_2 \cdot \frac{5 \cdot i_g}{d_{1.3}} + a_3 \cdot \frac{h}{d_{1.3}} + a_4 \cdot AVB_{50} \quad (11)$$

The logical value depends on tree diameter $d_{1.3}$, annual increment of tree basal area i_g , tree height h , and absolute height (site) class AVB_{50} . Absolute height (site) class is expressed as a potential top height in the simulation plot reached at the age of $t = 50$ years and it is **ecological sensitive**. The function of tree survival probability is then transformed to the function of tree mortality (in %) as follows:

$$Mrt\% = \frac{b_0}{e^{b_1 \cdot F(x,a)^{b_2}}} \cdot r(SD) \quad (12)$$

where $r(SD)$ is the value dependent on stand density (SD) determined by Stand Density Index according to REINEKE (1933). If stand density is greater than or equal to 0.7 (0.8 for pine), $r(SD)$ is equal to 1, otherwise it is equal to SD . The obtained value $Mrt\%$ is then compared with the random number drawn from uniform distribution from the interval $<0;100$). The tree i dies if the calculated value exceeds the random number:

$$M_i = \begin{cases} 1 = \text{alive} \Leftrightarrow Mrt\%_i \leq \text{Random}(100) \\ 0 = \text{dead} \Leftrightarrow Mrt\%_i > \text{Random}(100) \end{cases} \quad (13)$$

The age at which the tree dies is randomly generated from the 5-year interval. All coefficients are published in FABRIKA (2005).

Threshold stand density model is based on the reduction of the stand basal area, if this exceeds the maximum possible level. Maximum stand basal area is calculated as a weighted arithmetic mean of maximum basal areas of individual tree species (j) in the stand, while tree crown projections (cd_i^2) are used as weights:

$$G_{\max} = \frac{\sum cd_i^2 \cdot G_{\max}(h_{95\%_j})}{\sum cd_i^2} \quad (14)$$

Maximum stand basal area of a particular tree species is calculated from its top height ($h_{95\%}$) according to:

$$G_{\max}(h_{95\%}) = \frac{\pi}{16 \cdot a_0 \cdot h_{95\%}^{a_1} \cdot 10000} \cdot a_2 \quad (15)$$

Next, stand basal area of dying trees is obtained from the actual stand basal area (G) and the stand basal area of dead trees (G_{dead}) as follows:

$$G_{mort} = G - G_{max} - G_{dead}; \text{ if } G_{mort} > 0 \quad (16)$$

Then the trees with the highest probability of mortality are selected as dead trees in order to fill up the basal area G_{mort} .

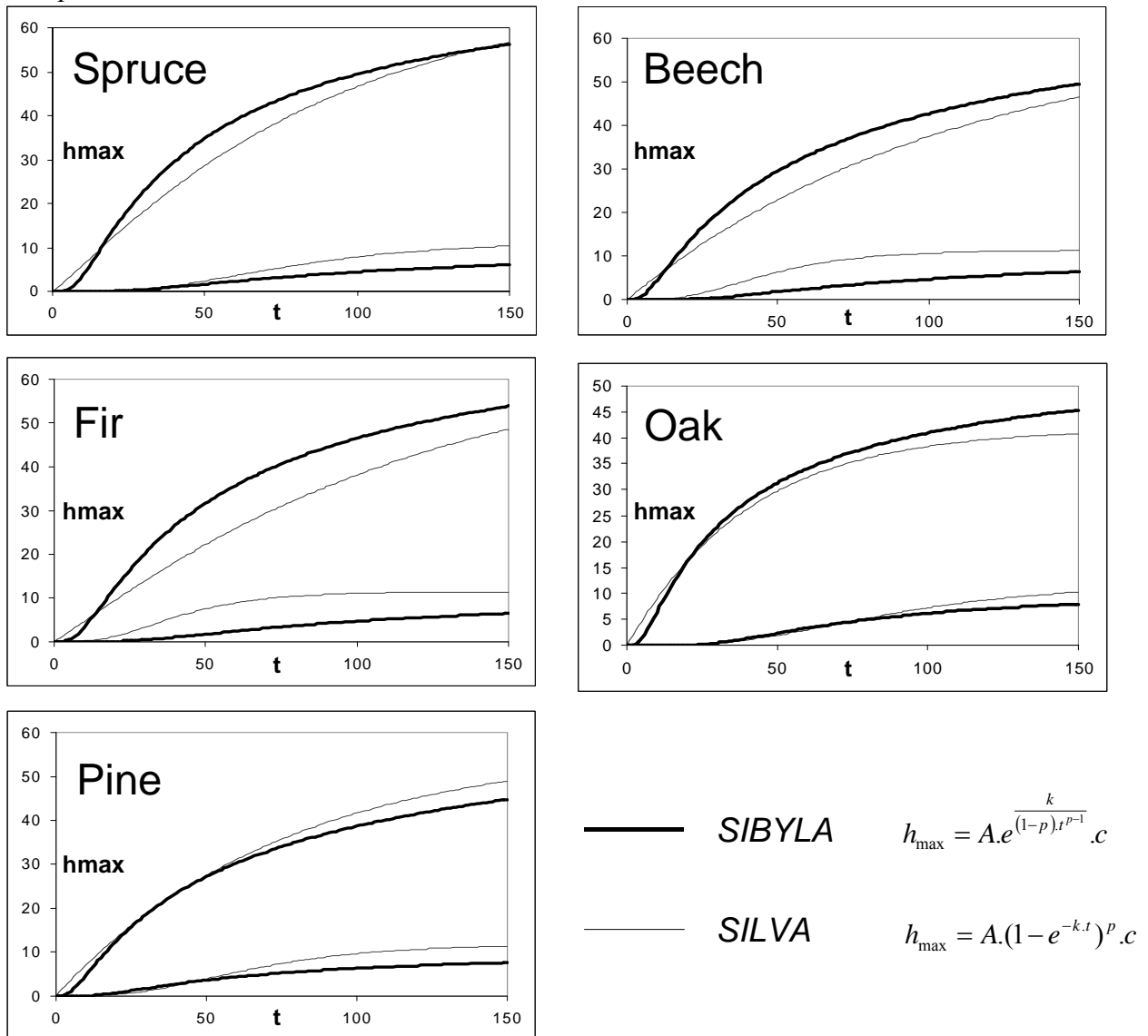


Fig. 3.2 Development of maximal tree height for optimal and pessimal stand conditions - comparison of SIBYLA and SILVA models.

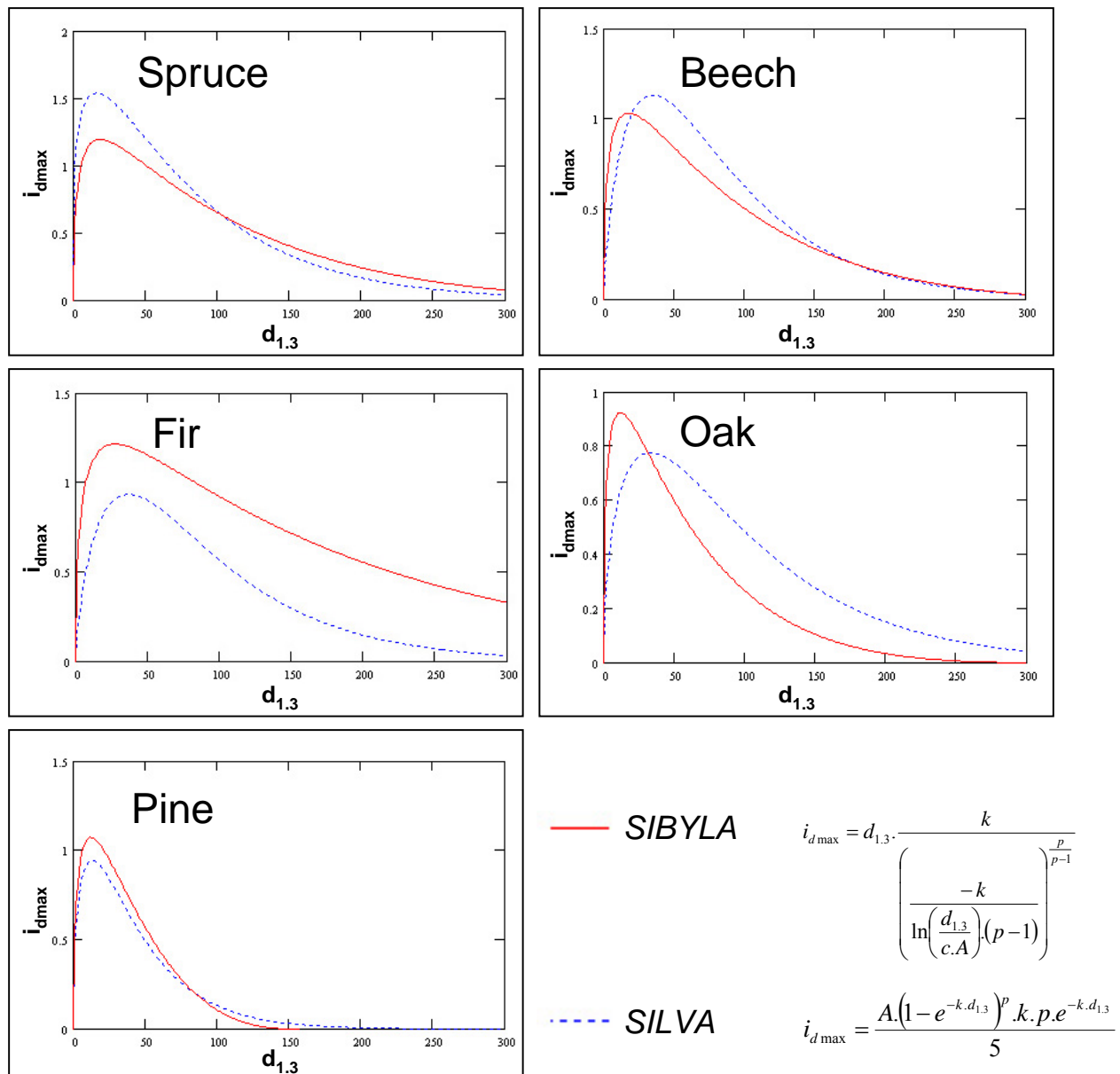


Figure 3.3 Development of maximal tree diameter increment at optimal stand conditions - comparison of SIBYLA and SILVA model.

3.2.1 Model calibration

The calibration of increment model was based on tree data from Slovak monitoring plots. We processed the data from 1189 permanent monitoring plots established in 1994. Plots have circular shape with size 200, 500 or 1000 m², depending on forest age and its cover in Slovakia. Repeated measurements of tree diameters and heights have been performed after 2-8 year periods, depending on monitored area. Number of processed trees is the following: 7358 spruce, 1137 fir, 1181 pine, 9213 beech, 3444 oak. For each plot, the representative plots (50 x 50 m) have been generated by expanding of circle plot area to representative area.

Growth simulations have been conducted without the mortality process. Model of thinning concepts has been replaced by direct trees selection on the basis of real cutting during the analysed periods. The growth simulation has been executed for 5 and 10 years period. Then predicted annual increment of diameter and height have been calculated and synchronised with real annual increment from the monitoring plots. Subsequently, modelled increments

(SIBYLA) and real increments (measured) have been compared. Significance of differences between SIBYLA increment and real increments ($i_{SIBYLA} - i_{REAL}$) has been tested. In general, bias has been detected for diameters and heights. Therefore, regression functions between differences (BIAS) and SIBYLA increments have been derived:

$$B_d = a_0 + a_1 \cdot i_d(SIBYLA) \quad (17)$$

$$B_h = a_0 + a_1 \cdot i_h(SIBYLA) \quad (18)$$

Subsequently, random error range has been derived as important quantity for the next statistical processing of data. Used method is as follows:

a) creation of SIBYLA increment classes and calculation of mean bias [$B(j)$] and standard deviation of biases [$s_B(j)$] for differences in each class,

b) derivation of regression model between standard deviations of biases and central points of SIBYLA increment classes [$s_B(j) = f(i_{SIBYLA}(j))$]

c) calculation of random error [E] on the basis of Gaussian distribution defined by bias and standard deviation of bias:

$$E_d = GAUSS(B_d, s_{B_d}) \quad (19)$$

$$E_h = GAUSS(B_h, s_{B_h}) \quad (20)$$

Final calibrated Slovak-specific increments are calculated by:

$$i_d(SK) = i_d(SIBYLA) - B_d + E_d \quad (21)$$

$$i_h(SK) = i_h(SILVA) - B_h + E_h \quad (22)$$

3.2.2 Model outputs

SIBYLA growth simulator is individual-tree distance-dependent model. Therefore individual tree data are produced and summarized for whole stand. SIBYLA growth simulator produces wide range of outputs: production, biomass, biodiversity, incomes, and costs. Production is quantified by tree counts, tree volume, mean age, mean diameter, mean height, mean tree volume, basal area per hectare, growing stock per hectare, projected crown area, canopy cover, stand density, total volume production, total current increment, and total mean increment. Biomass is quantified by dry weight of assimilates, branches, stem, and roots for individual trees and for whole stand and also carbon contents is calculated. Allometry functions are used for biomass calculation. Biodiversity is quantified by indices of species richness, heterogeneity, and balance, by indices of horizontal and vertical structures, and indices of structural differentiation. Incomes are quantified by specification of tree assortments and their financial value. Costs are specified by wages, material and social costs for harvesting and transport activities.

3.2.3 Methodology

Initial stand structures designed for the sensitivity analysis are the following (Tab. 3.1):

- pure beech stand (BK100),
- pure spruce stand (SM100),
- pure oak stand (DB100),
- three beech-oak mixed stands with different mixture:

- beech 20%, oak 80% (BK20DB80),
- beech 50%, oak 50% (BK50DB50),
- beech 80%, oak 20% (BK80DB20),
- three spruce-fir-beech mixed stands (Carpathian composition) with different mixture:
 - spruce 20%, fir 10%, beech 70% (SM20JD10BK70),
 - spruce 1/3, fir 1/3, beech 1/3 (SM33JD33BK33),
 - spruce 70%, fir 10%, beech 20% (SM70JD10BK20),

Individual tree data have been generated by SIBYLA structure generator. The principle of generation is the following:

Generation of diameter frequency distribution $f(d)$ depending on quadratic mean diameter (d_m), level of diameter variance (s_d), total number of trees (N) and size of diameter class (h , standard for simulator is 1):

$$f(d) = \frac{c}{b} \left(\frac{d}{b} \right)^{c-1} \cdot e^{-\frac{d^c}{b^c}} \cdot N \cdot h \quad (23)$$

Parameters b , c depends on d_m and s_d . This relation was derived from the empirical material of all Slovak area for spruce, fir, pine, beech and oak (HALAJ 1957). Fixing of input characteristics (mean diameter, mean height and growing stock per hectare) is preserved iteratively. In the first step, the generation of frequency distribution and back calculation of mean diameter is performed. The curve is shifted in direction of x axis, till mean diameter is equal to input diameter. In the second step, the number of trees is altered, till calculated growing stock is equal to the input growing stock.

2. Generation of single tree heights (h) on uniform height curves (ŠMELKO, PÁNEK and ZANVIT 1987), depending on quadratic mean diameter (d_m) and mean height (h_m):

$$h = 1,3 + (h_m - 1,3) \cdot e^{[(a_0 + a_1 \cdot h_m + a_2 \cdot d_m) \cdot (\frac{1}{d_{1,3}} - \frac{1}{d_m})]} \quad (24)$$

Generation of the crown diameters (b) and crown onsets (h_l) according to relations (PRETZSCH and KAHN 1998) :

$$b = e^{a_0 + a_1 \cdot \ln(d_{1,3}) + a_2 \cdot h + a_3 \cdot \ln(\frac{h}{d_{1,3}})} \quad (25)$$

$$h_l = h \cdot \left[1 - e^{\left(a_0 + a_1 \cdot \frac{h}{d_{1,3}} + a_2 \cdot d_{1,3} \right)} \right] \quad (26)$$

Generation of position co-ordinates (x , y) of single trees on basis of the Poisson's homogeneous process (PRETZSCH 1993).

Input data for structure generator have been derived from Slovak yield tables (HALAJ 1987). We used 4 different ages 40, 60, 80, and 100 years to cover the whole production range.

Stands younger than 40 years cannot be actually simulated in the SIBYLA model. We designed mean stand condition defined by mean site class in Slovak yield tables for each tree species. Average volume level 2.2 has been applied and stand density 0.9 have been used. Mean variance of diameter have been applied for structure generation.

The experimental plots were distributed in three forest eco-regions with natural dominance of spruce, beech and oak. Then we selected four different vegetation zones in each eco-region specified by different altitude and different forest type (site). Model stands have been located in the appropriate forest eco-regions and rotated in the frame of several vegetation zones. Thus 9 stand structures, 4 age classes and different sites (eco-region + vegetation zone + forest type) produced 240 variants of forest stands.

The representative sample plots used for the simulations are listed in the Table 3.1. The table contains stand parameters for generating the individual trees in the frame of square plots with size 0.25 hectares. The stands cover wide range of typical stands compositions with different species mixtures. The stands have been placed into 3 eco-regions (oak, beech, spruce), each with 4 different altitudinal vegetation zones defined by typical forest type (see Table 3.2). Such range covers vertical differentiation of natural conditions in Slovakia. The plots have been rotated in each eco-regions and respective vegetation zones in order to asses the influence of changed climate condition on stands development and their vulnerability.

Tab.3.1 Representative sample plots.

stand	Age	density	volume level	percentage				Site class				
				spruce	fir	beech	oak	spruce	fir	beech	oak	
BK100	40/60/80/100	0.9	2.2			100					24	
BK20DB80	40/60/80/101	0.9	2.2			20	80				24	24
BK50DB50	40/60/80/102	0.9	2.2			50	50				24	24
BK80DB20	40/60/80/103	0.9	2.2			80	20				24	24
SM20JD10BK70	40/60/80/104	0.9	2.2	20	10	70		28			24	
SM33JD33BK33	40/60/80/105	0.9	2.2	100/3	100/3	100/3		28			24	
SM70JD10BK20	40/60/80/106	0.9	2.2	70	10	20		28			24	
DB100	40/60/80/107	0.9	2.2				100					24
SM100	40/60/80/108	0.9	2.2	100				28				

Tab. 3.2 Eco-regions, their altitudinal vegetation zones (AVZ) and forest types.

Eco-region	Plot ID	AVZ	Description
Oak	4825	1	Oak-hornbeam forests on loess with <i>Brachypodium sylvaticum</i>
Oak	4973	2	Oak-beech forests with <i>Poa nemoralis</i> and <i>Luzula luzuloides</i>
Oak	5121	3	Beech-oak forests with <i>Carex pilosa</i> and <i>Galium odoratum</i>
Oak	5567	4	Beech forests with <i>Galium odoratum</i>
Beech	5713	4	Beech forests with <i>Luzula luzuloides</i>
Beech	5715	5	Beech-fir forests with ferns
Beech	6010	5	Beech-fir forests with <i>Galium odoratum</i>
Beech	6159	6	Sycamore-beech forests on rocky slopes with ferns and <i>Petasites albus</i>
Spruce	6605	7	Spruce-rowan forests on rocky slopes
Spruce	6607	8	Dwarf pine communities with <i>Pinus cembra</i> and <i>Larix deciduas</i>
Spruce	6609	5	Acidophilous beech forests on sandstone with grasses
Spruce	6752	6	Fir-beech forests with <i>Oxalis acetosella</i>

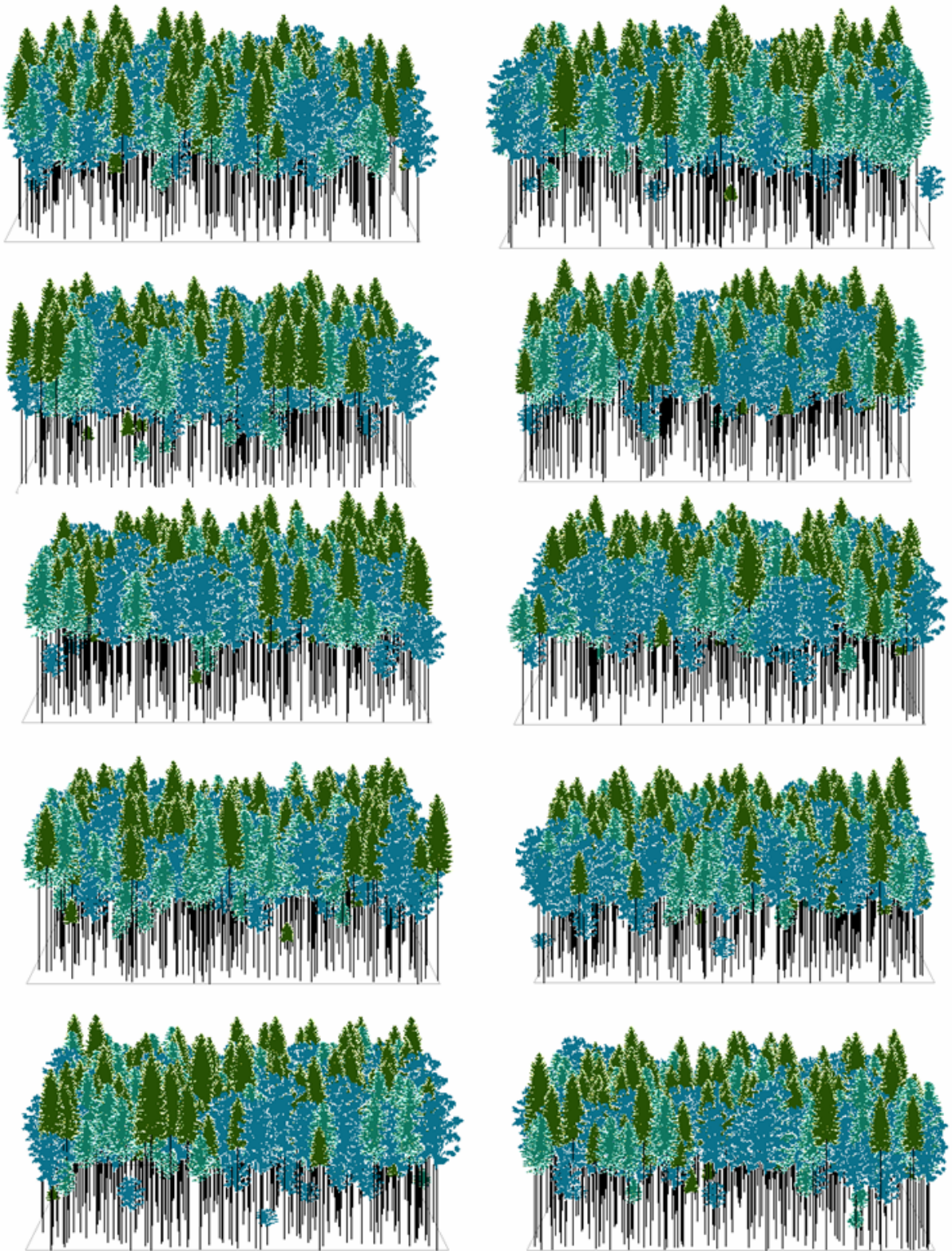


Fig. 3.4. Comparison of 10 different initial situations for 1 selected stand structure (SM33JD33BK33, Carpathian mix with balanced tree composition), age = 60 years.

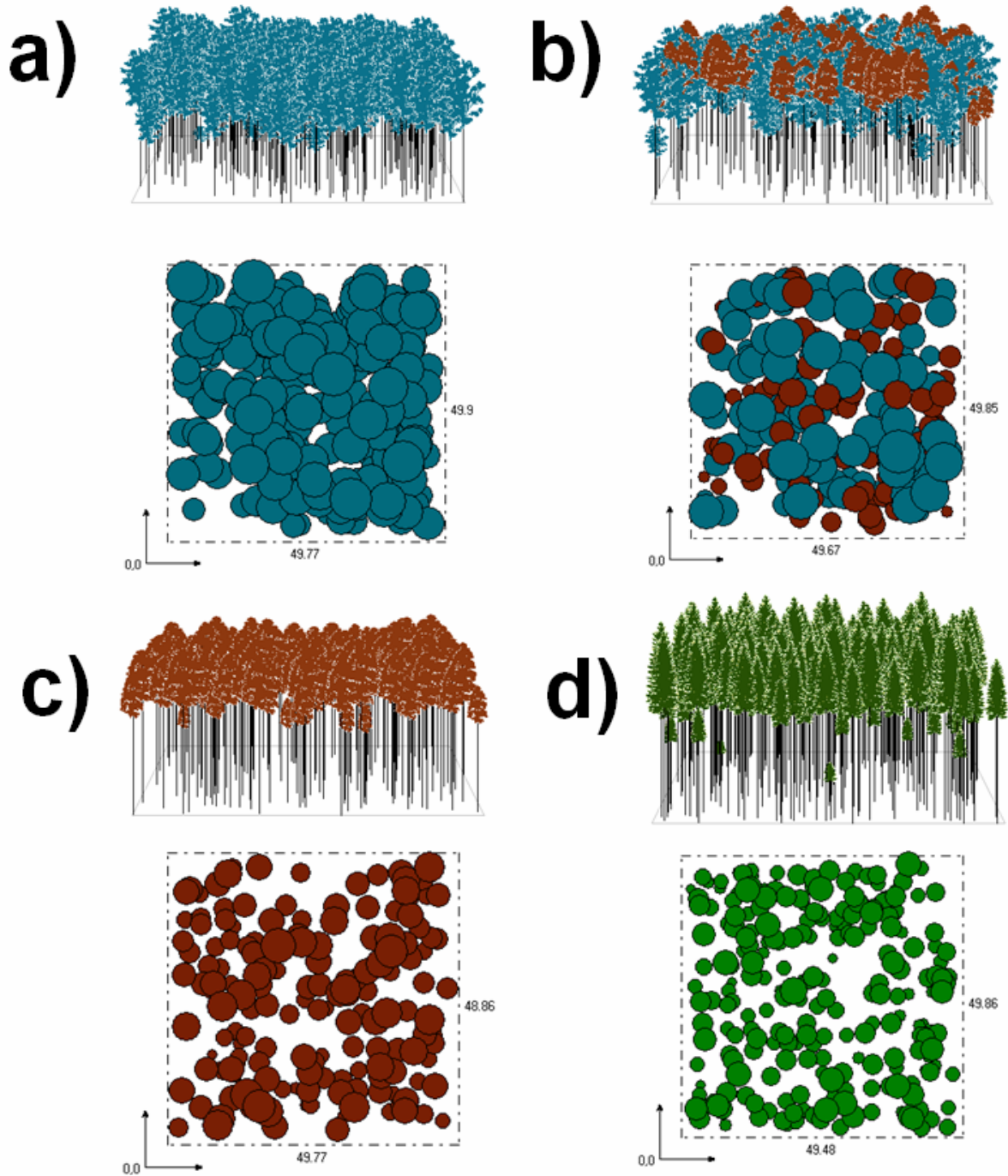


Fig. 3.5 Comparison of 4 different initial stands: a) beech stand, age = 80 years, b) beech-oak stand (50%-50%), age = 80 years, c) oak stand, age = 80 years, d) spruce stand, age = 80 years.

3.3 Results

The results describe the sensitivity of production and mortality of analyzed forest tree species and stands with various species, age composition and site conditions. The average values of production and natural mortality of 70, 90, 110 and 130 years old forest stands at the end of 30 years simulation periods (1961-1990, 2021-2050, 2071-2100) are investigated in relation to altitudinal vegetation zones (AVZ hereinafter), specific species compositions and stand conditions. The simulations were run under the following conditions:

1. No management has been applied except for the removal of dead trees
2. Only the natural trees mortality has been considered (no disturbances)
3. Stand density of 0.9 has been considered for each plot
4. Mean site class and mean volume level has been considered
5. Total volume production (TVP) and cumulative volume of death trees (CVDT) at the end of simulations have been the analyzed quantities

The following procedures have been applied to allow for the statistical analysis of simulation outputs:

1. Ten random stand structures were generated for each experimental plot, altering trees distribution at a plot
2. Each growth simulation has been run 10 times for each stand structure, stochastically altering the increments and mortality

Provided the interpretations were focused on responses of a single tree species, the simulated values were recalculated to species full coverage at a stand, to allow for inter-species and inter-stand comparisons. Both TVP and CVDT are investigated either in $\text{m}^3 \cdot \text{ha}^{-1}$ or in the ratios of future production/mortality vs. the reference period. The 97.5% confidence bands are displayed in all charts to allow for the visual assessment of the investigated quantities at $\alpha = 5\%$.

The results of simulations are interpreted in relations to so-called altitudinal vegetation zones, which reflect the altitudinal arrangement of forest vegetation and are frequently used in forestry. Because AVZ were designed for vegetation distribution under the normal climate, they also represent the reference state which the simulations under the climate change scenario can be referred to. The altitudinal vegetation zones of Slovakia are as follows:

1. Oak AVZ – forests of the lowest elevations up to 300 m a.s.l., outside the distributional range of beech
2. Beech-oak AVZ – 200-500 m a.s.l., transitional zone between oak and beech zones
3. Oak-beech AVZ – 300-700 m a.s.l., forest with dominance of beech
4. Beech AVZ – 400-800 m a.s.l., forest with high abundance of pure beech stands, often without any ground vegetation
5. Fir-beech AVZ – 500-1000 m a.s.l., beech stands with admixture of fir and occasionally spruce
6. Spruce-beech-fir AVZ – 900-1300 m a.s.l. continuation of fir-beech AVZ, with occasional prevalence of coniferous, mainly in nutrient-poor stands
7. Spruce AVZ – 1250-1550 m a.s.l., spruce dominated forest, form a narrow belt along the upper tree line
8. Dwarf pine AVZ – above 1550 m a.s.l.

To allow for better understanding of the next text we define the following terms and abbreviations:

TVP – total volume production calculated as the sum of growing stock on the end of simulation period and mortality during the simulation period

Periodic volume increment – calculated as difference between TVP on the end of simulation period and initial growing stock status

Natural mortality – volume of death trees during the simulation period, the mortality is caused without any outstanding activity of disturbance agents

CVDT – cumulative volume of death trees, sum of naturally died trees during the simulation period

3.3.1 Spruce (*Picea abies*) sensitivity to climate change

The results of simulation indicate that spruce is highly sensitive to the projected changes of climate (Figs. 3.4-3.5). Changes in both TVP and CVDT of stands with certain share of spruce were in most cases statistically significant. Changes in TVP exhibit increasing trend along the AVZs with significant differences between reference and future time periods.

Similarly, increasing trend along AVZs was also observed in case of CVDT, although being less pronounced. CVDT in the future periods differ significantly from the reference period almost in all AVZs. However, differences in mortality between NFC and FFC are not significant. This means that spruce mortality remains stable in the future, and it may be considered a less sensitive component of the total volume production.

Response of spruce production is similar as in case of all investigated tree species – declining production in the lower elevations due to projected impact of drought periods and heat stress; and rising production in the higher elevations due to tempering the climate at species upper distributional limit.

Productivity of spruce stands and stands with admixture of spruce in the 4th AVZ (beech) was projected to decline in the future by 5-25 %. The decline is much bigger in the FFC. Reduced production is accompanied by decrease of mortality by 10-20 %. Such findings indicate a change in total stands structure towards ecologically stable stands dominated by smaller volume trees. In the other words, decreased mortality indicates that ecological stability of investigated spruce stands should remain comparable to the reference period, although the production declines. This means that despite expected more pronounced drought in the lower elevations, spruce vitality increases (10-20% on average) and drought impacts mainly spruce increment.

Projected impacts on spruce stands in the 5th AVZ (fir-beech) are similar to those in the 4th AVZ, however in the FFC only. The production was projected to decline by 10% accompanied by approximately 20% decrease of mortality. In the NFC, both TVP and CVDT remain comparable to the reference period. In general, ecological stability of spruce stands and spruce vitality should not worsen in the 5th AVZ.

Significant increase of productivity of spruce stands was projected in 6-8th AVZs (spruce-beech-fir, spruce, dwarf pine). The increase ranges from 10-40% being more pronounced in the FFC and in higher AVZs. Increased TVP is accompanied by increase of spruce mortality by 20-40% comparing to the reference period. This indicates more productive but ecologically less stable stands, mainly in higher elevations. Forest stands structure changes towards bigger trees competing for resources with the remainders, thereby increasing a total spruce mortality. Extreme variability of mortality projected to the FFC in the 8th AVZ indicates unbalanced forest development. Anyway, milder climate in the alpine zone is supposed to result in significant increase of forest biomass.

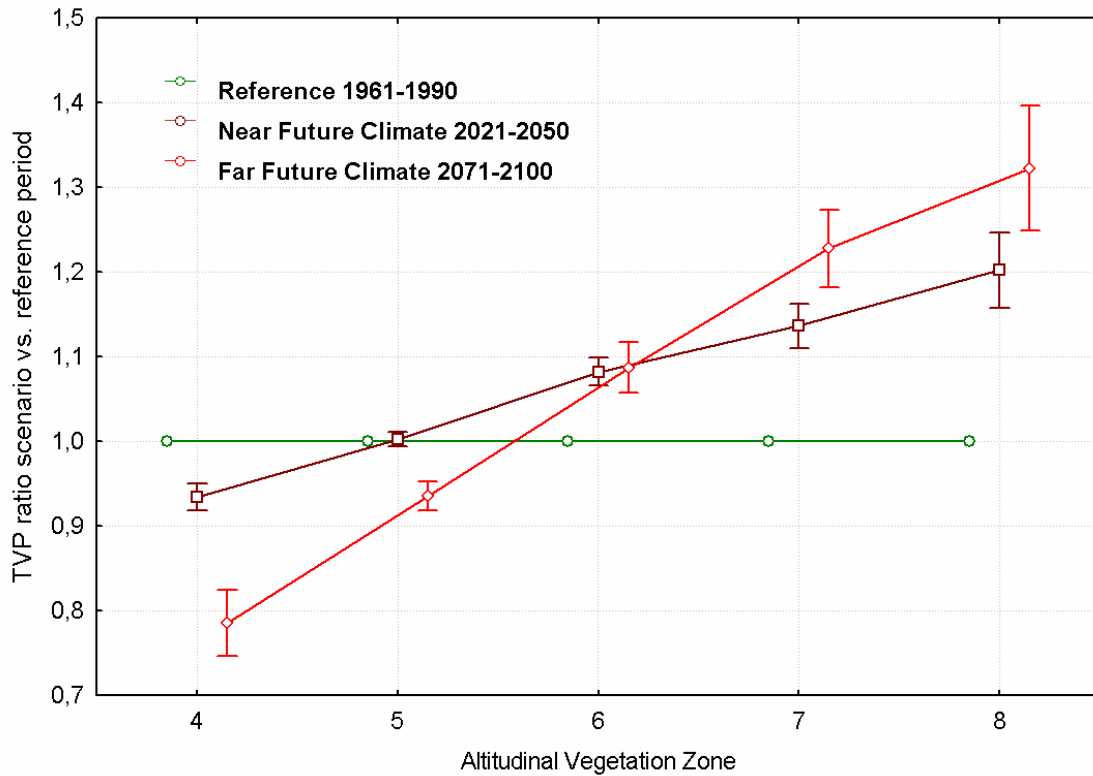


Fig. 3.6 Ratio of spruce total volume production between future and reference time periods within altitudinal vegetation zones.

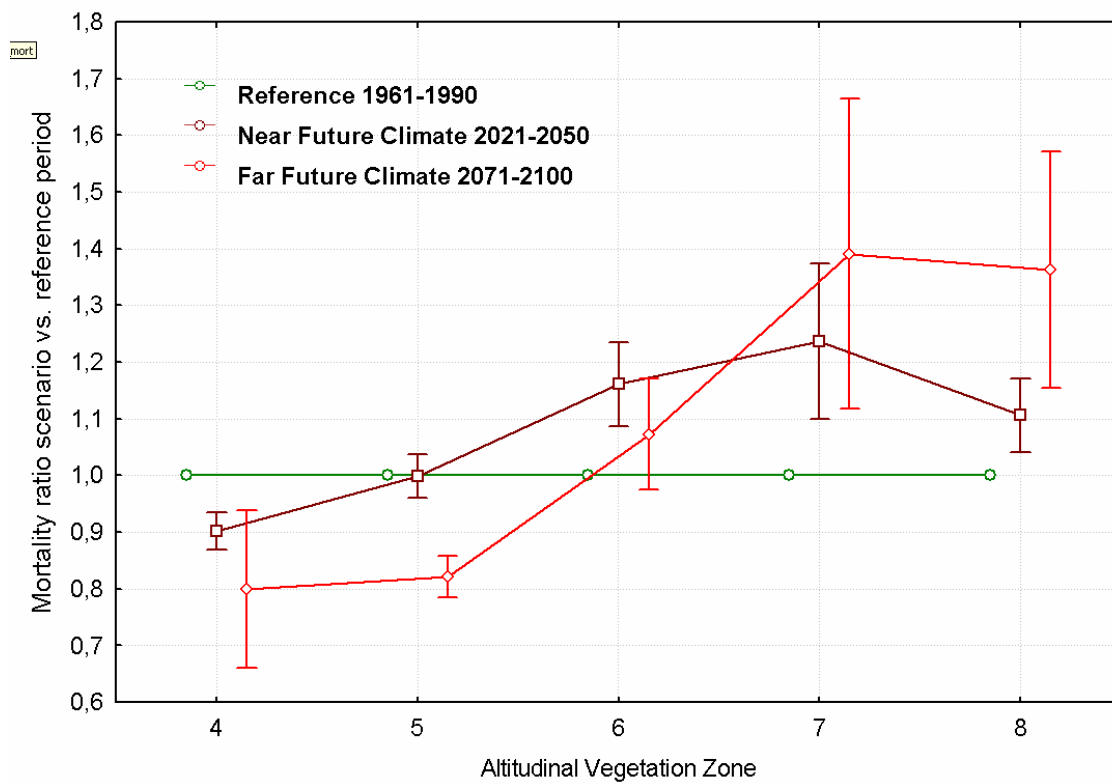


Fig. 3.7 Ratio of spruce cumulative volume of death trees between future and reference time periods within altitudinal vegetation zones.

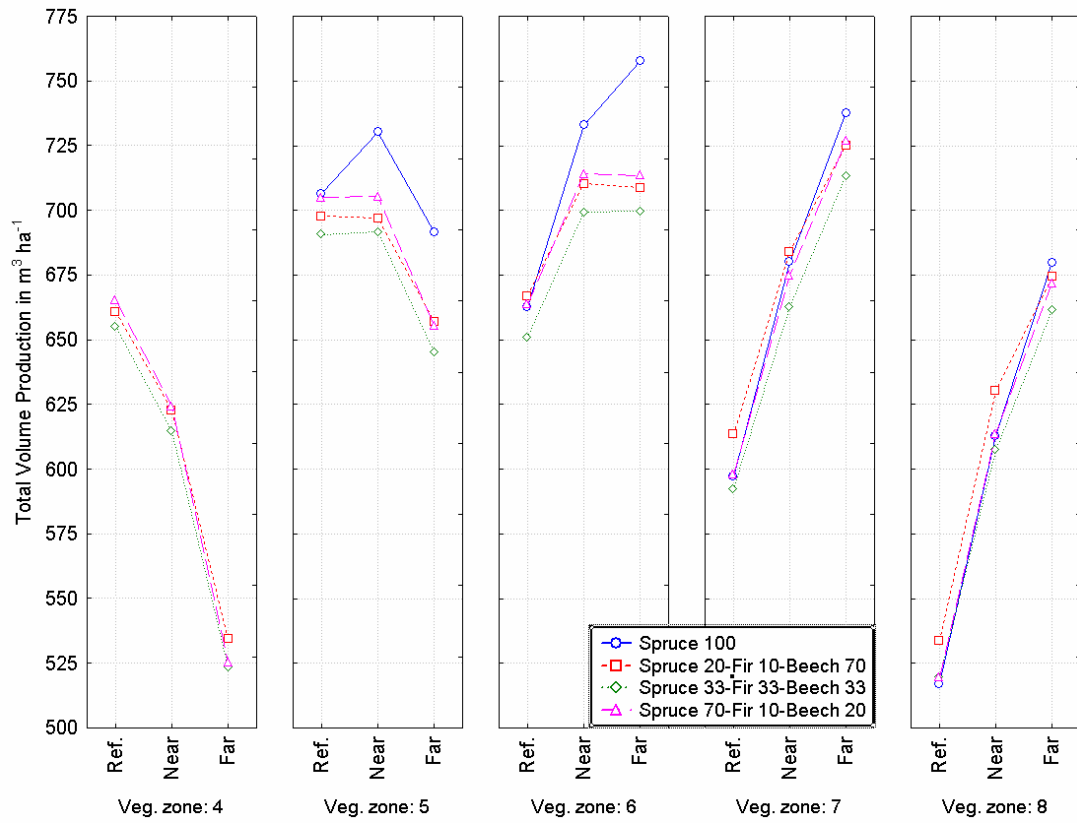


Fig. 3.8 Total volume production in model stands with presence of spruce under reference and future climate

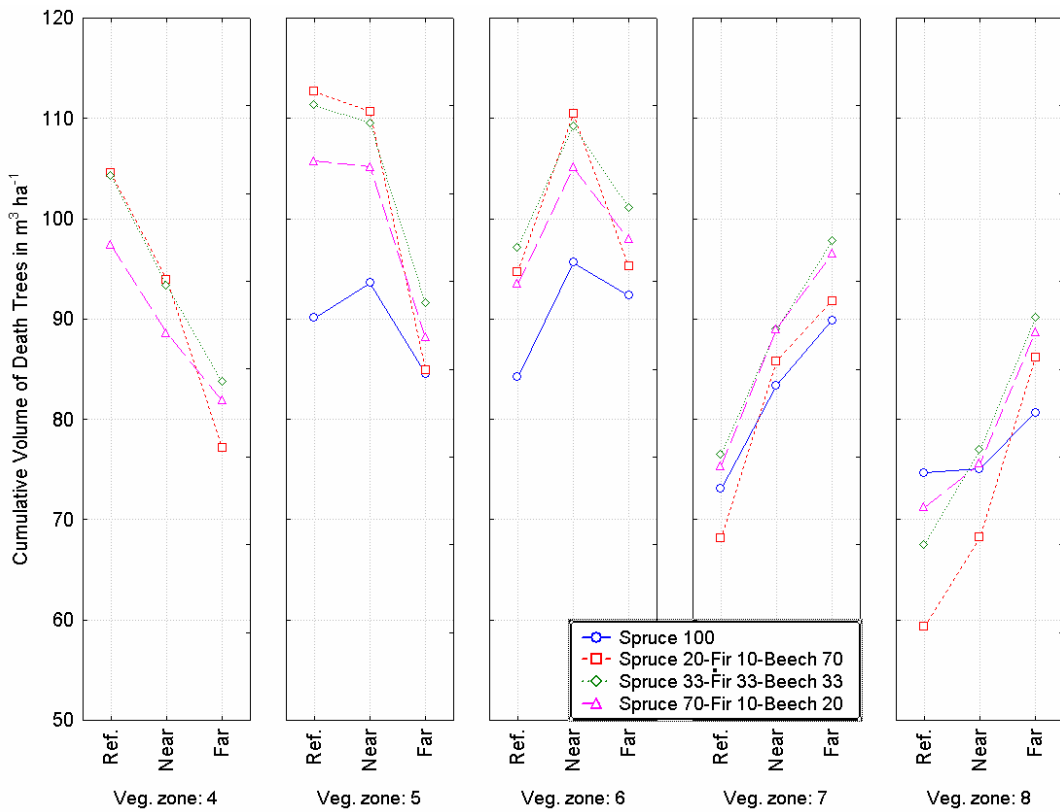


Fig. 3.9 Cumulative volume of death trees in model stands with presence of spruce under reference and future climate

Impact of species composition on spruce production and mortality is not clear at all (Figs. 3-4). The simulations indicate that pure spruce stands in 4-6th AVZ will resist better to projected production decline. In the same time, mortality of such stands was projected to be lower than in the mixed stands. The reason of this is spruce low competitiveness in these AVZs, thus only spruce pure stands can maintain their productivity. Such process is however not sustainable, mainly because of spruce high vulnerability by various disturbances. Similar response as in the 4-6th AVZ was also observed in the higher AVZs (7-8th), although the trend is less pronounced.

Investigation of absolute amounts of TVP ($\text{m}^3 \text{ha}^{-1}$) indicated that production increases in the 7-8th AVZs (spruce, dwarf pine) in the FFC, approaching the production of 5-6th AVZs under the reference climate. In the 5-6th AVZ the production remains stable or even improves. In general, spruce production optimum shifts by one AVZ and spruce stands in 6-7th AVZ will be the most productive. This is particularly true for spruce monocultures. In the same time, spruce mortality in these AVZs remains stable.

3.3.2 Fir (*Abies alba*) sensitivity to climate change

Fir's responses are similar to those of spruce (Figs. 3.10-3.11), although the trends are less intensive (fir's sensitivity to climate change is lower comparing to spruce). Changes of fir's production and mortality are in most cases statistically significant both between AVZs and future vs. reference time periods. Production response function lies in most AVZs above or close to the threshold of the reference period production, thus climate change impact on fir production is more-les positive.

Fir's mortality significantly increases in the NFC in all AVZs except for 4th, which is comparable with the reference. Increase of mortality is in general bigger than increase of increments (except for 8th AVZs). This indicates that ecological stability of fir stands will decline in the future. This is particularly true for the 4-5th AVZ, where increased or stable mortality is not accompanied by increments increase.

Production of pure fir stands and stands with fir admixture is projected to decline in the 4-5th AVZ by 5-15% and rise in the 6-8th AVZ by 5-35%. As in case of spruce, the differences are more significant in the FFC. Differences between future vs. reference time periods are statistically significant in lower (declining) AVZs (4-5th).

In the FFC, fir's vitality (indicated by change in mortality) improves comparing to the reference in its production optimum (4-5th AVZ), while in the 6th -AVZ it is projected to be comparable with the reference. Increase of mortality comparable to the increase of increments was projected in the higher elevations (7-8th AVZ).

Fir's production in the 7-8th AVZ will approach to actually the most productive 5-6th AVZs. This indicates that fir's production optimum shifts by one AVZ, without any negative impact on fir's vitality. This can positively influence forests production at a national scale.

Impact of species composition of fir's production and mortality is not significant (Figs.3.12-3.13). Regardless of beech or spruce prevalence at a stand, fir's responses are almost identical.

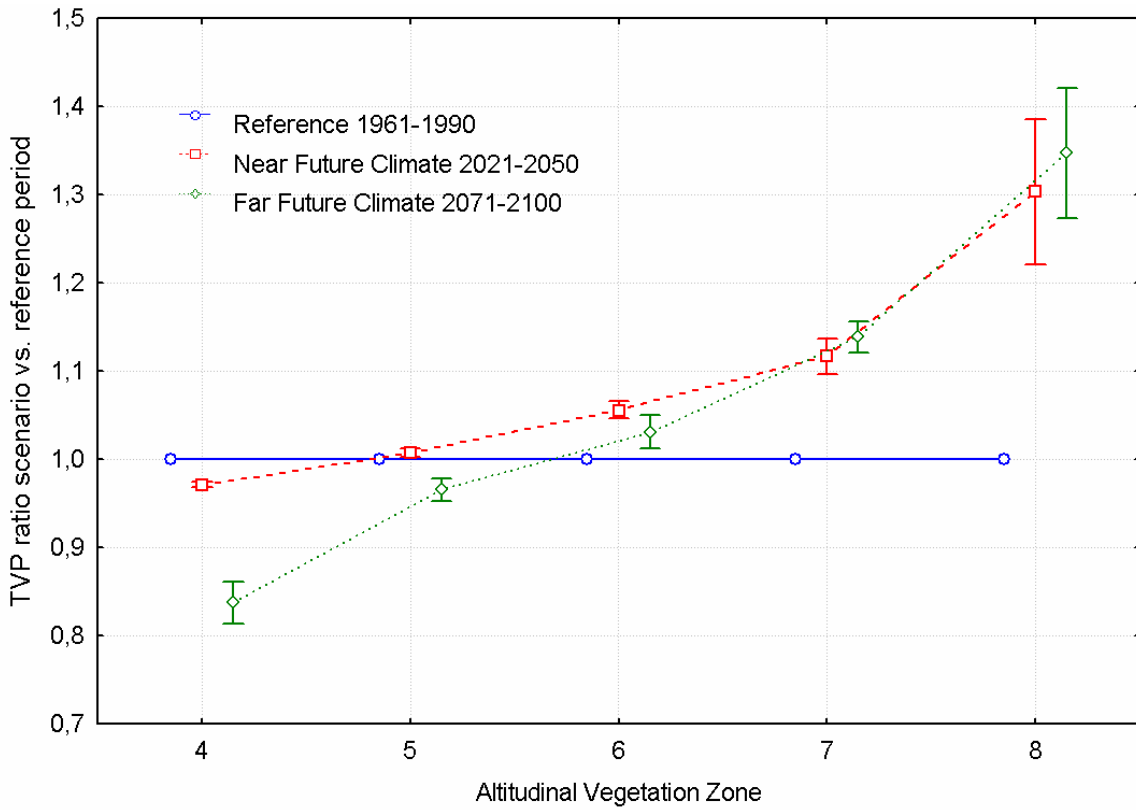


Fig. 3.10 Ratio of fir total volume production between future and reference time periods within altitudinal vegetation zones.

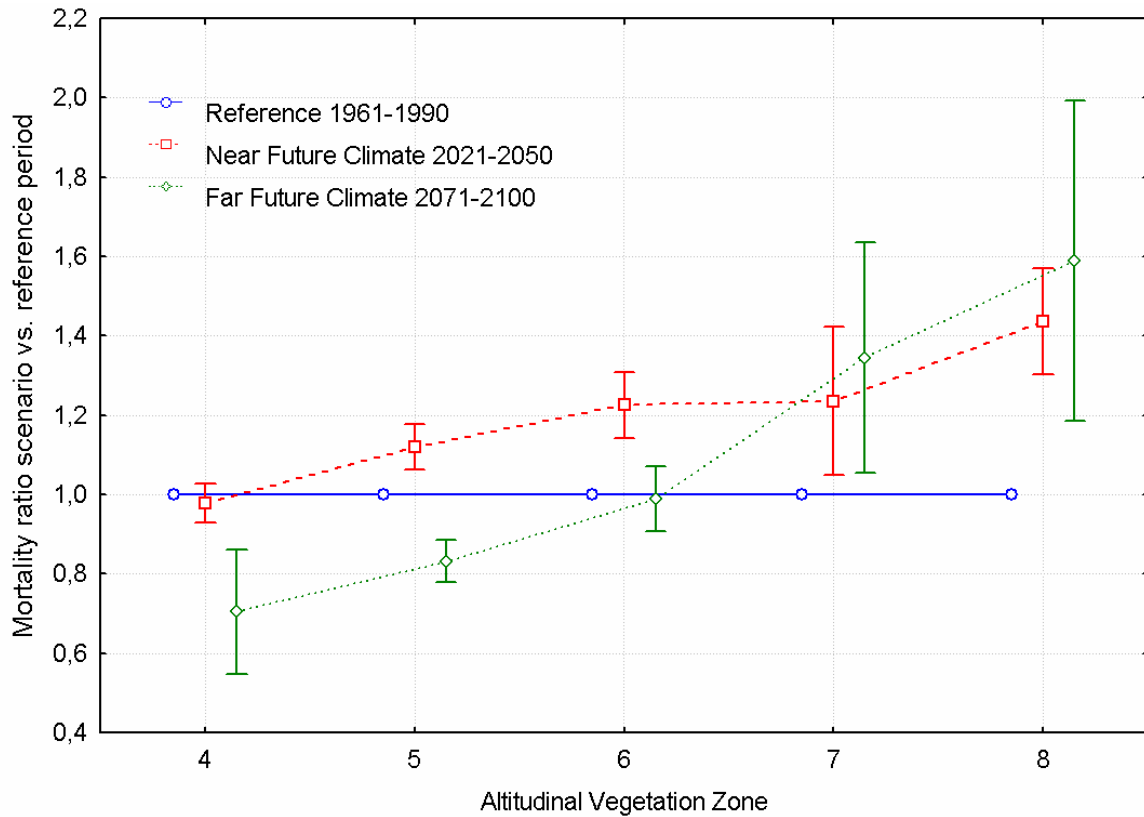


Fig. 3.11 Ratio of fir cumulative volume of death trees between future and reference time periods within altitudinal vegetation zones.

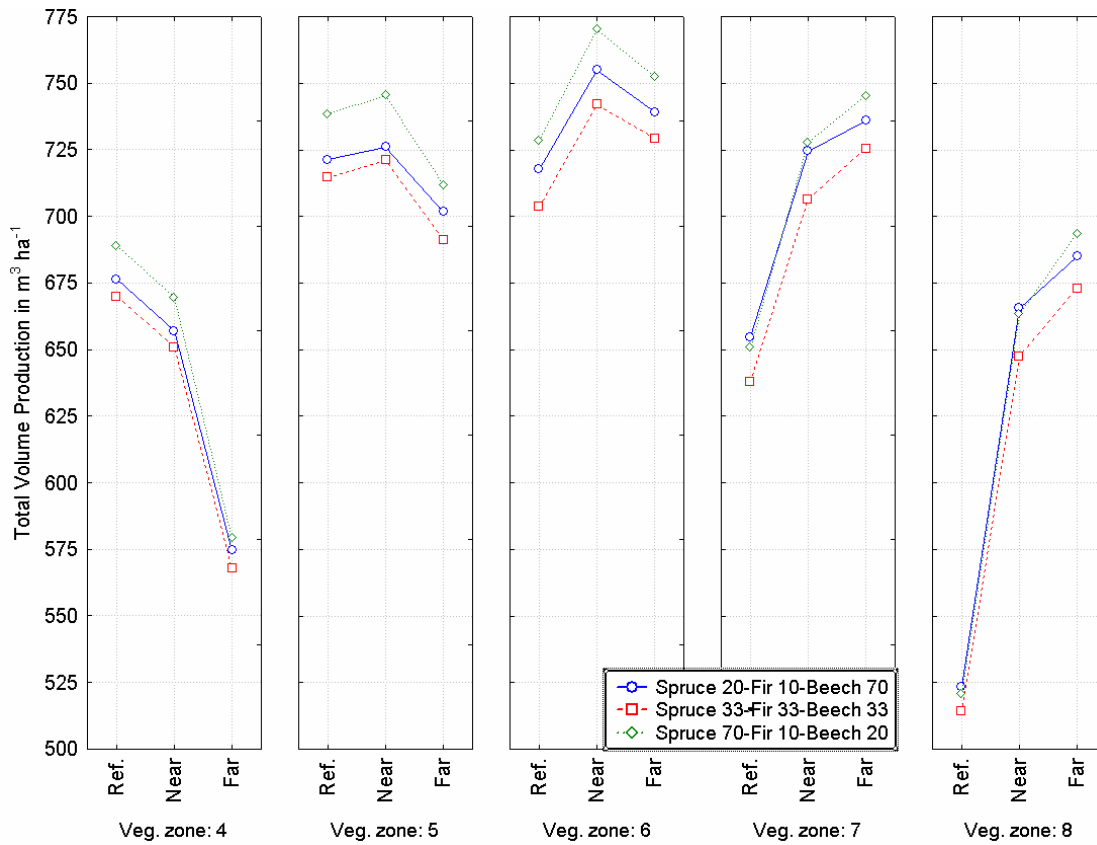


Fig. 3.12 Total volume production of model stands with presence of fir under reference and future climate

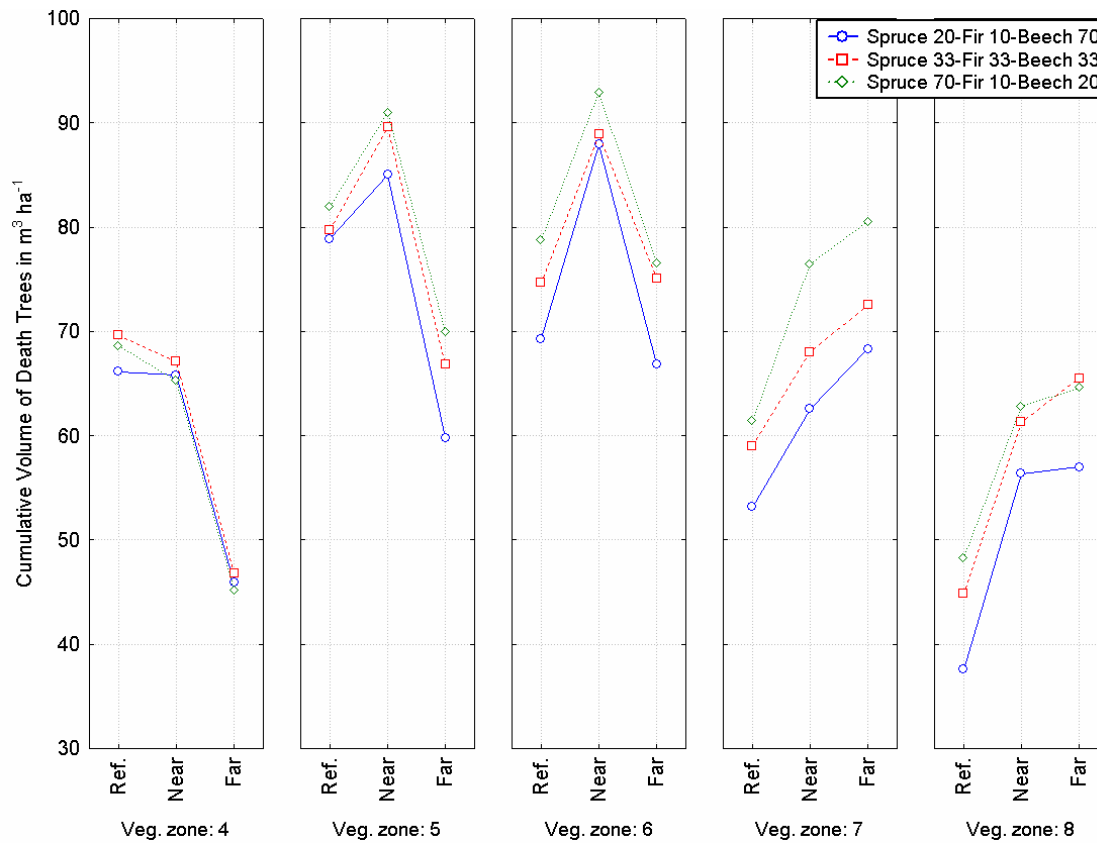


Fig. 3.13 Cumulative volume of death trees in model stands with presence of fir under reference and future climate

3.3.3 Beech (*Fagus sylvatica*) sensitivity to climate change

Beech, as shadow-tolerant species with wide ecological amplitude and flexible increment responses, was found to be the most sensitive tree species to expected climate change. Projected changes in production and mortality are significant between both AVZs and time periods at $\alpha = 5\%$. The response of TVP shows clear and well-interpretable trend. Mortality response is not as clear as in case spruce and fir, thus the proposed interpretations should be considered cautiously (Figs. 3.14-3.15).

Simulations indicate that in the NFC beech production will slightly decline (by 5-10%) in pure and mixed stands of 1st-2nd AVZ, where oak naturally dominates. Production decline will be accompanied by decrease of mortality up to 10%, what indicates development of ecologically relatively stable stands.

Decrease of beech production up to 5% was also projected in the 3rd-5th AVZs (naturally dominated by beech), particularly in nutrient-rich and calcic stands with deeper soils. This is accompanied by statistically significant increase of beech mortality by 5-7%. Such findings indicate potential decrease beech TVP in beech actual production optimum. Ecological stability of beech stands in these AVZs is supposed to decline.

In contrast, production of pure and mixed beech stands was projected to increase in the 6-8th AVZs (outside actual production optimum) by 10-30%. In the same time, statistically significant decrease of beech mortality by 5-15% was projected. This indicates improvement of ecological stability of beech stands in the in the higher elevations as well as shift of beech production optimum. Improved production in 6-7th AVZs could partially compensate production decline in beech actual production optimum.

Described tendencies remain similar in the FFC, however much more intensive. Beech productivity declines in 1st-2nd AVZs by 30-40%. Production significantly declines also in beech actual ecological optimum (3rd-5th AVZs) by 5-35%. This could have significant impact on total biomass of Slovak forests with more than 30% share of beech.

Negative development of beech mortality is much more pronounced in the FFC. Fig. 3.15 describes significant increase of mortality in 1st-6th AVZs (20-45%), with peak in actually the most productive 3rd-4th AVZs.

Intensive increase of beech mortality and production decline in the FFC could result in critical reduction of growing stock, potentially leading to local forest decline. In contrast, absence of any biotic disturbance acting as beech's primary mortality agent make beech perspective tree species, mainly in higher AVZs (6-8th).

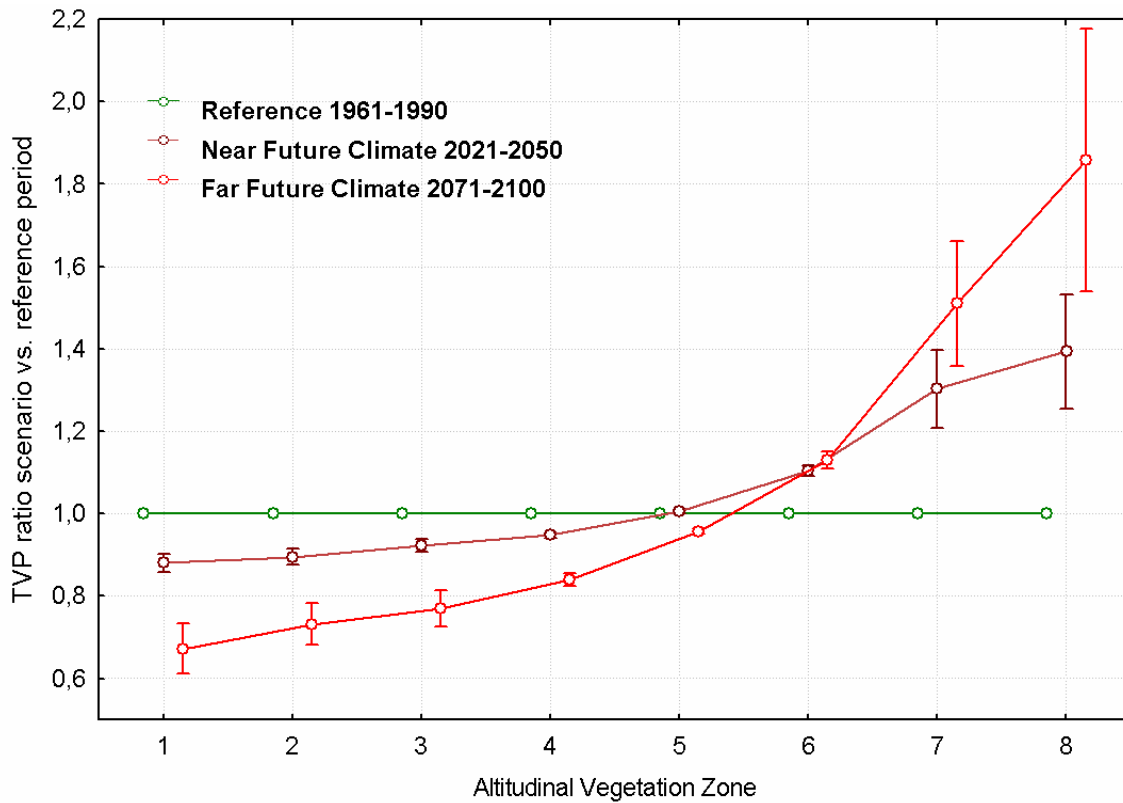


Fig. 3.14 Ratio of beech total volume production between future and reference time periods within altitudinal vegetation zones.

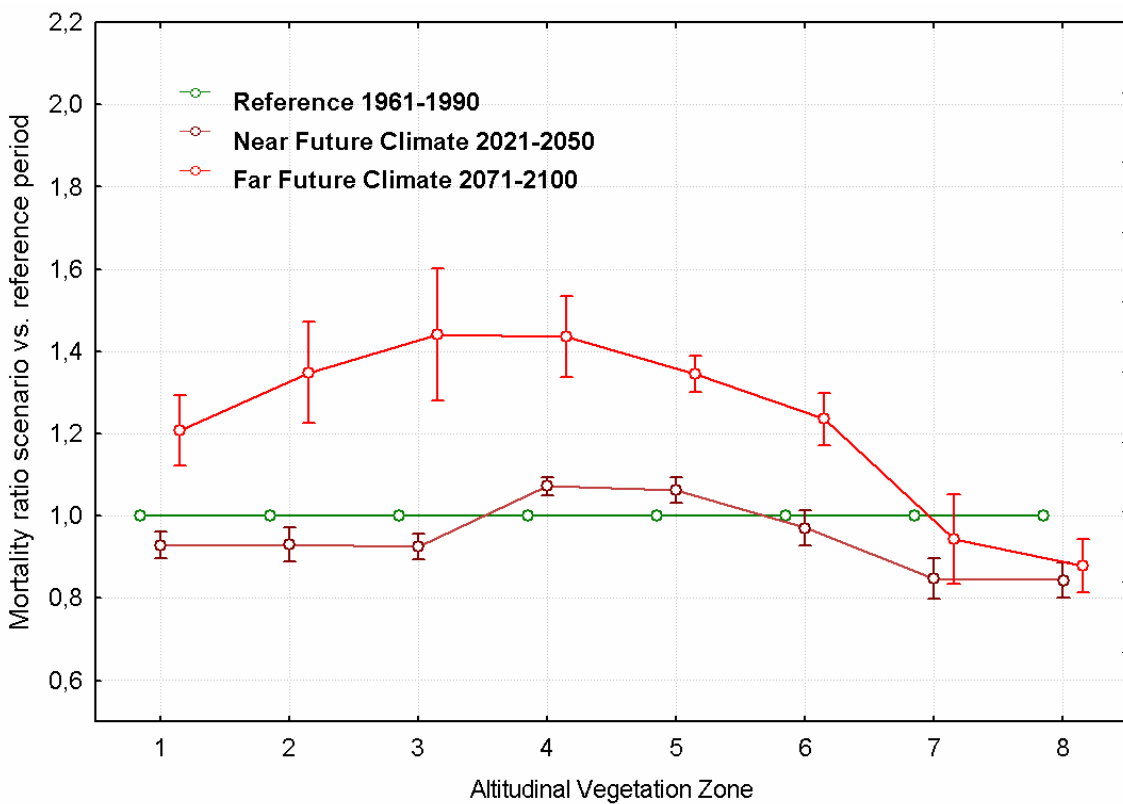


Fig. 3.15 Ratio of beech cumulative volume of death trees between future and reference time periods within altitudinal vegetation zones.

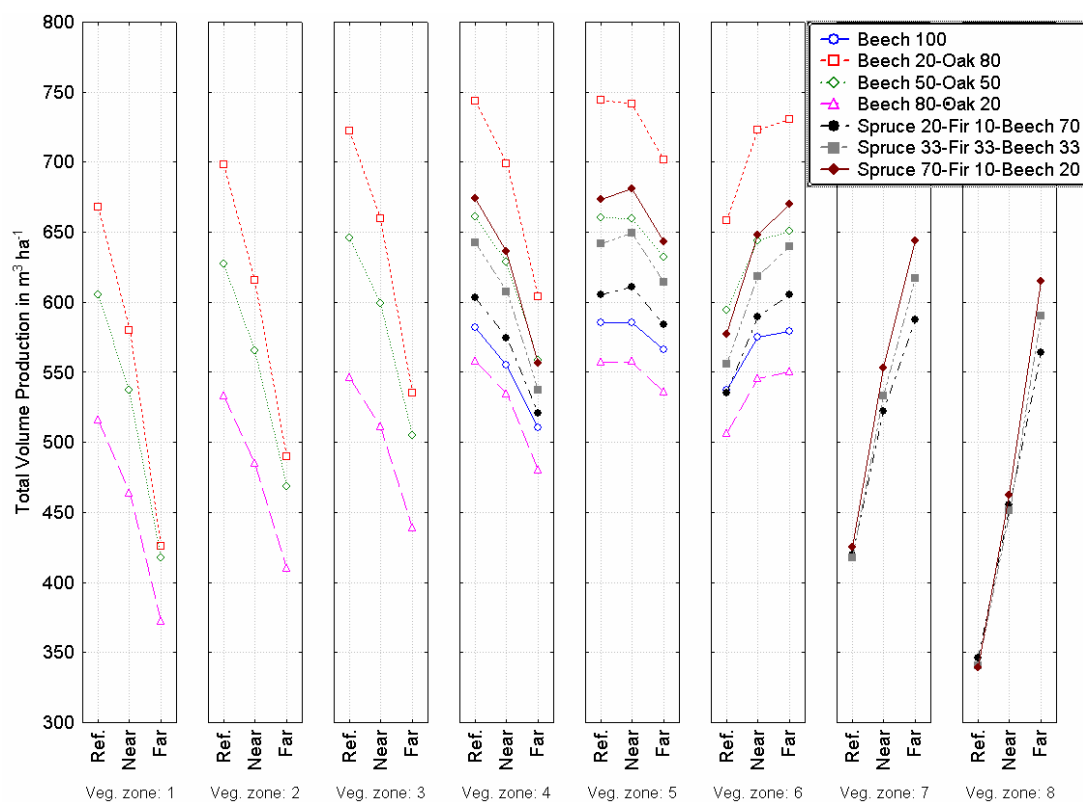


Fig. 3.16 Total volume production in model stands with presence of beech under reference and future climate

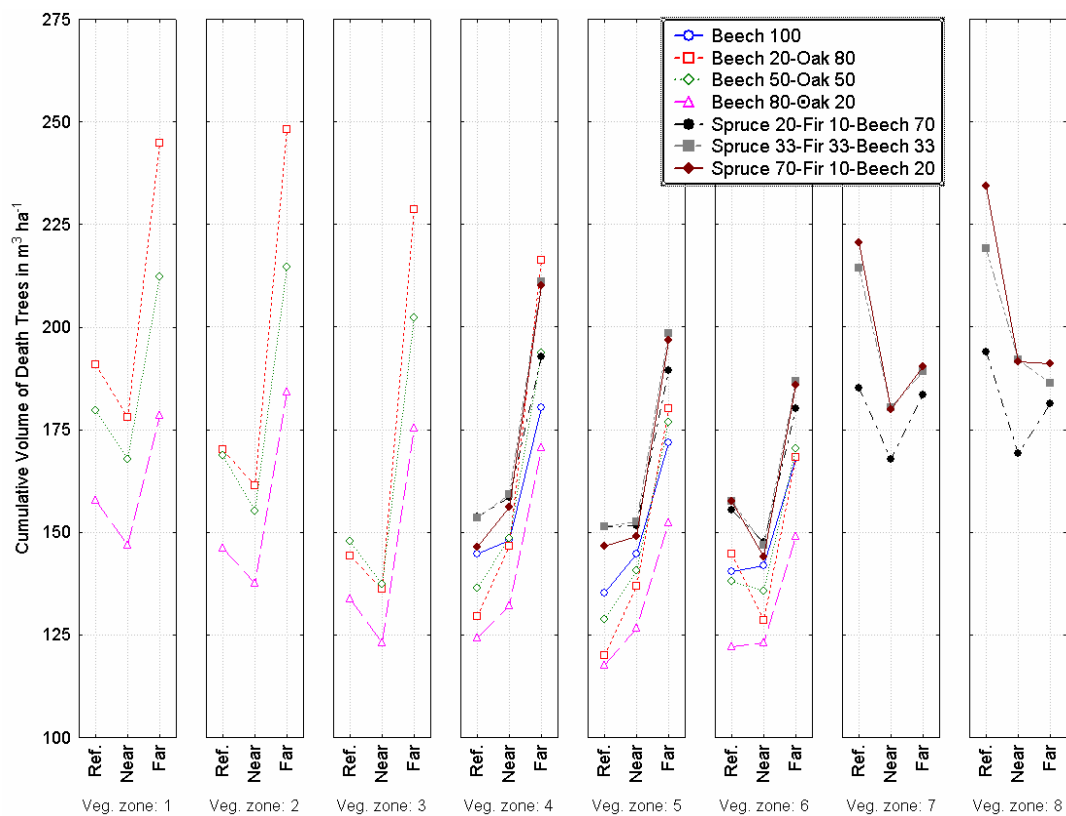


Fig. 3.17 Cumulative volume of death trees in model stands with presence of beech under reference and future climate

Described tendencies can be, in a limited way, compensated by rising production in the 6-8th AVZs (50-75%) accompanied by 5-15% decrease of mortality.

However, such development in the AVZs naturally dominated by coniferous (beech forms mostly a minor admixture of coniferous stands) is not likely to compensate production decline in the lower elevations. In addition, site conditions, such as oligotrophic and shallow soils of the higher elevation are not suitable for beech growth at all.

Impact of species composition on beech production in the 1st-4th AVZs indicates that beech production in mixed beech–oak stands improves, comparing to pure beech stands (Figs. 3.16-3.17). The reason of this is probably high competitiveness of oak in these AVZs. Simulations indicate that in the 5-6th AVZs, beech production improves in mixed stands and such tendency remains to the future. This fact is remarkable mainly in the 6th AVZ. As far as impact of admixture of various tree species, the production was mainly improved by presence of oak followed by coniferous. Such positive effect is evident in stands where beech act as the admixture species rather than the main species, particularly in 7-8th AVZs.

3.3.4 Oak (*Quercus* sp.) sensitivity to climate change

Simulations indicated low sensitivity of oak to climate change in both future time periods (Figs. 3.18-3.19). Despite this, production response function is similar to that of previous investigated species, however it rises up only in the elevations at upper distributional limit of oak. Changes in productivity and natural mortality of pure and mixed oak stands along the AVZs and between future vs. reference time periods in the actual distributional range of oak (1st-4th AVZ) do not exceed $\pm 3\%$, in most cases statistically not significant at $\alpha = 5\%$.

Increase of oak productivity by 2-8%, keeping the mortality unchanged, was projected in the higher AVZ (5-6th) at the upper distributional limit of oak in Slovakia.

Slight decline of productivity of pure oak stands accompanied by increase of mortality was projected in the 1st-4th AVZs, while in the oak-beech stands such trend is in contrary to this. This indicates positive effect of maintaining mixed oak-beech stands, which are supposed to be more productive. In addition, oak's productivity 5-6th AVZs was projected to be equal to 1-4th AVZs, thereby slightly increasing the forest biomass in the elevations above 500 m a.s.l. (Figs. 3.20-3.21).

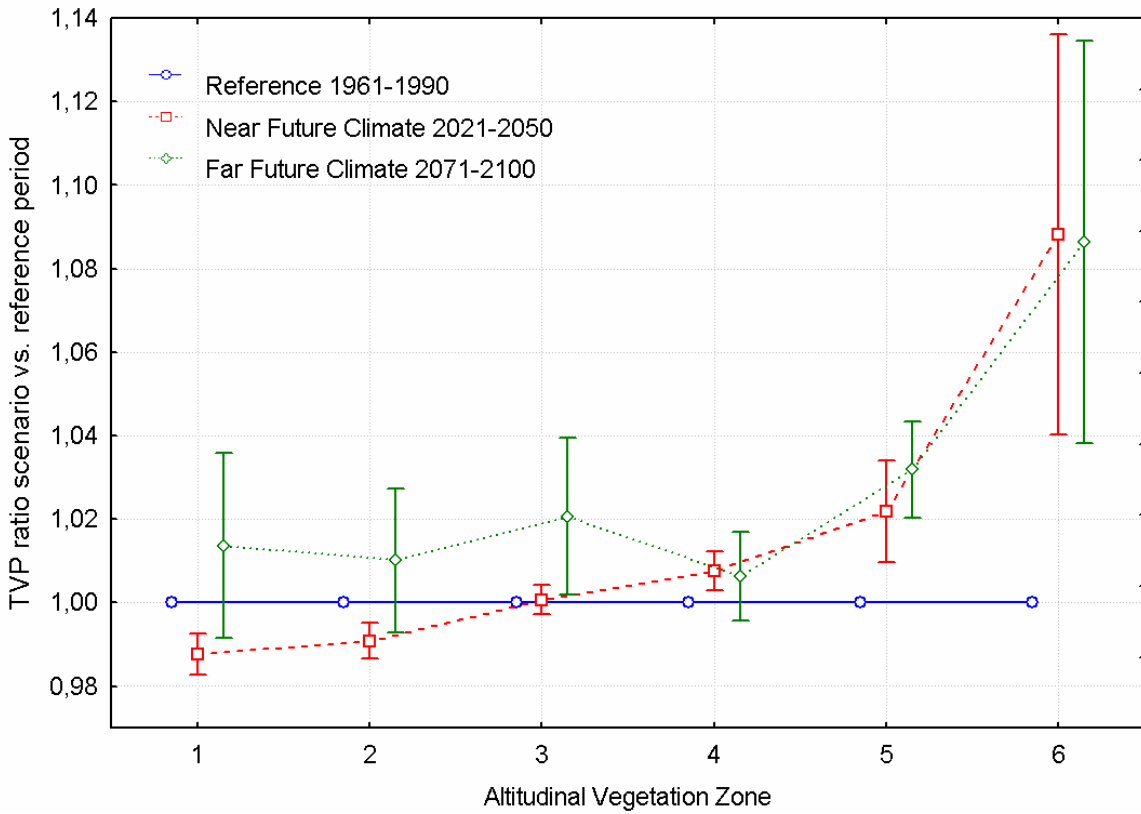


Fig. 3.18 Ratio of oak total volume production between future and reference time periods within altitudinal vegetation zones.

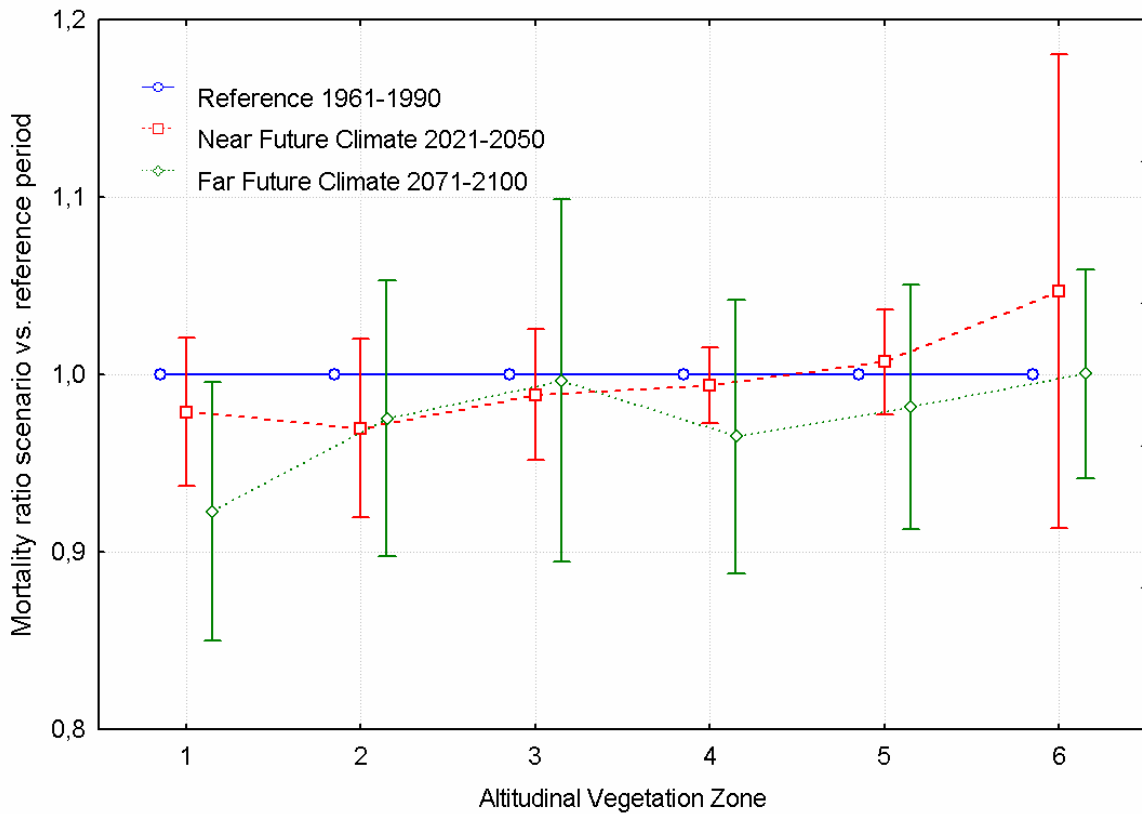


Fig. 3.19 Ratio of oak cumulative volume of death trees between future and reference time periods within altitudinal vegetation zones.

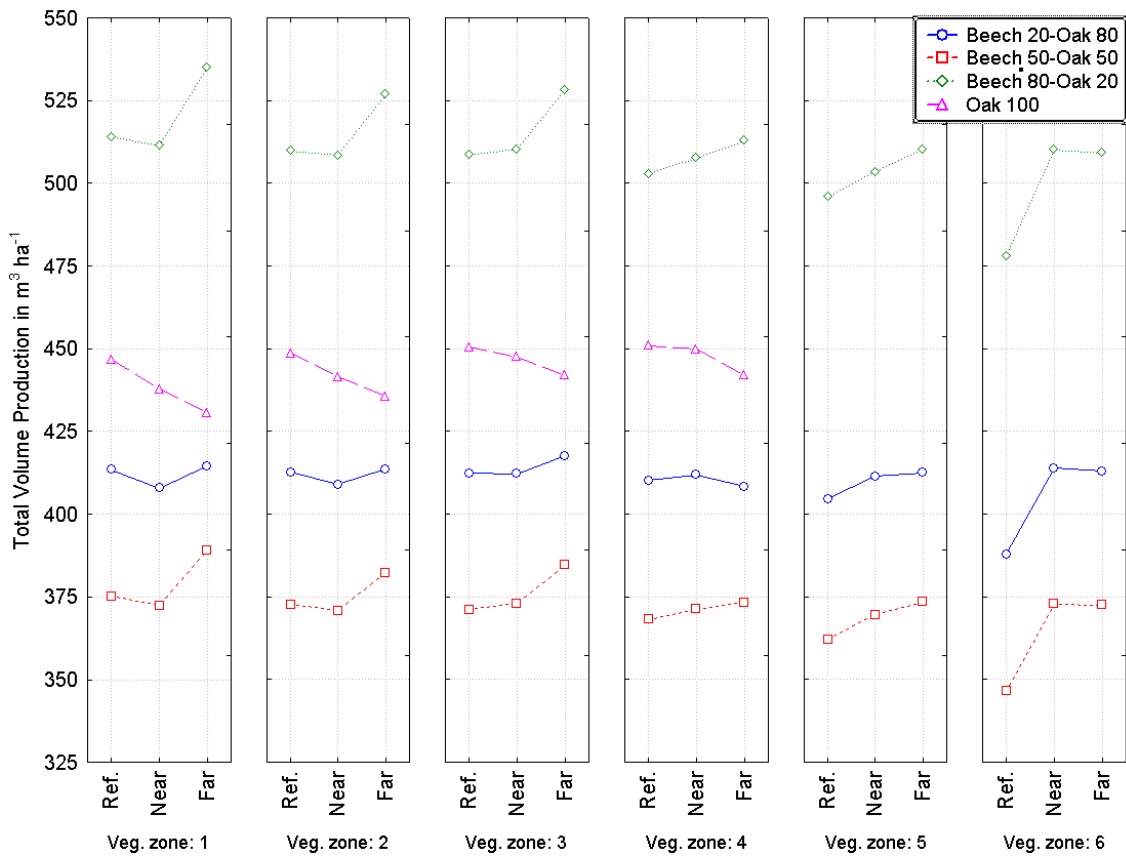


Fig. 3.20 Total volume production in model stands with presence of oak under reference and future climate

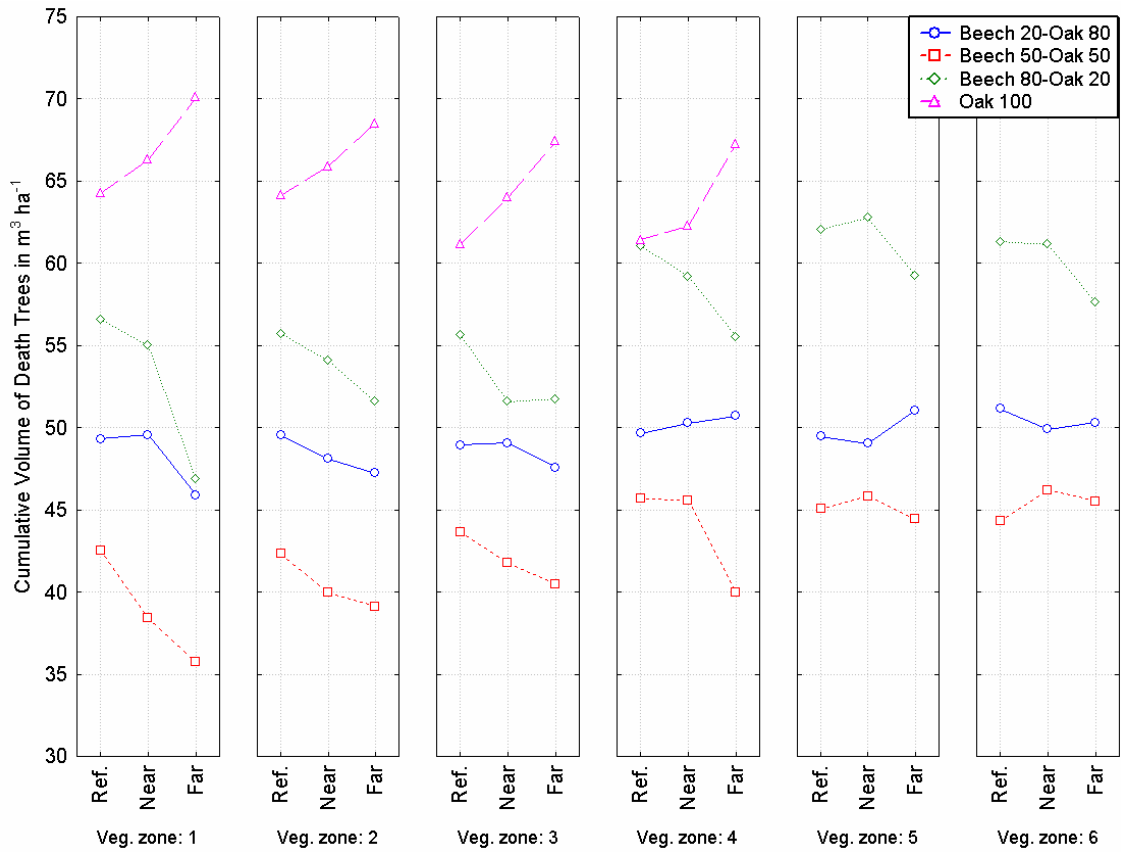


Fig. 3.21 Cumulative volume of death trees in model stands with presence of oak under reference and future climate

3.4 Conclusions

Analysis of forest tree species responses to climate change indicated clear and interpretable trend in production, which intensity and shape differed between species. In general, production declines in the lower elevations up to a certain extent and improves along the elevation gradient. The main differences are between the intensity of such response and position of point where such response function passes through the production threshold reached under the reference climate. Mortality responses differ between species, i.e. mortality either increases or decreases along the elevation gradient. In addition, the magnitude of change differs between near and far future climate. Thus the interpretation of climate change impacts on forest trees production and natural mortality is based on the relations between the production and mortality response functions.

To the future, oak (*Quercus sp.*) is very promising forest tree species, with low sensitivity to projected changes of climate. Changed climate in higher elevations allows for oak's expansion to lower mountain regions being limited mainly by soil parameters and competition of coniferous. Projected changes of productivity in oak's current production optimum are negligible, and ecological stability (indicated by changes in mortality) will either remain at the reference level or improve. Oak will probably expand to 5-6th AVZ, especially in nutrient-rich stands, where it is supposed to form, in an increased rate, mixtures with coniferous. Such mixed stands can be found in these elevations also at present, but they are mostly not formed naturally. Risk from biotic pests should not be considered at present (except for periodic defoliations by Gypsy moth, Deliverable 6.7), anyway monitoring systems of newly established pest should be developed.

Productivity and mortality of pure and mixed beech stands is projected to significantly change in the future. Beech in the 1st-2nd AVZs and in its actual production optimum (3rd-4th AVZ) is projected to suffer from significantly increased natural mortality accompanied by reduced production. Especially 3rd and 4th AVZs, i.e. the zones of beech natural dominance, are supposed to undergo in the next 40-70 years an intensive reduction of beech abundance. Beech is supposed to better resist the climate change in compositions with higher share of beech, probably because of high competition of other tree species (mainly of oak, which productions optimum shifts to 5th or even 6th AVZ). In the higher elevations, beech will be faced to increased competitiveness of coniferous. Projected decrease of beech abundance in 1st-5th AVZ (indicated by increased mortality of beech in mixed stands) to the favor of less productive oak; and increased mortality of beech in vast areas of 3rd and 4th AVZ could negatively impact the total forest biomass in Slovakia.

Spruce and fir were found to be the most sensitive species to climate change. Spruce and fir production in both pure and mixed stands in the higher elevations will rise, being accompanied by stable or even increased mortality. To the contrary, in the lower elevations (4-5th AVZ) the production is projected to decline (more intensively in case of fir). Both species will better resist to competition of broadleaved in stands with spruce and fir prevalence. In fact, expected increased pressure of bark beetle makes older pure spruce stands extremely vulnerable, therefore such knowledge has a very limited use for practical forest management. Intensive increase of fir and spruce production in the 8th AVZ indicates the shift of upper tree line into higher elevations, further being limited by soil parameters. Increased productivity of physiologically highly productive coniferous, but also of beech in 6th and 7th AVZ, can have significant positive impact on the total forest biomass in Slovakia.

4 AGRICULTURE – THE SLOVAK REPUBLIC

4.1 Introduction

Evaluated crops: winter wheat
spring barley
corn maize

Region: Western Slovakia

Subregions: Danubian lowland
Záhorie lowland

Soils:

Regions	Soil type	Classification
Danubian lowland	Loamy	Chernozems
	Loamy	Fluvisol
	Loamy	Luvisol
Záhorie lowland	Sandy loam	Mollic Fluvisol
	Sandy loam	Regosol

Time slices: 1971 - 2000 – Reference period of years
2021 – 2050
2071 - 2100

CO₂ concentration: SRES A1B (IPCC, 2007)

Simulation crop model: DAISY

Evaluation of the climate change impacts on soil water regime under field crops was based on simulations by agro-ecological model DAISY. DAISY is a one-dimensional model simulating water, energy, nitrogen and soil organic matter balance. Crop development and yield is possible to simulate in dependence on crop rotation and various management strategy. DAISY simulates plant growth and development, including the accumulation of dry matter and nitrogen content in different plant parts. The main plant-growth processes considered in DAISY are photosynthesis, respiration, partitioning of assimilates, stress factors and leaf and root development. DAISY allows for building complex management scenarios (Hansen et al. 1990; Hansen 2000).

4.1.1 Sensitivity of field crop yields with respect to agro-climatic conditions

Sensitivity of yields was evaluated comparing average and 90% probability (percentile) of grain yields in period of years 1971-2000 (Fig. 3.22).

Variability of spring barley, winter wheat, and maize grain yields are influenced first of all by availability of soil water. The highest yields are simulated in regions of Žitný Ostrov (except for shallow soils on gravels) and nearby rivers Nitra, Váh and Hron. Range of yields in regions with available water in soil profile are relatively small (green areas on both right and left figures). We can find in these regions also the most fertile soils of Slovakia.

On the other hand the high variability of yield we can find on sandy loams, luvisols and fluvisol of whole western Slovakia. Shortage of precipitation in some years make sandy soils very vulnerable especially in northern part of the region. Seasonal distribution of rainfall significantly influence variability of field crops yields on shallows and sandy soils.

Winter wheat rooting system is better prepared for occurrence of drought during growing season and so grain yields vary less the yields of winter barley. Especially during ripening transport of assimilates is blocked due to very high temperatures and shortage of water in June. Average winter wheat yields exceed $5,5 \text{ t}\cdot\text{ha}^{-1}$ on the most of the evaluated territory and 90% probability of winter wheat grain yields is more than $4,5 \text{ t}\cdot\text{ha}^{-1}$.

Average spring barley yields are higher than $4,5 \text{ t}\cdot\text{ha}^{-1}$ on the most of the evaluated territory and 90% probability of winter wheat grain yields is more than $3,5 \text{ t}\cdot\text{ha}^{-1}$.

Corn maize is very often considered as a perspective plant due to resistance on drought in agro-climatic conditions of Slovakia. Average corn maize yields are higher than $7,5 \text{ t}\cdot\text{ha}^{-1}$ on the most of the evaluated territory and 90% probability of winter wheat grain yields is more than $5,5 \text{ t}\cdot\text{ha}^{-1}$.

Fig. 3.22 A, Winter wheat

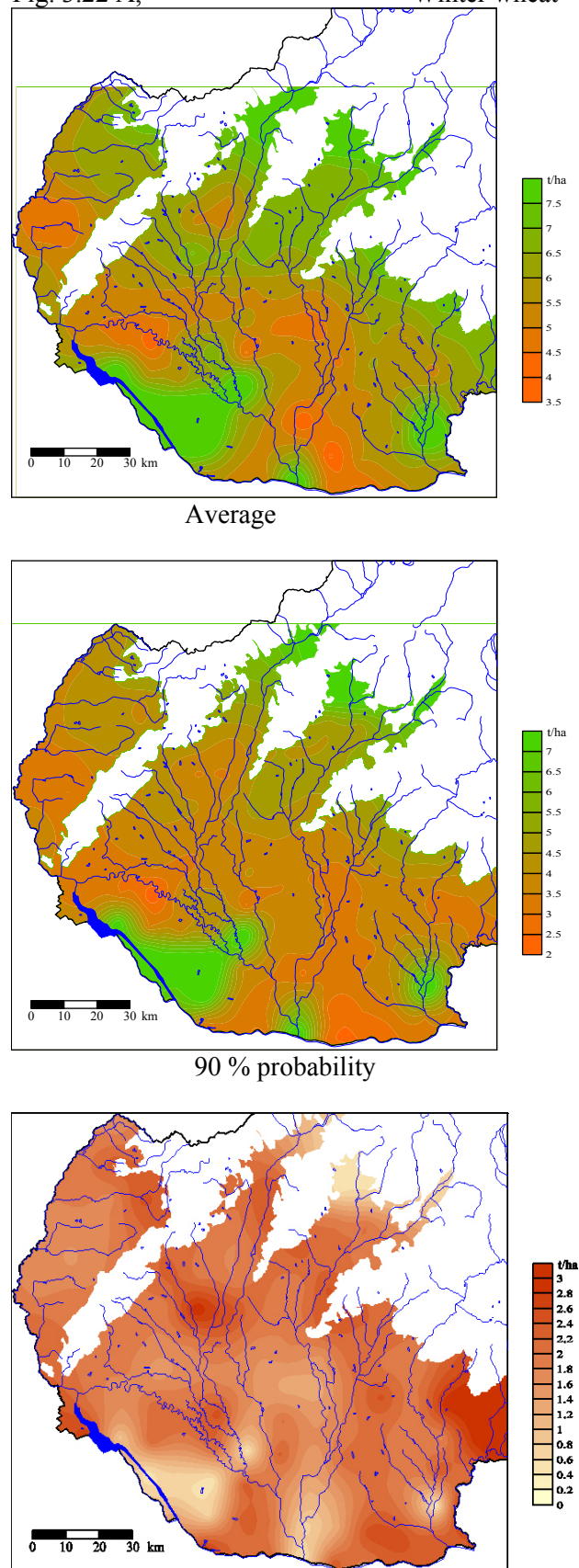
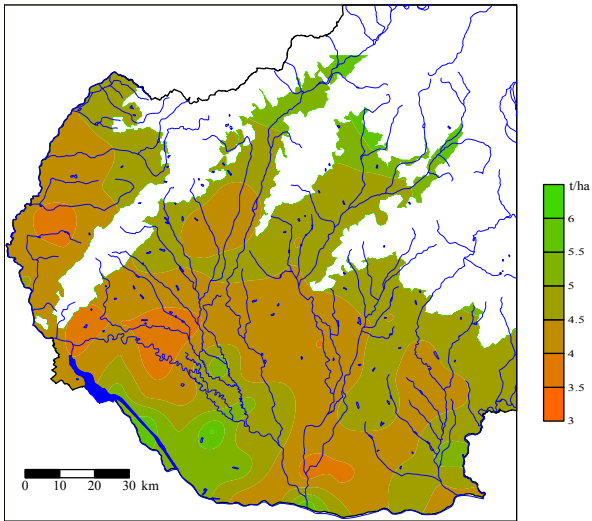


Fig. 3.22 Spatial distribution of field crops in Western Slovakia - reference period of years 1971-1990

Difference (AVG-90%)

Fig. 3.22 B,

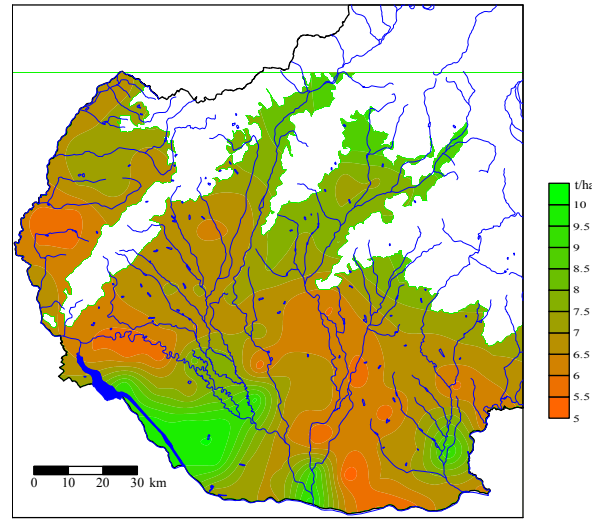
Spring barley



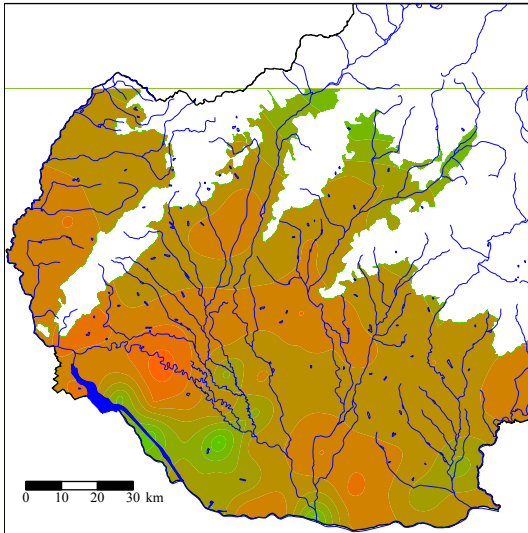
Average

Fig. 3.22C,

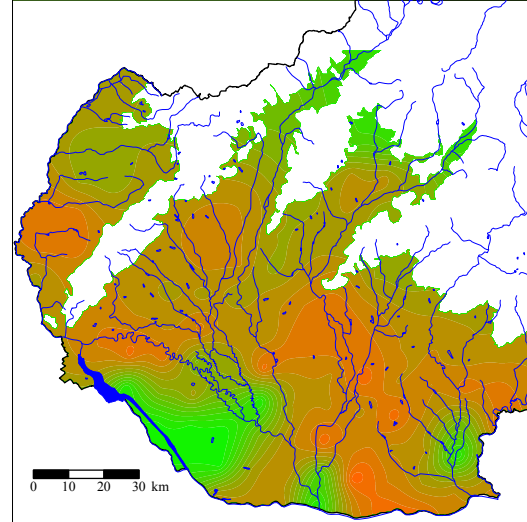
Corn maize



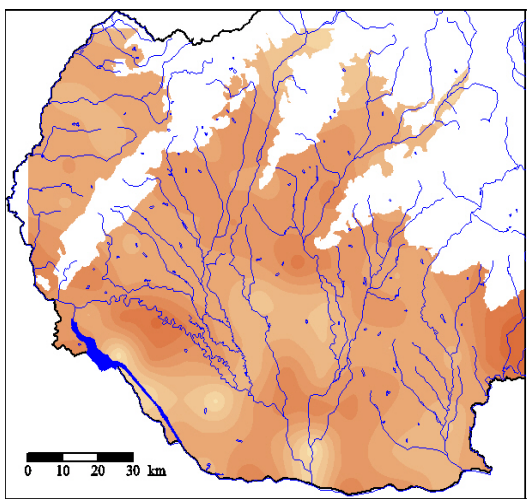
Average



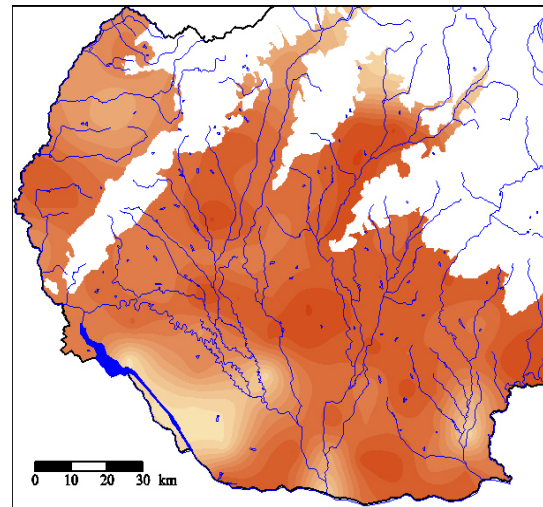
probability90%



90 % probability



Difference (AVG-90%)

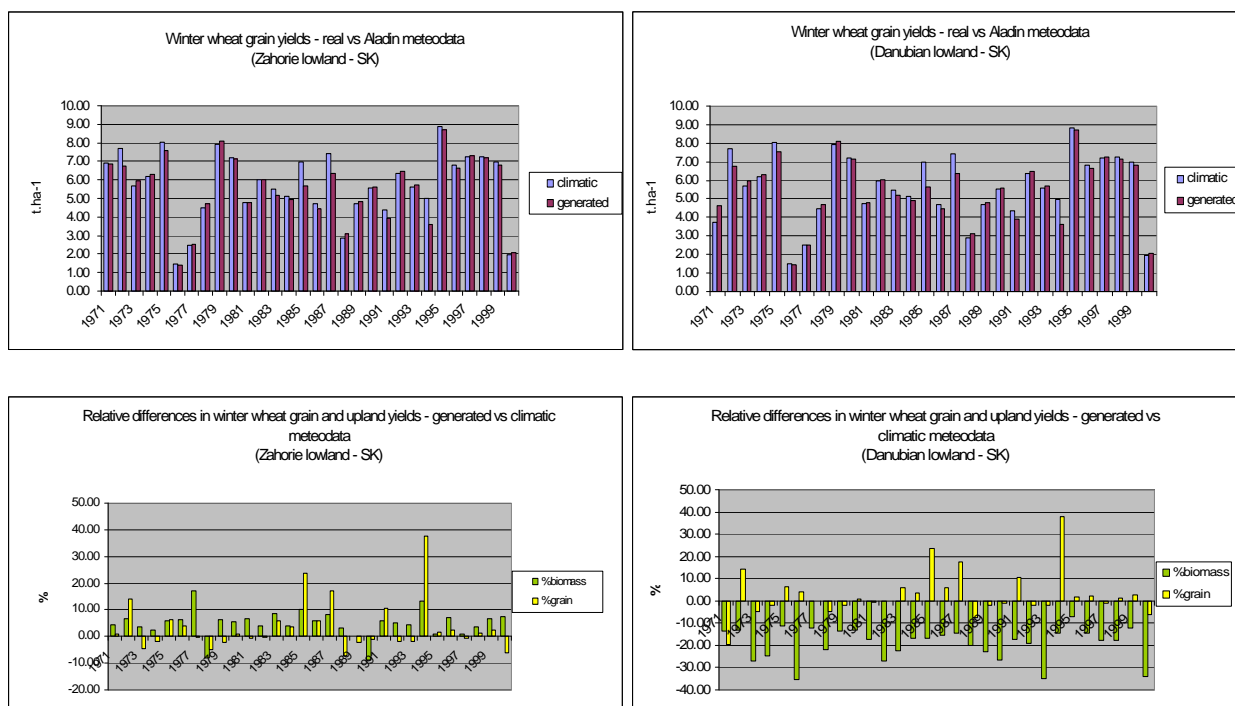


Difference (AVG-90%)

4.1.2 Sensitivity of field crop yields with respect to meteorological datasets

Variability of field crops yields were evaluated separately in Záhorie and Danubian Lowland. Yields were simulated with two different climatic datasets for the period of 1971-2000: data generated by Aladin model and with measured climatic data characteristic for the particular locality.

Fig. 3.23 Winter wheat grain yields and their deviations simulated according to generated and measured climatic data for Danubian lowland (grid 4522 vs. meteodata for Hurbanovo – left) and Záhorie lowland, (grid 5252 – vs. meteodata for Bratislava- right) - datasets in years 1971-2000

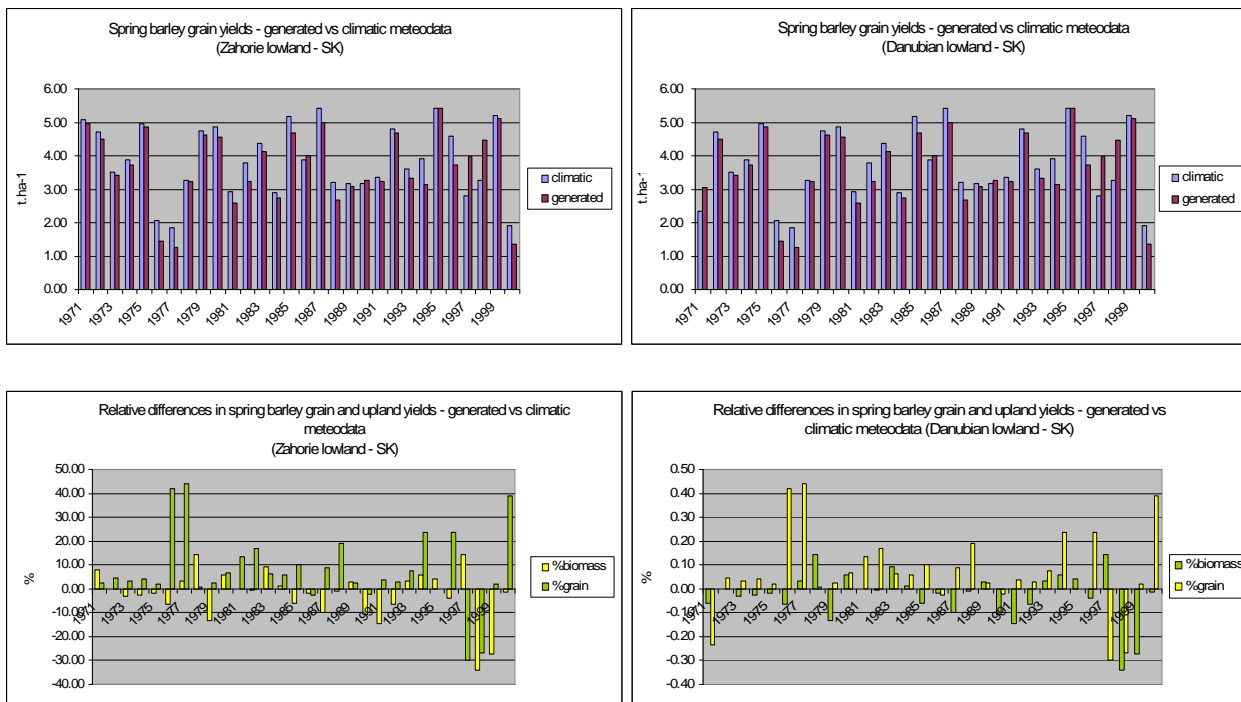


Winter wheat	Harvest	Generated [t.ha ⁻¹]		Measured [t.ha ⁻¹]		Δ [t.ha ⁻¹]		Δ [%]	
		grain	upland biomass	grain	upland biomass	grain	upland biomass	grain	upland biomass
Záhorie lowland	26.7	5.55	11.70	5.73	12.26	-0.18	-0.56	-3.41	-4.93
Danubian lowland	25.7	5.93	12.89	4.59	10.55	1.34	2.34	24.69	19.16

Tab. 3.3 Comparison of simulated winter wheat yields according to generated (Aladin) and climatic data for Danubian lowland (grid 4522 vs. meteodata for Hurbanovo,) and Záhorie lowland, (grid 5252 – vs Bratislava) - datasets in years 1971-2000

Winter wheat yields in Záhorie and Danubian Lowlands were simulated with two different climatic datasets for the period of 1971-2000: data generated by Aladin model and with measured climatic data characteristic for the particular locality. As seen from the results (Fig. 3.23, Table 3.3), model with generated data overestimates grain as well as upland biomass yields of winter wheat in Danubian Lowland (+24.69 % in grain and +19.16 % in upland biomass yields). On the other hand, model with generated data underestimates both grain and upland biomass winter wheat yields in Záhorie Lowland in comparison with usage of measured data (-3.41 % in grain and -4.93 % in upland biomass yields).

Fig. 3.24 Spring barley grain yields and their deviations simulated according to generated and measured climatic data for Danubian lowland (grid 4522 vs. meteodata for Hurbanovo – left) and Záhorie lowland, (grid 5252 – vs. meteodata for Bratislava- right) - datasets in years 1971-2000



Spring barley	Harvest	Generated [t.ha ⁻¹]		Measured [t.ha ⁻¹]		Δ [t.ha ⁻¹]		Δ [%]	
		grain	upland biomass	grain	upland biomass	grain	upland biomass	grain	upland biomass
		Záhorie lowland	12.7	3.68	8.36	3.86	8.12	-0.18	0.24
Danubian lowland	11.7	3.54	8.26	3.20	7.24	0.34	1.02	13.07	13.45

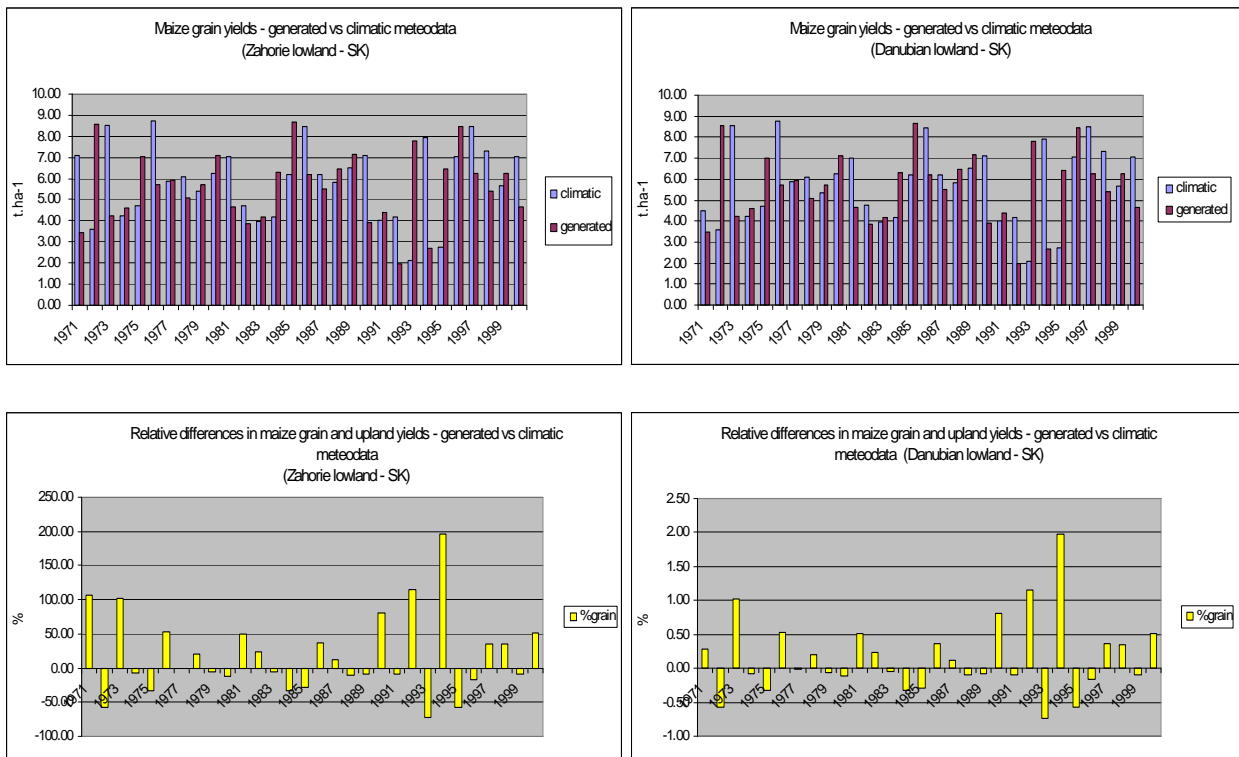
Tab. 3.4 Comparison of simulated spring barley yields according to generated (Aladin) and climatic data for Danubian lowland (grid 4522 vs. meteodata for Hurbanovo,) and Záhorie lowland, (grid 5252 – vs Bratislava) - datasets in years 1971-2000

Spring barley yields in Záhorie and Danubian Lowlands were also simulated with two different climatic datasets for the period of 1971-2000 and the yields were finally compared (Fig. 3.24, Tab. 3.4) Model with generated data overestimates grain as well as upland biomass yields of spring barley in Danubian Lowland (+13.07 % in grain and +13.45 % in upland biomass yields). Model with generated data underestimates grain yields of spring barley in Záhorie Lowland

(-7.88 %) and overestimates upland biomass (+2.19 %) at the same time.

Corn maize grain yields in Záhorie and Danubian Lowland were also simulated with the climatic datasets for the period of 1971-2000 and with generated data and the yields were compared. Model with generated data overestimates grain yields of corn maize by 8.82 % in Danubian Lowland. Model with generated data underestimates grain yields of corn maize in Záhorie Lowland (-3.83 %).

Fig. 3.25 Corn maize grain yields and their deviations simulated according to generated and measured climatic data for Danubian lowland (grid 4522 vs. meteodata for Hurbanovo – left) and Záhorie lowland, (grid 5252 – vs. meteodata for Bratislava- right) - datasets in years 1971-2000



Maize	Harvest	Generated	Measured	Δ	Δ
		[t.ha ⁻¹]	[t.ha ⁻¹]	[t.ha ⁻¹]	[%]
Záhorie lowland	30.9	5.62	5.83	-0.21	-3.83
Danubian lowland	29.9	5.11	4.61	0.50	8.82

Tab. 3.5 Comparison of simulated maize grain yields according to generated (Aladin) and climatic data for Danubian lowland (grid 4522 vs. meteodata for Hurbanovo,) and Záhorie lowland, (grid 5252 – vs Bratislava) - datasets in years 1971-2000

4.1.3 Sensitivity of field crop yields with respect to climate change impacts

Phenology

Harvest maturity of selected crops was evaluated up to time slices. There were not found significant differences in simulation of harvest time between data simulated according to generated (Aladin) and measured meteorological data both for Danubian and Záhorie lowlands. Difference of harvest maturity 1 day in average between Danubian and Záhorie lowlands was found.

Comparison of yields simulated according to meteorological data from station Hurbanovo.

Winter wheat yields in Záhorie and Danubian Lowland were simulated with two different climatic datasets for the period of 1971-2000: data generated by Aladin model and with measured climatic data characteristic for the particular locality.

Maturity of all crops grown on different soil types is accelerated towards time slices. Due to increase of air temperature the maturity of spring barley should be accelerated by about 6 days, winter wheat by about 17 days and corn maize by about 17 days in average in the time slice 2071-2100 as compared to the reference period of years 1971-2000.

Biomass and grain yield

Increase of CO₂ concentration and consequent increase of photosynthesis rate positively affect the yields of spring barley and winter wheat, especially towards more distanced time horizons. While winter wheat and spring barley yield increase towards time slices almost on whole the territory of Western Slovakia (except for spring barley on Luvisol in Nitra region in time slice 2071-2100 (Fig. 3.28)), depression of maize yields was found in time slice 2071-2100 on the whole area (Fig. 3.27).

On the other hand high temperatures generated by GCM during growing seasons (especially in ripening time) frequently led to the fall of simulated yields.

Generally, the yield increase in conditions of climate change do not correspond to the theoretical level of efficiency of photo synthetically active radiation for both spring barley and winter wheat crops (calculated in

dependence upon CO₂ concentration in the Fig. 3.27 Harvest maturity of spring barley, winter wheat and corn maize in Western Slovakia up to time slices 1971-200, 2021-2050 and 2071-2100

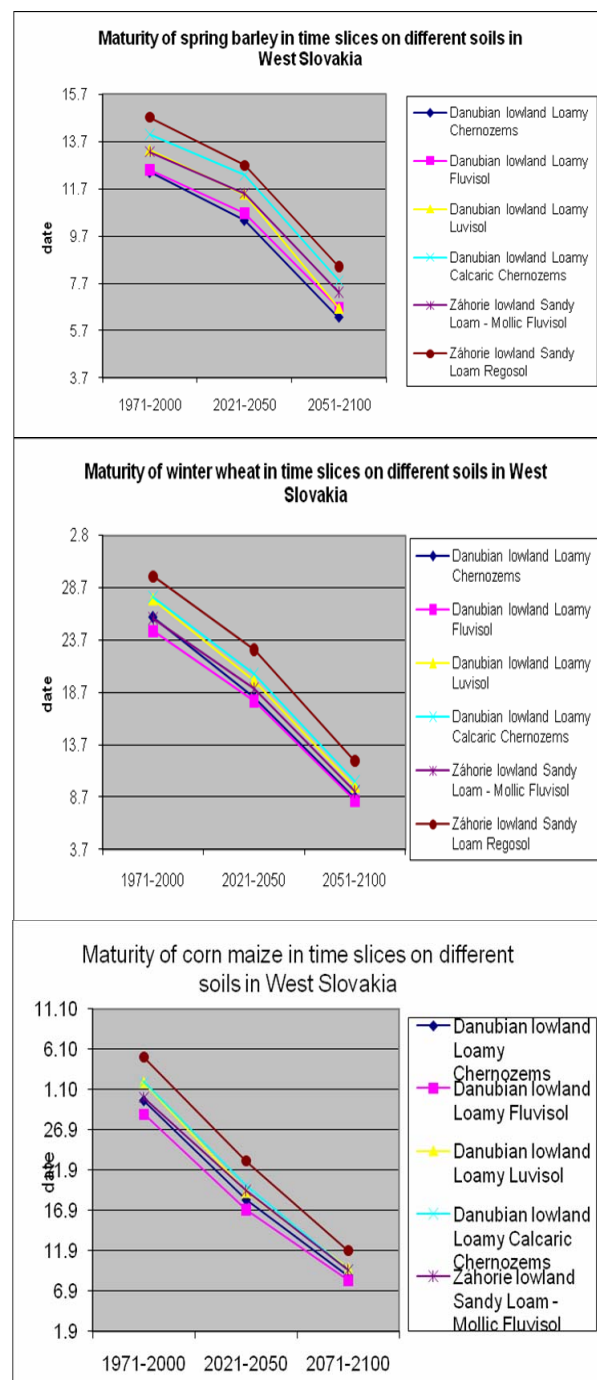


Fig. 3.26 Harvest maturity of winter wheat, spring barley and corn maize in time slices in Western Slovakia

Increase of CO₂ concentration and consequent increase of photosynthesis rate positively affect the yields of spring barley and winter wheat, especially towards more distanced time horizons.

While winter wheat and spring barley yield increase towards time slices almost on whole area of Western Slovakia (except for spring barley on Luvisol in Nitra region in time slice 2071-2100), depression of maize yields was found in time slice 2071-2100 on the whole area (Fig. 3.27).

On the other hand high temperatures generated by GCM during growing seasons (especially in ripening time) frequently led to the fall of simulated yields.

Generally, the yield increase in conditions of climate change do not correspond to the theoretical level of efficiency of photo synthetically active radiation for both spring barley and winter wheat crops (calculated in dependence upon CO₂ concentration in the atmosphere for emission scenarios SRES A1B (IPCC, 2007)).

Soil water content seems to be the main limiting factor of spring barley yields. Spring barley biomass and grain yields decline in Nitra and Trnava region is caused by the lack of available soil water in local soils, which further decreases due to the higher temperatures projected according to the SRES A1B scenario. The crop is more sensitive to the lack of water supply after the winter. Yields have increasing tendency on the rest of the sites, which have better soil conditions with enough soil water content.

Grain yields of corn maize have decreasing tendency. Fertilization effect of CO₂ concentration is not significant, corn maize belongs to C4 crops with different type of photosynthesis.

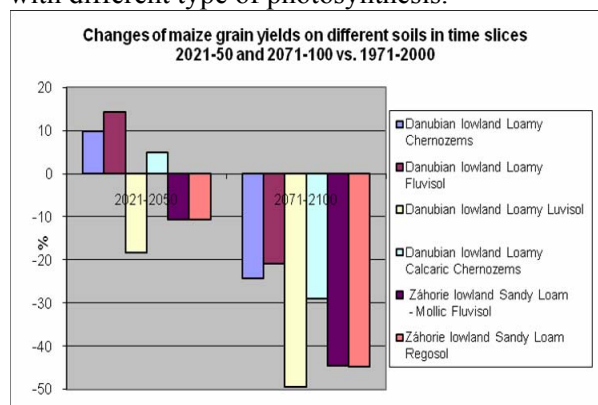


Fig. 3.27 Relative changes of grain yields of corn maize - comparison of slices 2021-2050 and 2071-2100 vs. 1971-2100

Harvest index of winter wheat is gradually decreasing in the period of years 2071-2100, but it is still much higher than in 1971-2000, especially in Žitný Ostrov. The only exception is northern Záhorie, where the harvest index is constantly lower than in the reference period (Fig. 3.31).

Harvest index of spring barley in Žitný Ostrov, Trnava region and southern Záhorie is higher than in the reference period, but gradually declines, in spite of the rest of the localities with significant decline of the index in the whole future time period (Fig. 3.29).

Top dry biomass yield will be formed mainly by straw yield in future climate. Grain yields will be probably reduced by higher temperatures during ripening. Transport of assimilates from other parts of the plant into grains is not so effective because of accelerating effect of high temperatures on ripening of cereals. Based on the simulation results, fertilization effect of CO₂ on spring barley and winter wheat grain and biomass yield is evident. Increasing temperature and CO₂ concentration will cause the increase of yields up to the year 2075, when the yields will gradually begin to decline.

4.2 Conclusions

- Except for regions of Žitný ostrov (Rye island) and some stands near big river of western Slovakia most of the evaluated area was recognized as the vulnerable region according to variability of yields. Shortage of precipitation in some years make all evaluated sandy loam soils and loamy soils (luvisols, fluvisols and chernozems) very dry especially in northern part of the region.
- Increase of CO₂ concentration and consequent increase of photosynthesis rate will positively affect the biomass and grain yields of winter wheat and spring barley in Western Slovakia. The highest effect was simulated for Haplic Chernozems on Danubian lowlands (Žitný ostrov)
- Rise of spring barley and winter wheat yields were simulated for time slices 2021-2050 and 2071-2100 for most of the Western Slovakia as compared with 1971-2000
- But yields of winter wheat and spring barley will decline after 2070 on all evaluated soils.
- Grain yields of corn maize have decreasing tendency practically during whole evaluated periods.
- Level of yields conditions of climate change will not correspond with the theoretical positive effect of CO₂ photo synthetically active radiation for spring barley and winter wheat crops for emission scenarios SRES A1B.

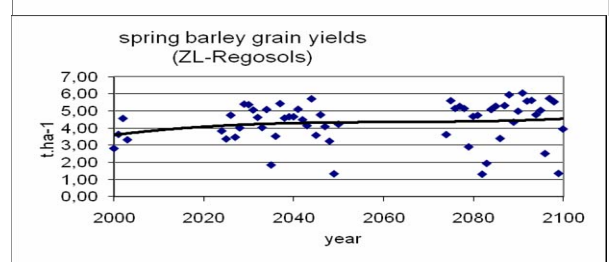
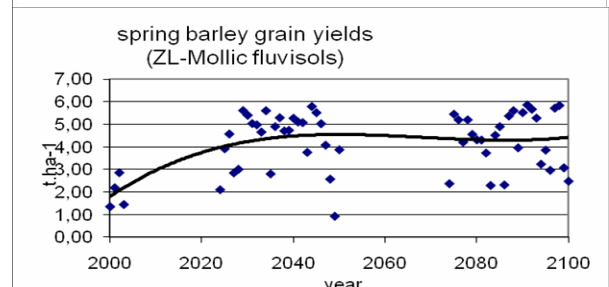
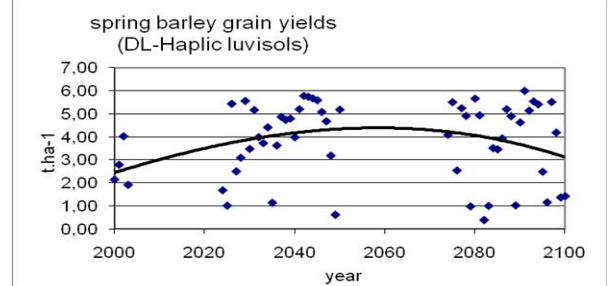
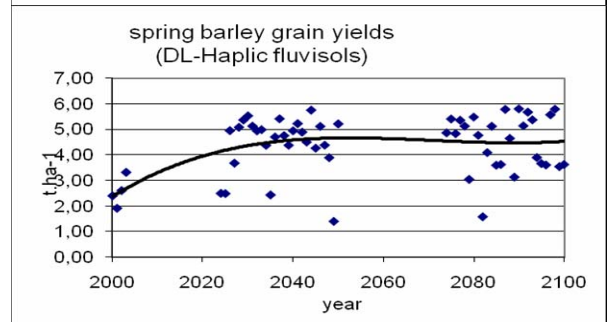
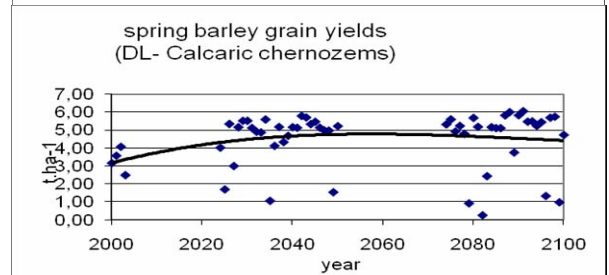
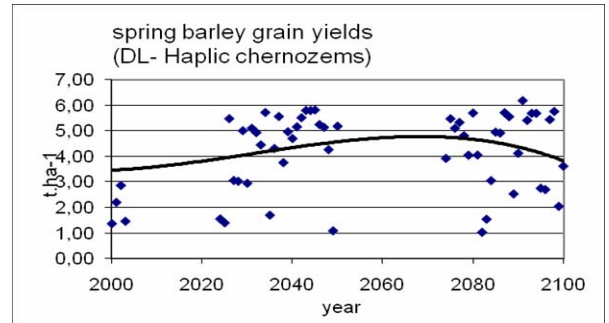
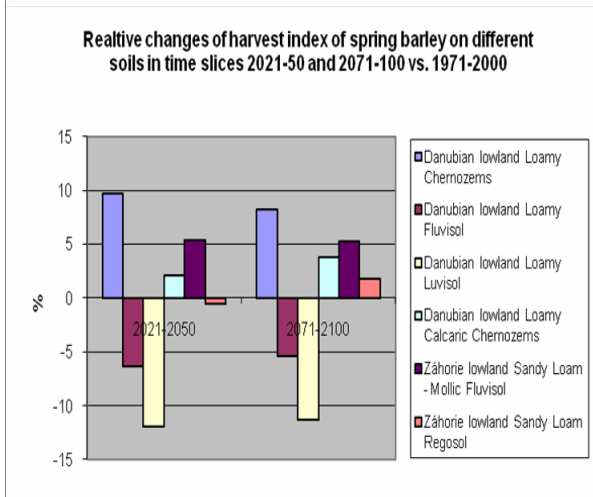
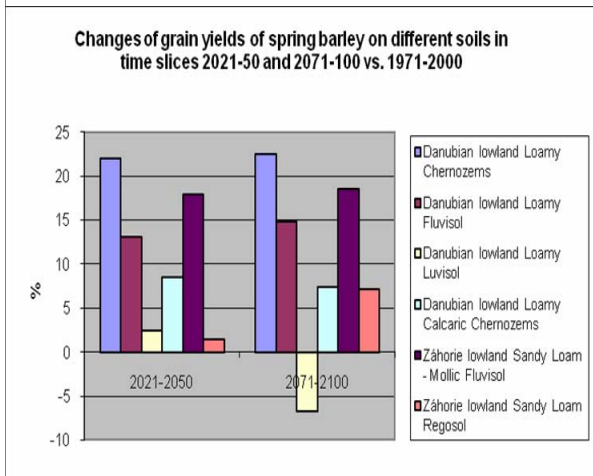
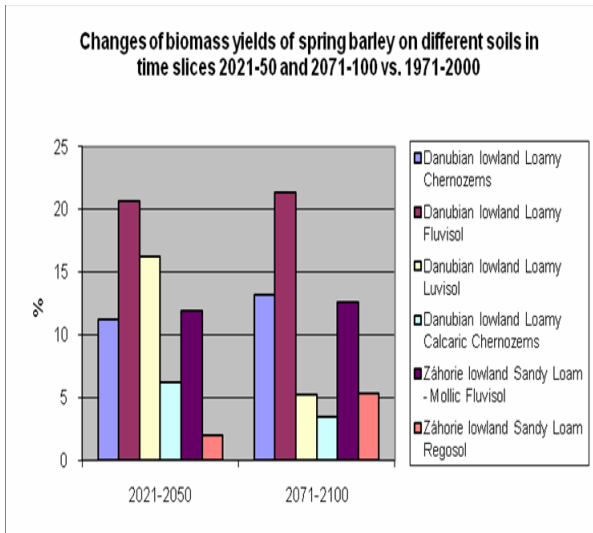


Fig. 3.28 Relative changes of grain and upland biomass and harvest index of spring barley on different soils -comparison of slices 2021-2050 and 2071-2100 vs. 1971-2000

Fig. 3.29 Grain yields of spring barley 2000 -2100

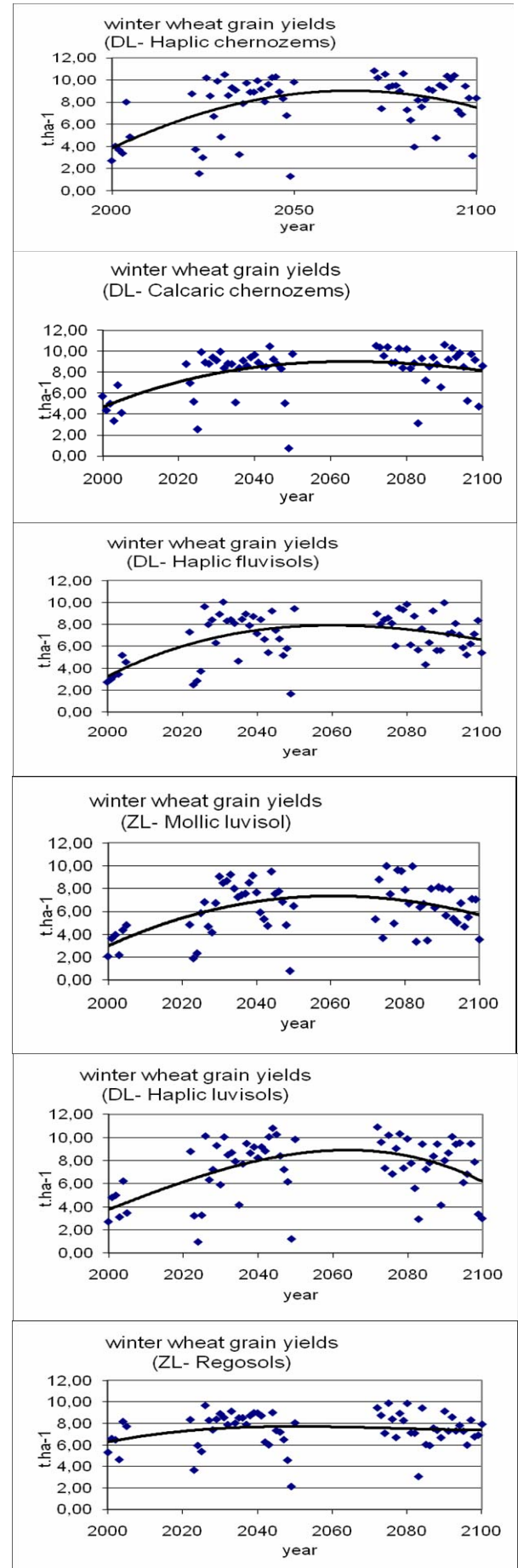
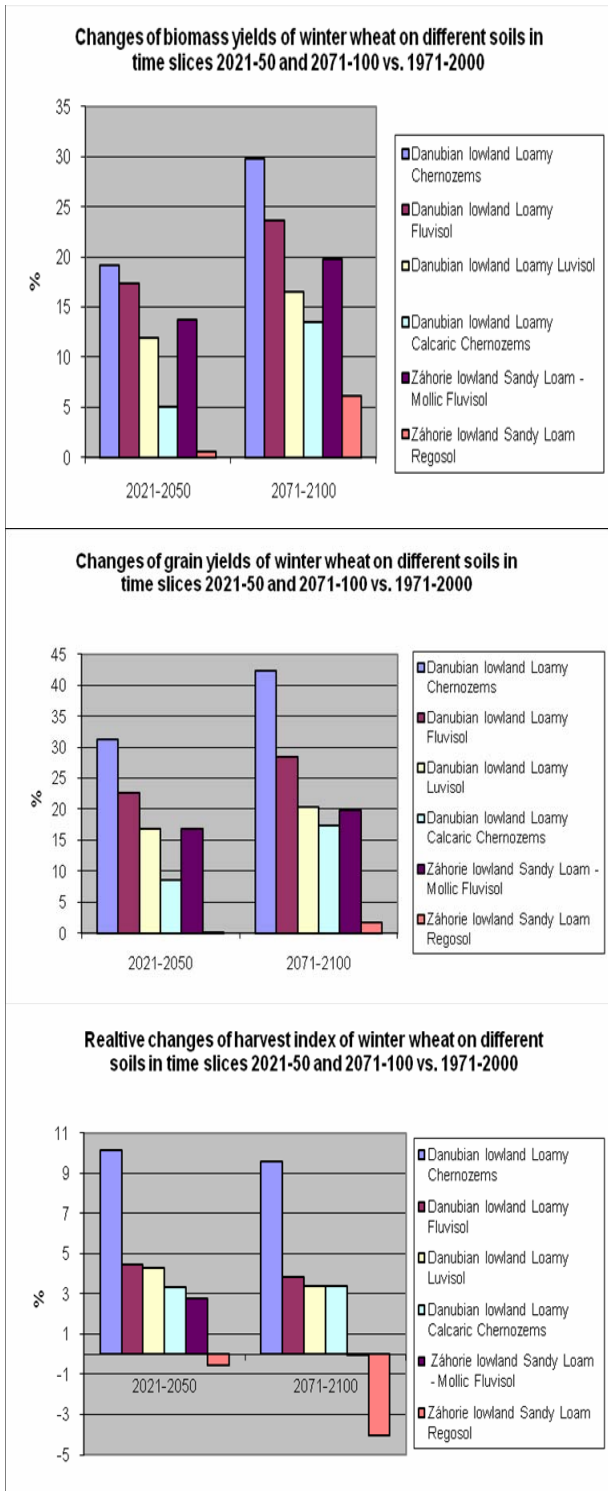


Fig. 3.30 Relative changes of grain and upland biomass and harvest index of winter wheat on different soils of Danubian and Záhorie lowlands -comparison of slices 2021-2050 and 2071-2100 vs. 1971-2000

Fig. 3.31 Grain yields of winter wheat 2000 - 2100

Fig. 3.32 Upland biomass and grain yields of spring barley for different soils on Danubian and Záhorie lowlands and time slices 1971-2000, 2021-2050, 2071-2100 (statistical distribution)

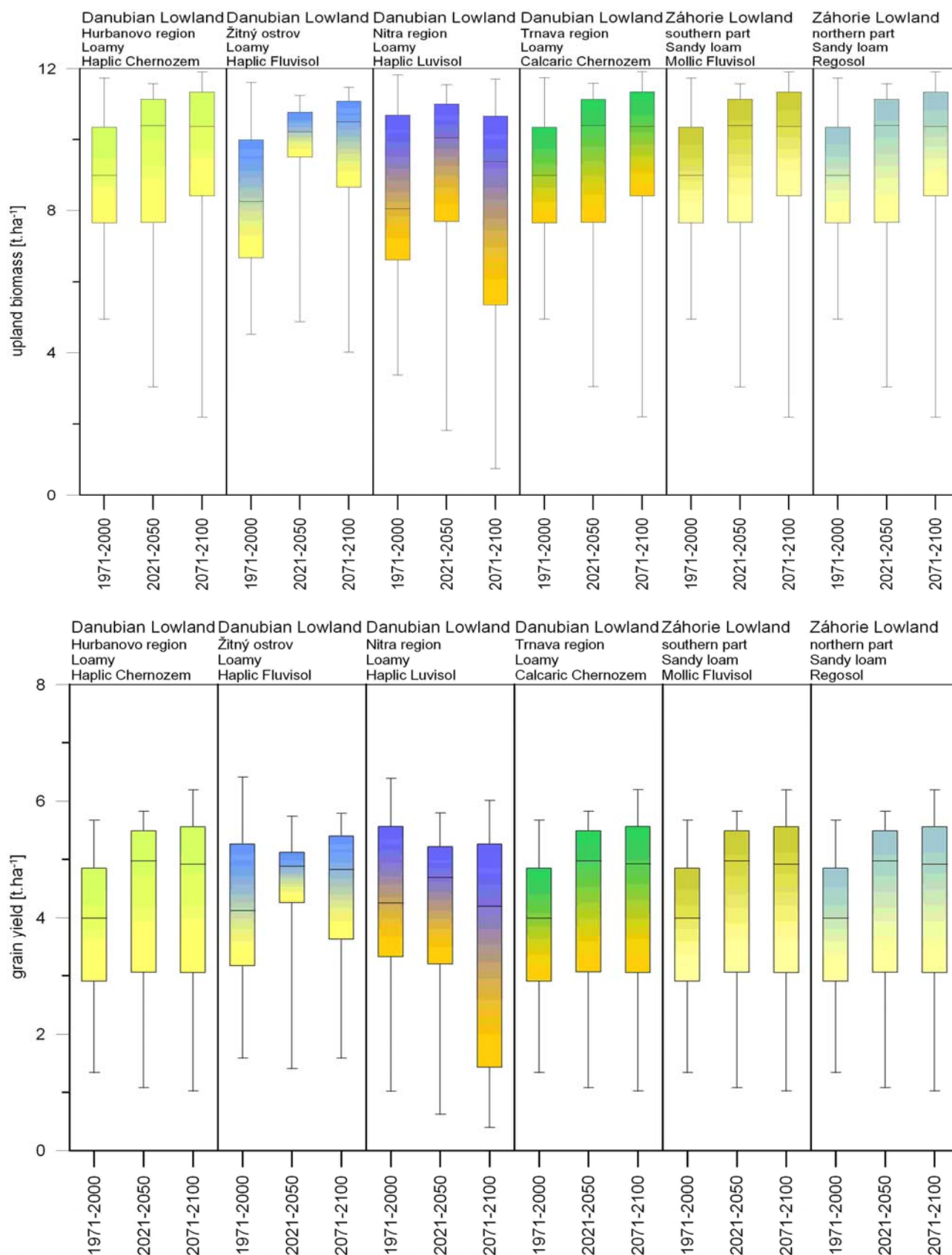


Fig. 3.33 Upland biomass and grain yields of winter wheat for different soils on Danubian and Záhorie lowlands and time slices 1971-2000, 2021-2050, 2071-2100 (statistical distribution)

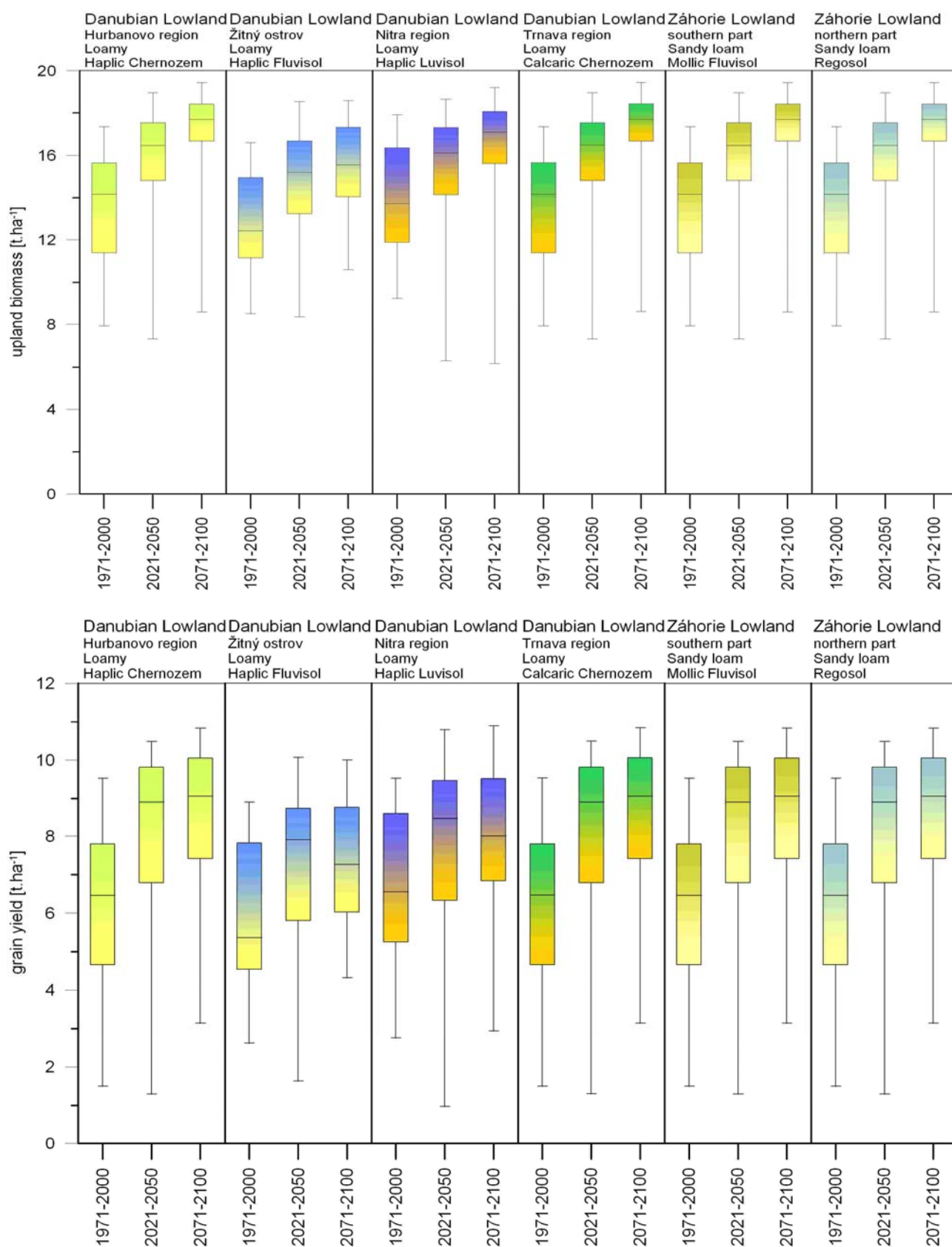
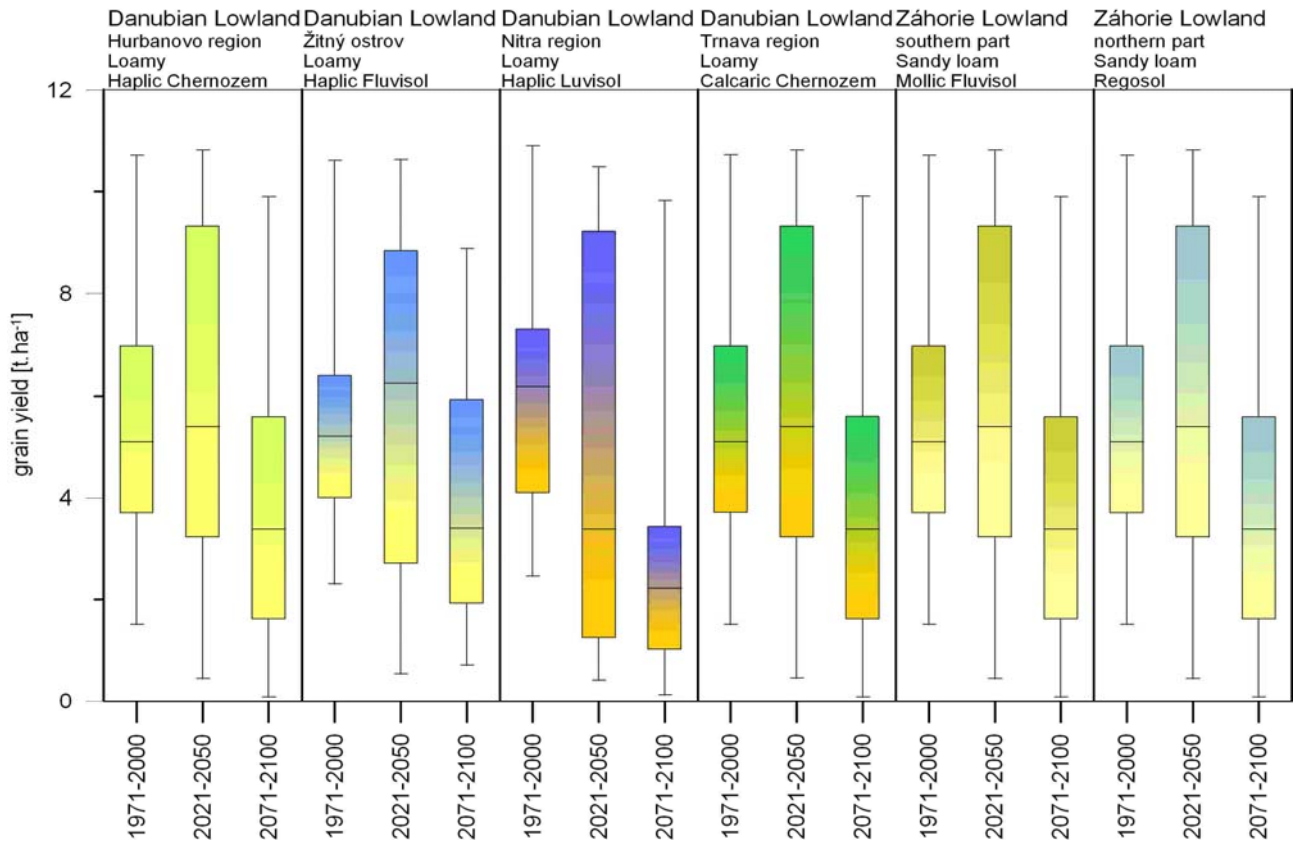


Fig. 3.34 Grain yields of corn maize for different soils on Danubian and Záhorie lowlands and time slices 1971-2000, 2021-2050, 2071-2100 (statistical distribution)



5 FOREST ECOSYSTEMS – POLAND

5.1 Introduction

The main objective of WUT was to study possible impacts of climate changes on forest ecosystems sensitivity to atmospheric deposition of sulphur and nitrogen.

Sensitivity of natural ecosystems to atmospheric pollution is quantitatively characterized by so called “critical loads” (CL) specifying this amount of atmospheric deposition of a given pollutant which is safe for their structure and functioning. In case of atmospheric deposition of nitrogen two major adverse effects are recognized i.e. acidification caused simultaneously by nitrogen and sulphur deposition and eutrophication caused by nutrient nitrogen solely.

Critical load of acidity is by definition the highest deposition of acidifying compounds as sulfur and oxidized and reduced nitrogen, that will not cause chemical changes leading to long-term harmful effects on ecosystem structure and function

The **critical loads of acidity** are represented by a function defined by three quantities: $CL_{max}(S)$, $CL_{min}(N)$ and $CL_{max}(N)$, where:

- $CL_{max}(S)$ is a maximum critical load of sulphur, which is the maximum tolerable sulphur deposition in case of zero deposition of nitrogen,
- $CL_{min}(N)$ is a minimum critical load of nitrogen, which equals to long-term net removal and immobilization of nitrogen in soil,
- $CL_{max}(N)$ is a maximum critical load of nitrogen, which is the harmless maximum deposition of nitrogen in case of zero sulphur deposition:

Critical load of eutrophication – $CL_{nut}(N)$ is the highest deposition of nutrient nitrogen below which harmful eutrophying effects in ecosystem structure and function do not occur according to present knowledge.

To calculate critical loads a number of biogeochemical input parameters are needed of which some key parameters are directly dependant on climatological factors.

The recently internationally approved methodology to calculate and map critical loads is summarized in the “Mapping Manual on Methodologies and Criteria for Modelling and Mapping Critical Loads & Levels and Air Pollution Effects, Risks and Trends” (UBA, 2004). This methodology is based on the Simple Mass Balance model. We applied this methodology in our study.

The research have been conducted for two selected forested domains in Poland, characterized by different localization, air pollution pressure, meteorological conditions, soil and forest type and current forest health condition. Their localization in Poland is shown on Fig 4.1.

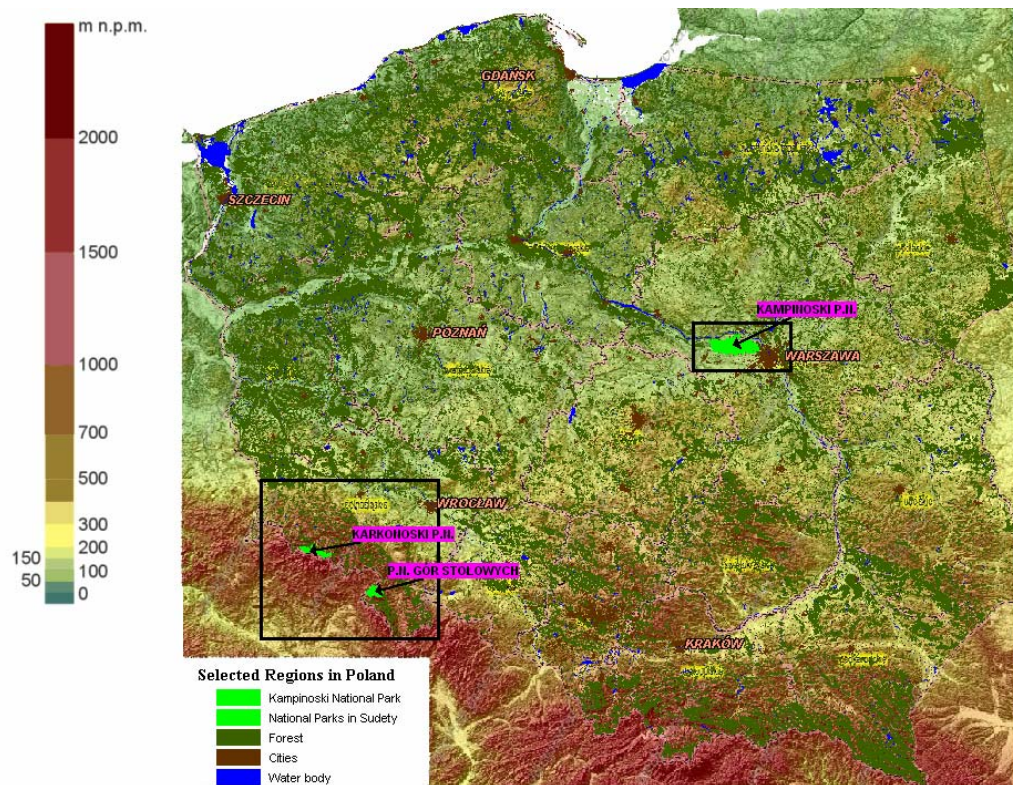


Fig. 4.1. The area of Poland with chosen domains and National Parks considered in the study.

The first domain is situated in the mountain climatic zone of west-southern part of Poland and belongs to the Sudety natural-forest region. The region represents the highest forest cover in Poland (38%) as well as one of the highest level of damage when compared to other natural-forest regions. The region represents a great ecological value and is protected by two Polish National Parks (NP): Karkonoski National Park - a UNESCO protected biosphere reserve, and National Park of Stolowe Mountains. It will be hereafter referred to as **Karkonosze domain**. The second domain is situated in central part of Poland and belongs to the Mazowsze-Podlasie natural-forest region. The region represents the lower forest cover in Poland (19,6%) and medium damage level. The unique feature of that region is localization of Kampinoski National Park in the vicinity of agglomeration (Warsaw). It will be hereafter referred as **Kampinos domain**.

The study domains have been established during second reporting period and based on the CORINE land-cover map the terrestrial ecosystems residing in the both domains have been identified, showing that in both domains coniferous forests prevail. The soil types have been identified using the EUROSOIL soil map.

The following tasks was worked on:

1. Acquisition of input data for critical loads of nutrient nitrogen
 - long-term net immobilization of nitrogen in soil organic matter
 - net removal of nitrogen in harvested vegetation
 - precipitation surplus in the soil root zone
 - acceptable nitrogen concentration in the soil leachate
2. Acquisition of input data for critical loads of acidity
 - Determination of chemical criteria for acid neutralizing capacity (ANC) estimation
 - Base cation atmospheric depositions

- Base cation weathering from soil minerals
 - Base cation uptake by vegetation
3. Development of input databases suitable for computational procedures
 4. Development of computer software to calculate and map critical loads of acidity and eutrophication
 5. Calculating and mapping critical loads of acidity and eutrophication
 6. Calculating and mapping current exceedances of critical loads of acidity and eutrophication
 7. Defining critical loads parameters sensitive to climate
 8. Extraction of climatic data for control period and for future decades from the outputs of RegCM (CUNI)
 9. Calculating total deposition of sulphur species for extended control period and for future decades (RegCM-CAMx).
 10. Calculating total deposition of oxidized nitrogen and reduced nitrogen species for extended control period and for future decades (RegCM-CAMx).
 11. Calculating and mapping of exceedances of critical loads of acidity and eutrophication for past and future time periods
 12. Analysis of sensitivity of selected critical loads parameters to predicted changes of chosen climatic factors

The mass balance models were used to calculate parameters of critical load functions of acidity and eutrophication of the selected forested areas in Poland, with a distinction into coniferous, deciduous and mixed forests. Based on the input data availability on one hand and the expected maximum obtainable accuracy on the other hand, the spatial resolution defined by a 1 x 1 km grid cell size has been chosen. Such a cell size provides that a unique sub-ecosystem type is represented in a cell and no statistical interpretation within a grid cell is required. This detailed spatial resolution resulted in 2078 records in the derived input and output data databases for the domain of Kampinos and 1979 for Karkonosze domain. The databases were generated and managed under the Microsoft Excel 2007 software. To produce thematic maps of input and output parameters the MapInfo Professional v. 9.02. software was used.

To calculate critical loads exceedances there is a need to compare them to deposition estimates. Within this study we use two sources of deposition data. For the calculation of current (2005) critical loads exceedances transboundary and local depositions fluxes of sulfur and nitrogen compounds calculated by EMEP model in 50x50 km grid covering most of Europe have been applied. The EMEP grid is a special case of the so-called polar stereographic projection where each point on the Earth's sphere is projected from the South Pole onto a plane perpendicular to the Earth's axis and intersecting the Earth at a fixed latitude Φ_0 . This spatial grid system has been adopted to calculate critical loads and their exceedances for forest ecosystems of the considered areas. After dividing every 50 sq km grid cell by 2500 a detailed grid was constructed with a grid cell of 1x1 km size. Based on this grid all numerical and geographical processing was performed. To bring the output databases back to a more common spatial system a next conversion is done from the stereographic coordinates to the geographic coordinates by assigning to the middle of each 1x1 km stereographic grid cell its geographic coordinates. So in the resulting databases each record is addressed by its geographical longitude and latitude.

For assessing climate change impacts on critical loads exceedances, the deposition have been calculated at WUT with much finer resolution of 10 x 10 km. Three time-slices have been considered: the so-called extended control period (1991-2000) and two future climate time-

slices: 2041-2050 and 2091-2100. The simulation have been performed under WP7 of CECILIA with coupled regional climate (RCM) - air quality (AQ) modeling system with constant emission database (for the base year 2000). The modeling system consists of RegCM-EMIL-CAMx models and have been implemented for the WUT modelling domain, centred over Poland (52.00°N, 19.30°E) on a grid with 120 x 109 points and a resolution of 10 km. The map projection choice was Lambert conformal. The high-resolution simulations were performed with GCM ECHAM5 meteorological fields to drive RCM. The RCM model applied was the improved version of RegCM3 for high resolution applications RegCM3-Beta (Pal et al., 2007), which is referred as RegCM (WUT). The AQ model applied was CAMx - a complex third-generation Eulerian Grid Model developed at ENVIRON International Corporation (Novato, California). Simulations have been carried out using CAMx v. 4.40. The emission model EMIL was originally developed at WUT. The model applies for Poland and creates the so called second-level emission database for the high resolution 10 km photochemical runs performed at WUT. Emission database applied for other, than Poland, countries belonging to modelling domain remains zero-level (based on EMEP inventory). The Lambert Conformal Conic spatial system in which deposition were calculated had to be converted into the EMEP polar stereographic projection system and the data disaggregated to a grid defined by a grid cell of 1x1 km size. Such a conversion produced 2079 grid cells for the domain of Kampinos and 1798 grid cells for the Karkonosze domain. After derivation of all needed input data for critical loads and their exceedances calculation, the input database have been completed.

5.2 Results

5.2.1 Critical load function of acidity

Applying the Simple Mass Balance model described in UBA (2004) all three parameters of the critical loads function have been calculated (CL_{max}(S), CL_{min}(N) and CL_{max}(N). The governing parameter of acidification is CL_{max}(S) while CL_{min}(N) is an auxiliary one and CL_{max}(N) derives from the first two parameters. The obtained CL_{max}(S) are presented on Fig. 4.2 and Fig. 4.3.

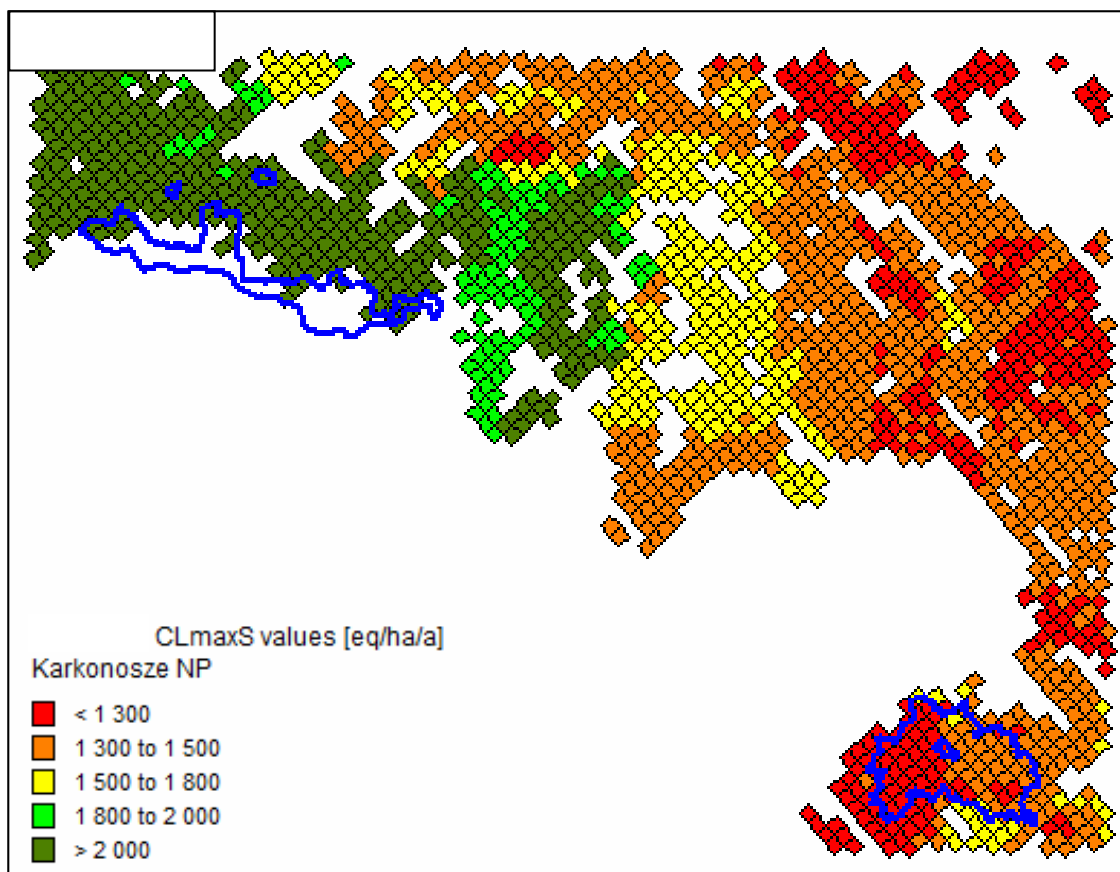


Fig. 4.2 $CL_{max}(S)$ values [$eq\ ha^{-1}a^{-1}$] in Karkonosze domain.

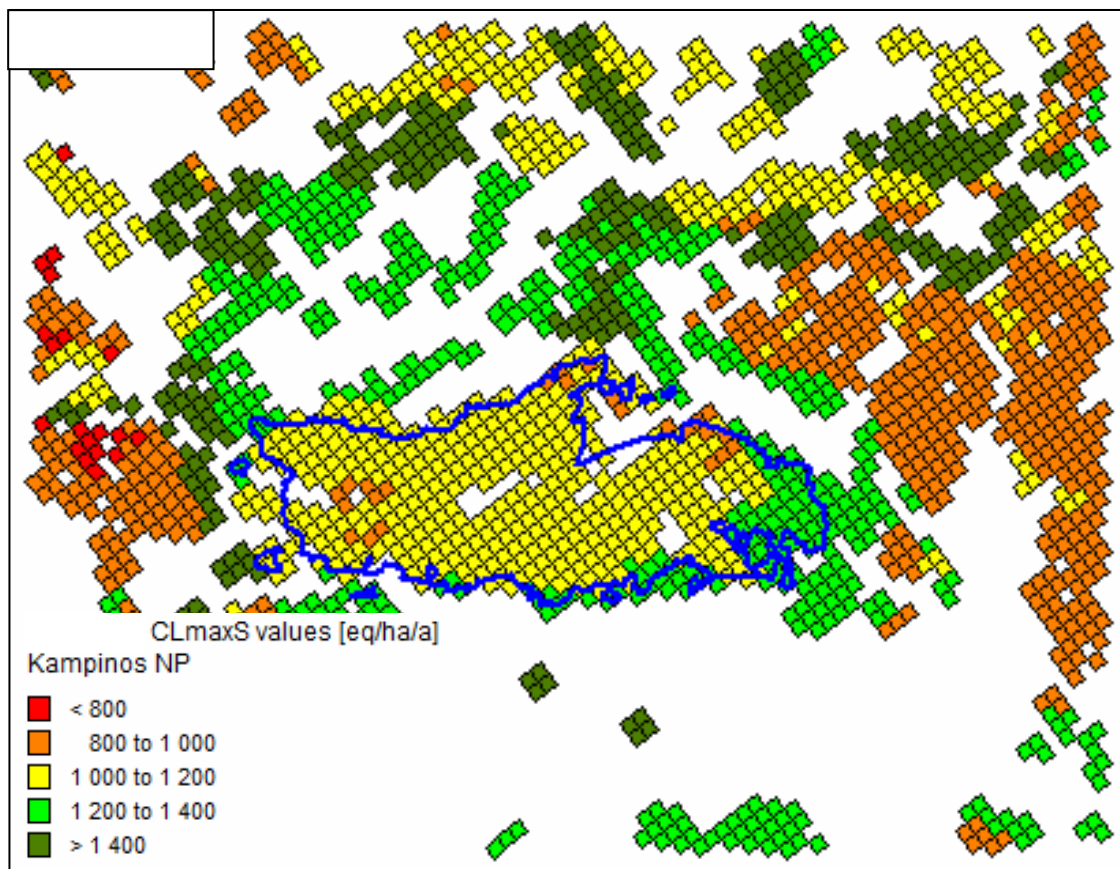


Fig. 4.3 $CL_{max}(S)$ values [$eq\ ha^{-1}a^{-1}$] in Kampinos domain.

For Karkonosze domain the most frequent values of CLmax(S) ranges between 1300 and 1500 eq ha⁻¹a⁻¹ occupying the east and south-east part. Within strict borders of the Karkonoski National Park (see Fig. 4.1) the highest values exceeding 2000 eq ha⁻¹a⁻¹ dominate. This is due to relatively high precipitation and base cation deposition values which overcompensate the effect of low values of base cation input from weathering being common to mountain areas. For National Park of Stolowe Mountains the lowest values (<1500 eq ha⁻¹a⁻¹) dominate.

For Kampinos domain the CLmax(S) values and spatial distribution is different. In here lower values between 1000 and 1200 eq ha⁻¹a⁻¹ prevail and the distribution is almost complete regular. Base cation weathering values are higher than in Karkonosze and precipitation surplus is significantly lower.

5.2.2 Critical load of nutrient nitrogen

To calculate critical loads of nutrient nitrogen the Simple Mass Balance model described in UBA (2004) was applied. Spatial distribution of the resulting CLnut(N) values for the both considered areas is given in Figures 4.4 and 4.5.

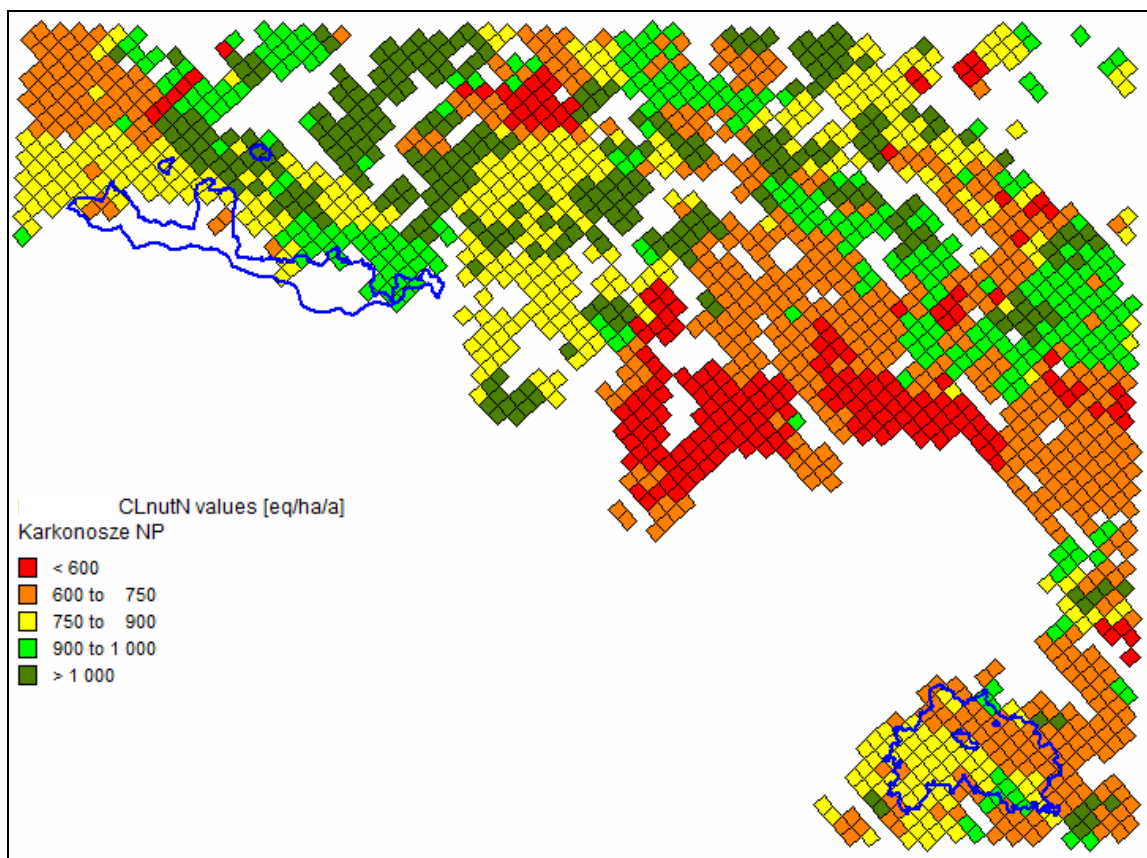


Fig. 5.4 $CL_{nut}(N)$ values [$eq\ ha^{-1}\ a^{-1}$] in Karkonosze domain.

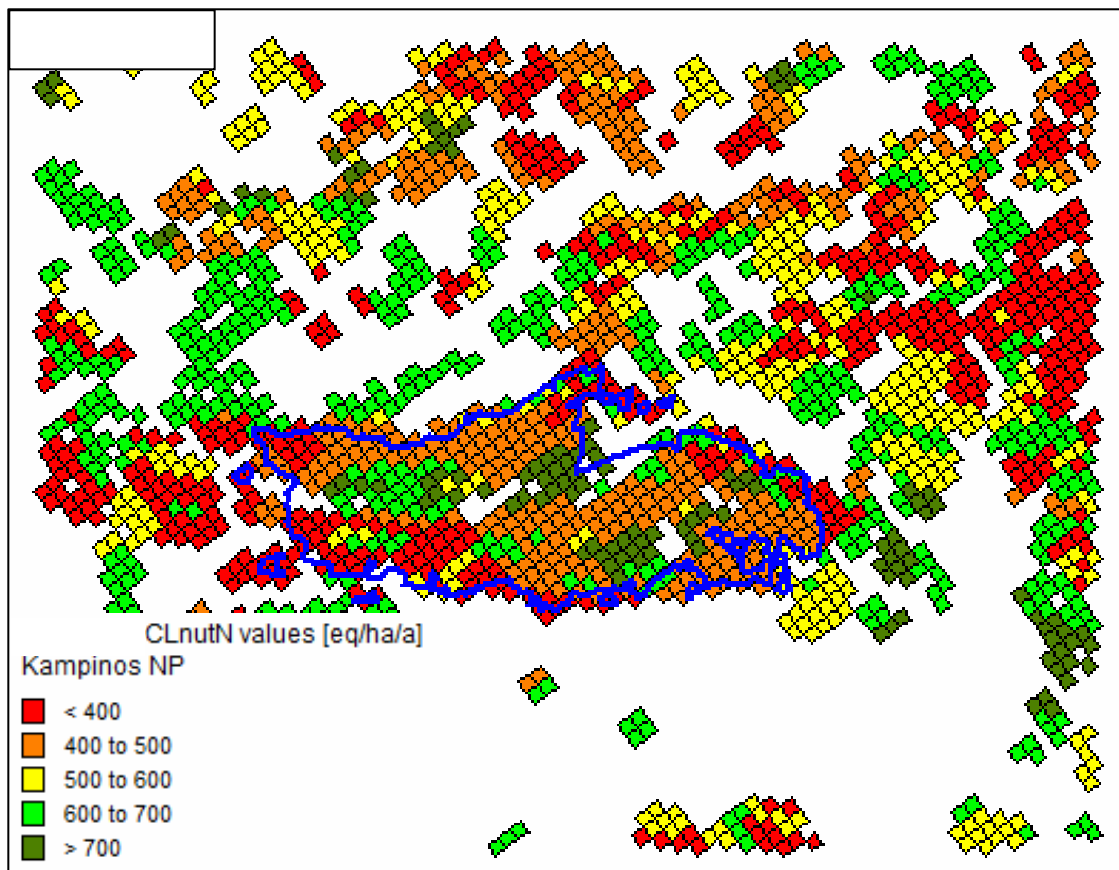


Fig. 4.5 $CL_{nut}(N)$ values [$eq\ ha^{-1}a^{-1}$] in Kampinos domain.

In the north-western part of the Karkonosze domain values of the range 900 to more than 1000 $eq\ ha^{-1}a^{-1}$ appear most frequently while within the south-eastern part lower values are observed varying between less than 600 up to 750 $eq\ ha^{-1}a^{-1}$ within the National Park of Stolowe Mountains. Within the border of the Karkonoski National Park the distribution is opposite i.e. in the north-western part the $CL_{nut}(N)$ values are lower than in the south-eastern part. In Kampinos domain the average $CL_{nut}(N)$ level as well as the spatial distribution is similar for both the whole domain and the National Park area. Within the National Park $CL_{nut}(N)$ values ranging between less than 400 to 500 $eq\ ha^{-1}a^{-1}$ evidently prevail. Comparing the two considered domains and their National Parks, it is to note that in average the Kampinos National Park with its lower range of $CL_{nut}(N)$ values is more sensitive to nutrient nitrogen deposition and therefore more vulnerable to eutrophication than the National Park of Stolowe Mountains and Karkonosze National Parks.

5.2.3 Current critical load exceedances

In general exceedance of a critical load of acidity or nutrient nitrogen is the excess of actual acid or nitrogen deposition over their critical values for a given ecosystem. In terms of ecosystem protection exceedance of critical load is a measure of the potential risk to functioning and structure of an ecosystem. For the calculation of current (2005) critical loads exceedances depositions fluxes of sulfur and nitrogen compounds calculated by EMEP model in 50x50 km grid covering most of Europe have been applied. Figures 4.6 and 4.7 present spatial distribution of $CL_{max}(S)$ and $CL_{nut}(N)$ exceedances of acidity and eutrophication respectively for the Karkonosze domain.

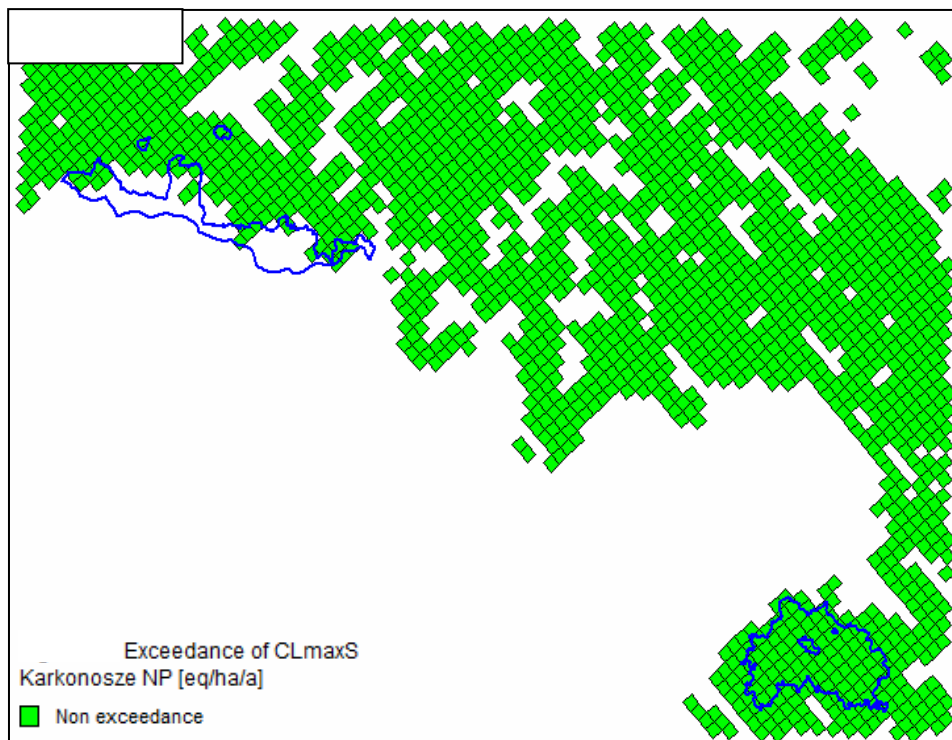


Fig. 4.6 Current exceedances of $CL_{max}(S)$ values [$eq\ ha^{-1}\ a^{-1}$] in Karkonosze domain.

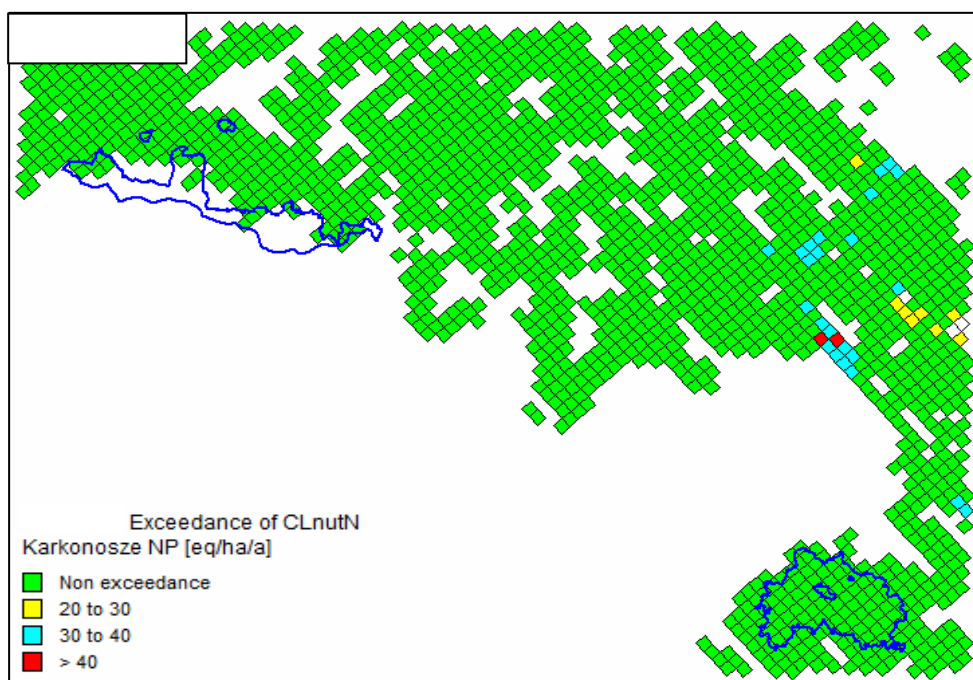


Fig. 4.7 Current exceedances of $CL_{nut}(N)$ values [$eq\ ha^{-1}\ a^{-1}$] in Karkonosze domain.

As shown at Figure 4.6 the acid deposition from 2005 doesn't cause any exceedance of the critical load of acidity in all the domain of the Karkonosze. From Figure 4.7 a relatively small exceedance of critical load of eutrophication is reported in the south-west part of the domain while the majority of its area shows non exceedance, including both national Parks. Spatial distributions of exceedances of acidity and eutrophication for Kampinos domain are shown in Figures 4.8 and 4.9 respectively.

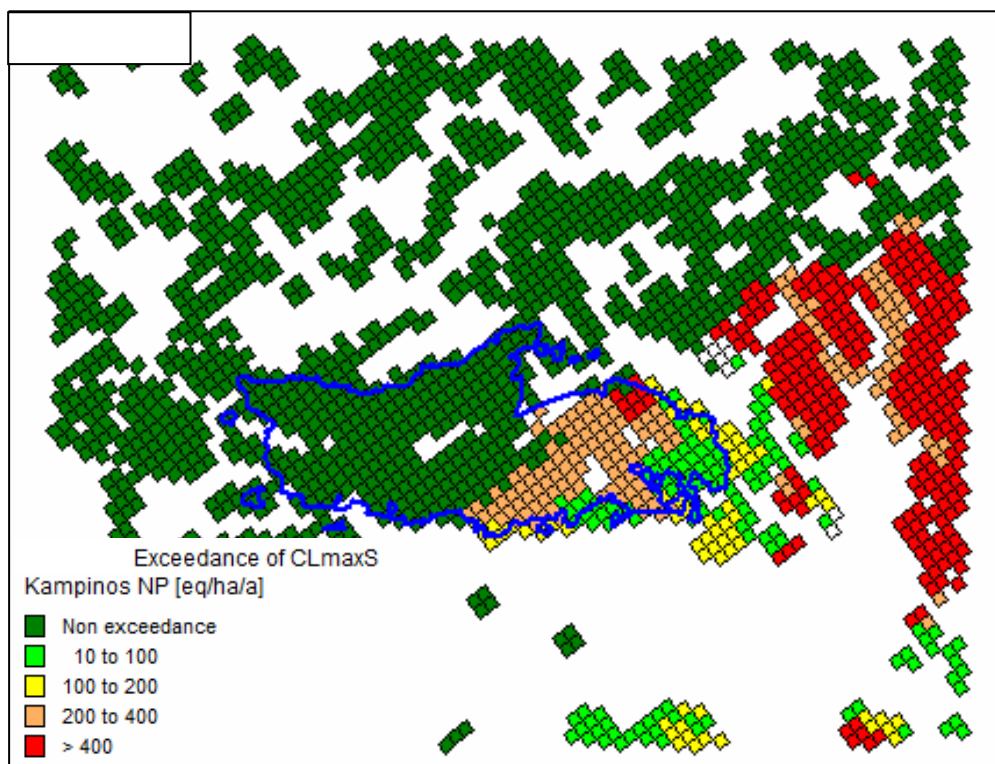


Fig. 4.8 Current exceedances of $CL_{max}(S)$ [$eq\ ha^{-1}a^{-1}$] in Kampinos domain.

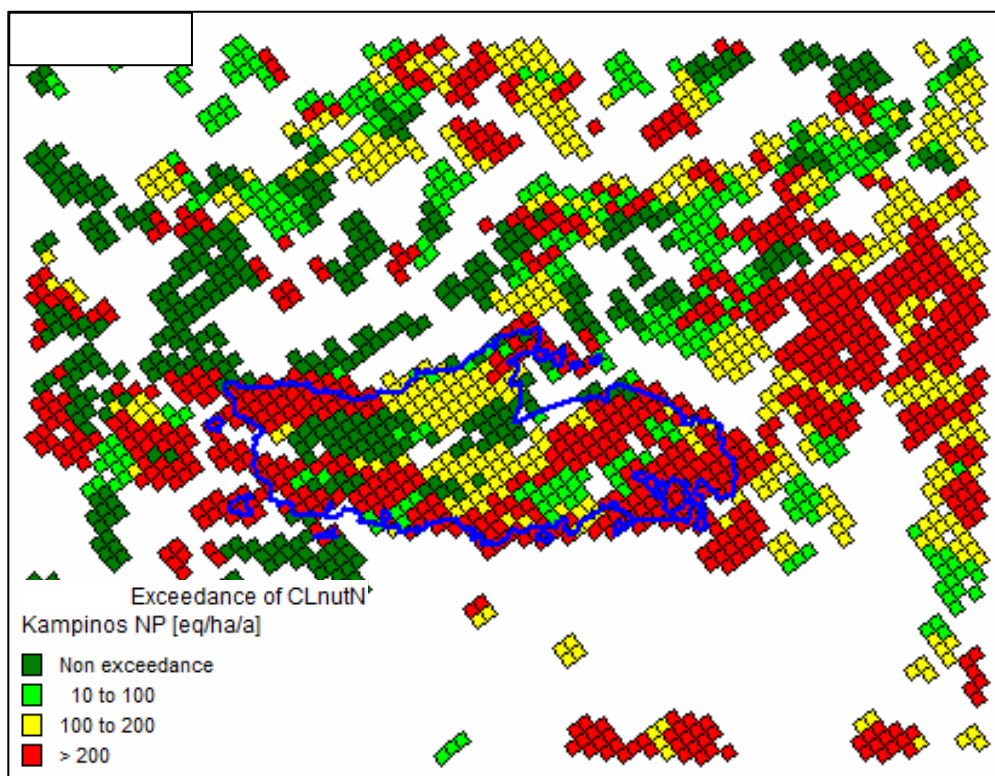


Fig. 4.9 Current exceedances of $CL_{nut}(N)$ [$eq\ ha^{-1}a^{-1}$] in Kampinos domain.

The exceedance of critical loads of acidity in Kampinos domain (Fig. 4.8) is ranging from non exceedance in the western part to relatively high exceedance in the eastern part. Such a distribution of exceedance should be attributed to the acid deposition fluxes from the Warsaw agglomeration.

The exceedance of critical loads of eutrophication (Fig. 4.9) has a more even spatial distribution what is explained by nitrogen deposition generated by low agricultural emission sources common for this part of the country.

5.2.4 Defining critical loads parameters sensitive to climate

The sensitivity of forest ecosystems to acidification and eutrophication, quantitatively defined by relevant critical loads, is combined with climate conditions. Air temperature and atmospheric precipitation are the both climatic factors that modify maximum critical loads of sulphur $CL_{max}(S)$ representing acidification and critical loads of nutrient nitrogen $CL_{nut}(N)$ representing eutrophication.

Concerning $CL_{max}(S)$, it is dependent on climate by dependence of leaching of acid neutralizing capacity (ANCl_e) on precipitation and dependence of base cation weathering (BC_w) on temperature.

Concerning $CL_{nut}(N)$, the acceptable load of nitrogen leaving the soil (Nle(acc)) is directly dependent on the precipitation surplus thus indirectly with precipitation.

5.2.5 Climate data from Regional Climate Model

To calculate critical loads changes driven by climate changes the following climate data were needed for the both studied domains: the average annual values of air temperature and atmospheric precipitation.

Climate scenario and control data was produced by WP2 of the CECILIA project for the time slices of 1961-2000 (control period), 2021-2050 and 2071-2100 using the A1B SRES scenario (Nakicenovic et al., 2000). We used output of regional climate model simulations performed by the Charles University of Prague in fine resolution of 10 x 10 km. The model is referred herein as RegCM (CUNI). Global climate model ECHAM5 provided the driving data for the RegCM (CUNI).

From the European climate data delivered by CUNI, the data for selected domains have been extracted for control period and for future decades and converted from NetCDF format to the format needed by database developed for this study. As there might be a systematic over- or underestimation in the precipitation scenarios we used the CRU TS 1.2 data and the simulation data from the reference period (1961-1990) to estimate bias. The calculated bias was used to correct the scenario precipitation data.

The final climate data consist of average monthly temperatures and precipitations for three time slices. For each of these periods annual averages have been calculated to satisfy the critical loads calculation method.

For the Kampinos domain the climatic data were prepared for 60 single nodes while for the Karkonosze domain for 255 nodes. The Lambert Conformal Conic spatial system was applied spatially to address the nodes positions. For CL calculation this spatial system had to be converted into the EMEP polar stereographic projection system and the data disaggregated to a grid defined by a grid cell of 1x1 km size. Such a conversion produced 2079 grid cells for the domain of Kampinos and 1798 grid cells for the Karkonosze domain.

Climate data - the Kampinos domain

For the climate data a trend analysis was done for each of the three time series. A trend analysis for the entire period 1961 - 2100 was done assuming a linear continuity. The following Figures (4.10,4.11) show how the temperature and precipitation changed within the considered periods:

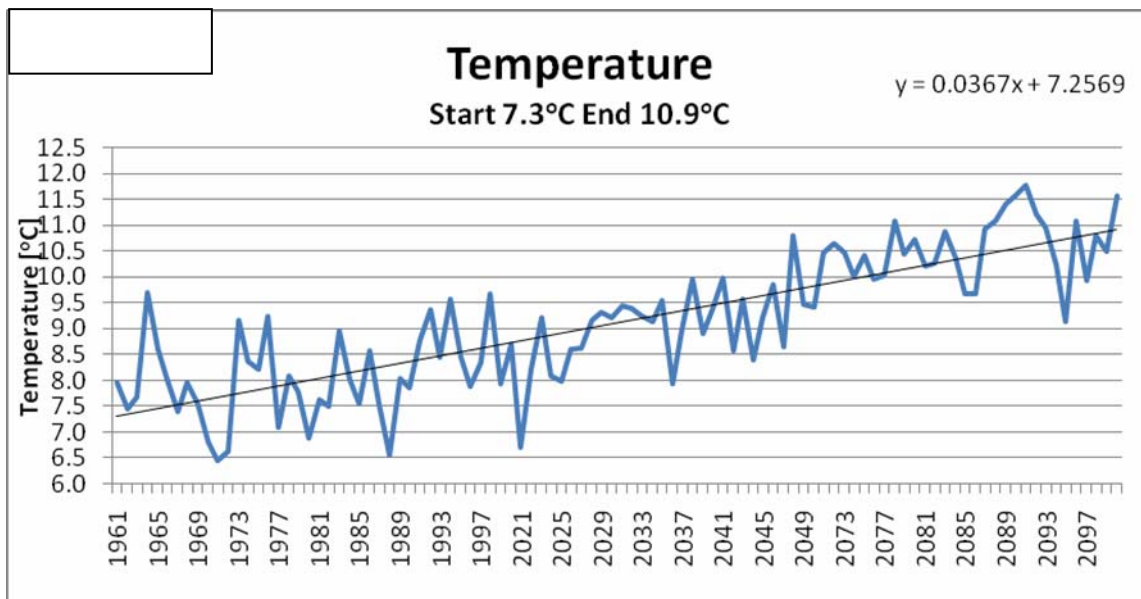


Fig. 4.10 Changes in average temperature [°C] between 1961 and 2100 in Kampinos domain. Within the entire 1961 - 2100 period a linear continuity was assumed.

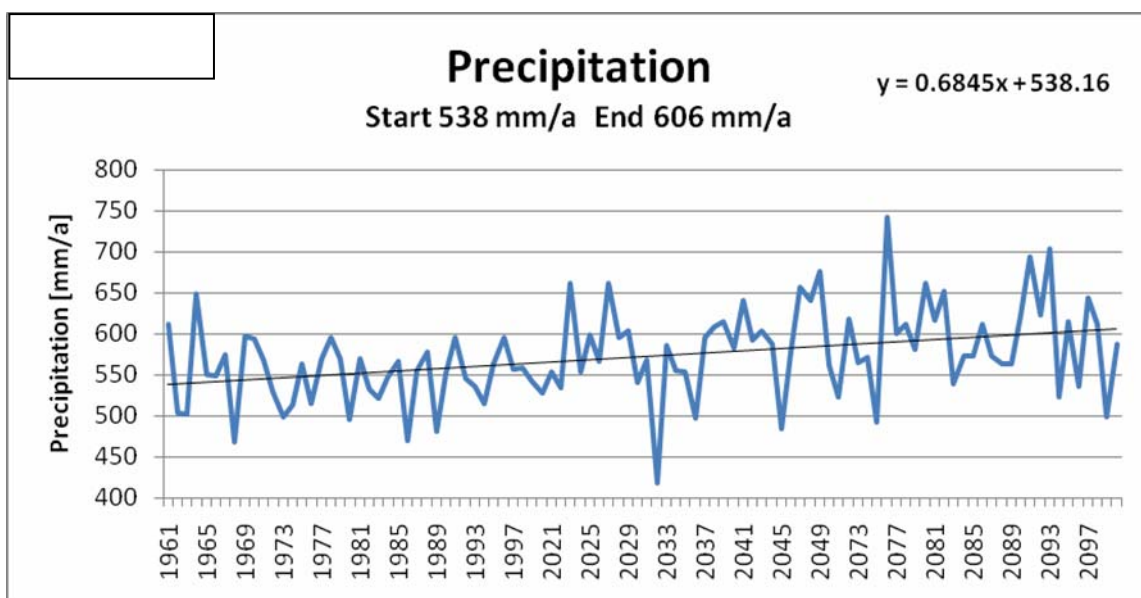


Fig. 4.11. Changes in average precipitation [mm a⁻¹] between 1961 and 2100 in Kampinos domain. Within the entire 1961 - 2100 period a linear continuity was assumed.

The entire period consisting of the three considered sub-periods reveals the most evident and clear increasing tendency in temperatures and precipitation. The forecasted temperature increase amounts to 3.6°C and the precipitation surplus equals to 68 mm a⁻¹.

Climate data - Karkonosze domain

Similarly as for the Kampinos domian, the climatic data for Karkonosze domain were subject to a trend analysis for each of the three time series and for the total time span from 1961 to 2100, assuming a linear continuity. The results are shown in Figures 4.12 and 4.13:

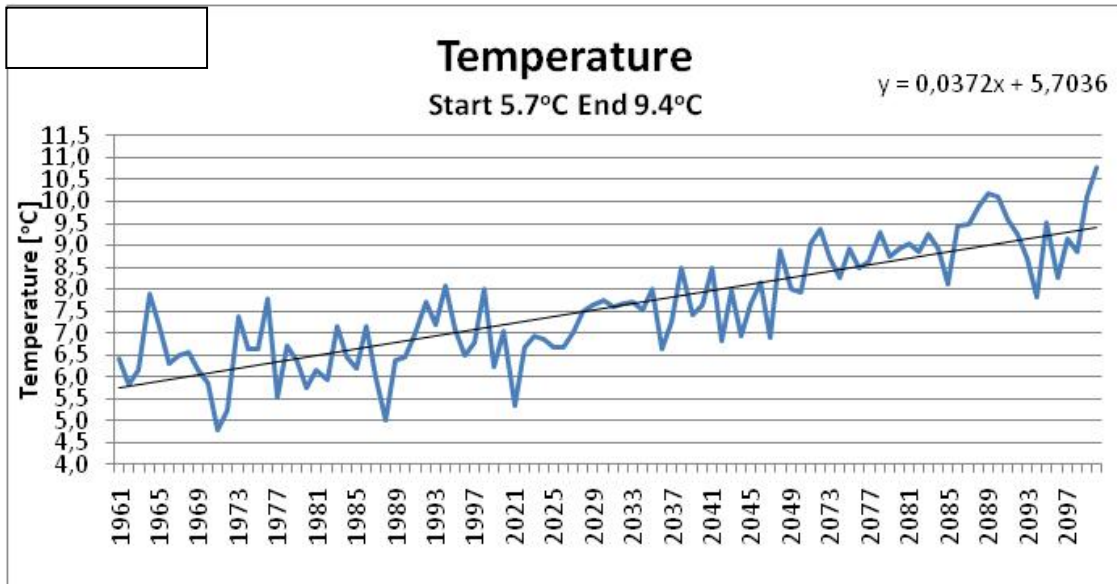


Fig. 4.12. Changes in average temperature [°C] between 1961 and 2100 in Karkonosze domain. Within the entire 1961 - 2100 period a linear continuity was assumed.

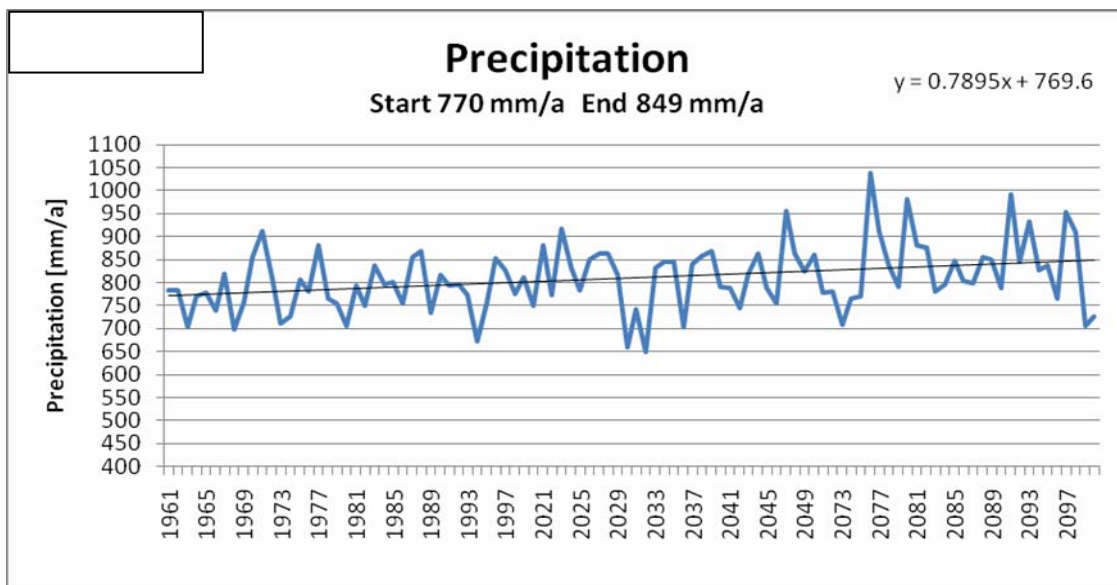


Fig. 4.13 Changes in average precipitation [mm a⁻¹] between 1961 and 2100 in Karkonosze domain. Within the entire 1961 - 2100 period a linear continuity was assumed.

The growing tendency of temperature changes in the entire analyzed period 1961-2100 is evident. The resultant temperature increase amounts to 3.7°C. In the same time span precipitation values are also showing an increasing trend while not of that range as temperature. The resultant increase of precipitation is 79 mm a⁻¹.

5.2.6 Deposition data from Regional Climate Model-Air Quality Modelling System

For assessing climate change impacts on critical loads exceedances, the deposition have been calculated at WUT with coupled regional climate-air quality model. The simulation have been performed with RegCM (WUT)-EMIL-CAMx modeling system for the WUT modelling with high resolution of 10 km.

Again, as for climate data, deposition data were extracted from the modeling results for selected domains (60 nodes for Kampinos domain, 255 nodes for Karkonosze domain in the Lambert Conformal Conic spatial system. The data were converted into the EMEP polar stereographic projection system and the data disaggregated to a grid defined by a grid cell of 1x1 km size.

Deposition data – the Kampinos domain

For the resulting data on sulphur and total nitrogen depositions a trend analysis was done for each of the three considered decades and for the joint time span from 1991 to 2100, assuming a linear continuity. The following Figures (4.14, 4.15) show the deposition changes in Kampinos domain throughout the considered periods:

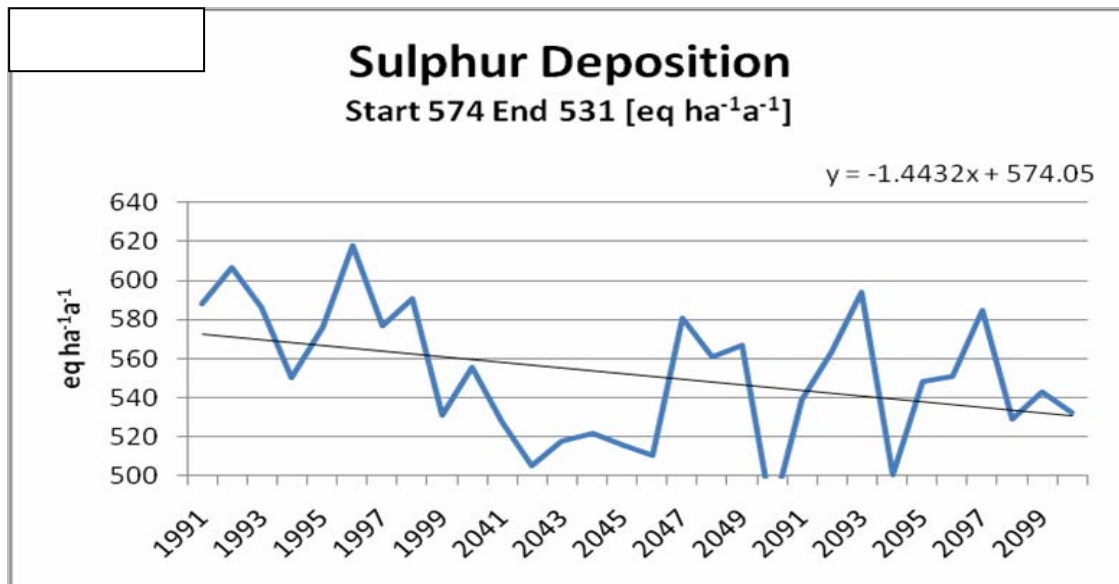


Fig. 4.14 Changes in sulphur deposition [eq ha⁻¹ a⁻¹] between 1991 and 2100 in Kampinos domain. Within the entire 1991 - 2100 period a linear continuity was assumed.

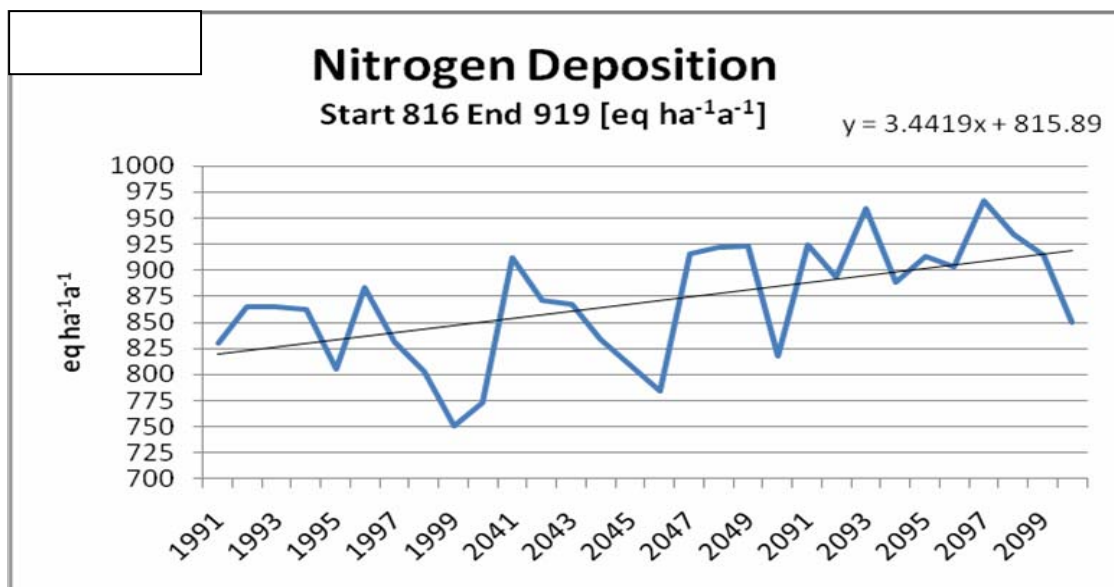


Fig. 4.15 Changes in nitrogen deposition [eq ha⁻¹ a⁻¹] between 1991 and 2100 in Kampinos domain. Within the entire 1991 - 2100 period a linear continuity was assumed.

Within the entire 1991 - 2100 period the resultant sulphur deposition is decreasing from the level 574 eq ha⁻¹a⁻¹ in 1991 to 531 eq ha⁻¹a⁻¹ in 2100. Concerning total nitrogen deposition, in spite of a markedly drop in the first 1991-2000 period, the overall tendency is growing within the entire considered period from 816 to 919 ha⁻¹a⁻¹.

Deposition data – the Karkonosze domain

As for Kampinos domain, from the Karkonosze domain deposition data a trend analysis was done for each of the three considered decades and for the joint time span from 1991 to 2100, assuming a linear continuity. The following Figures (4.16, 4.17) show the deposition changes in Karkonosze domain throughout the considered periods:

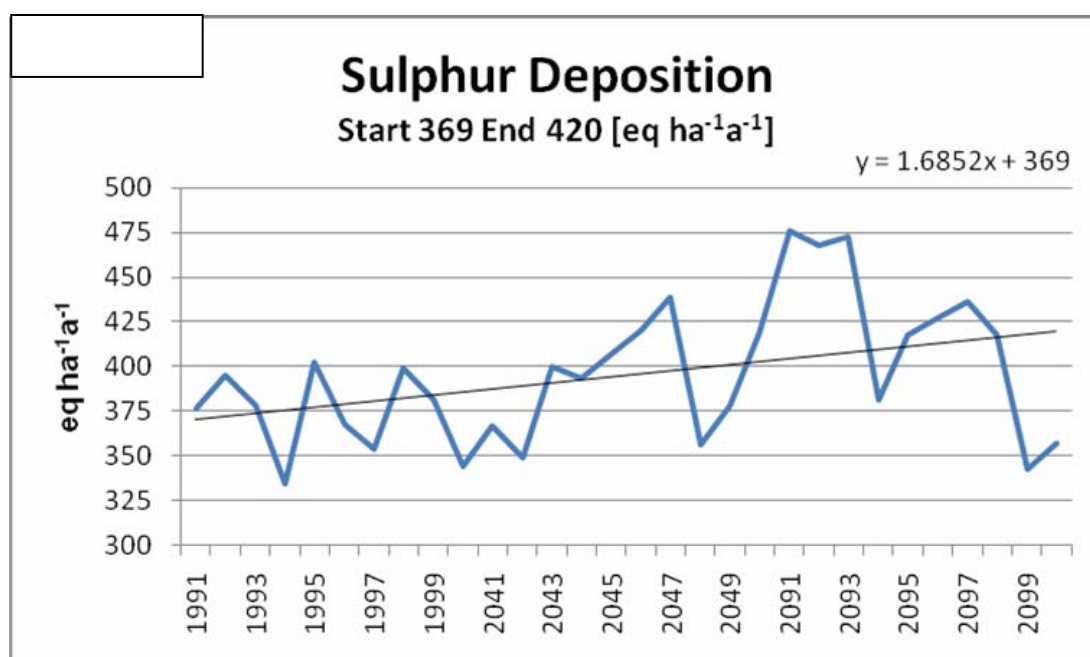


Fig. 4.16 Changes in sulphur deposition [eq ha⁻¹ a⁻¹] between 1991 and 2100 in Karkonosze domain. Within the entire 1991 - 2100 period a linear continuity was assumed.

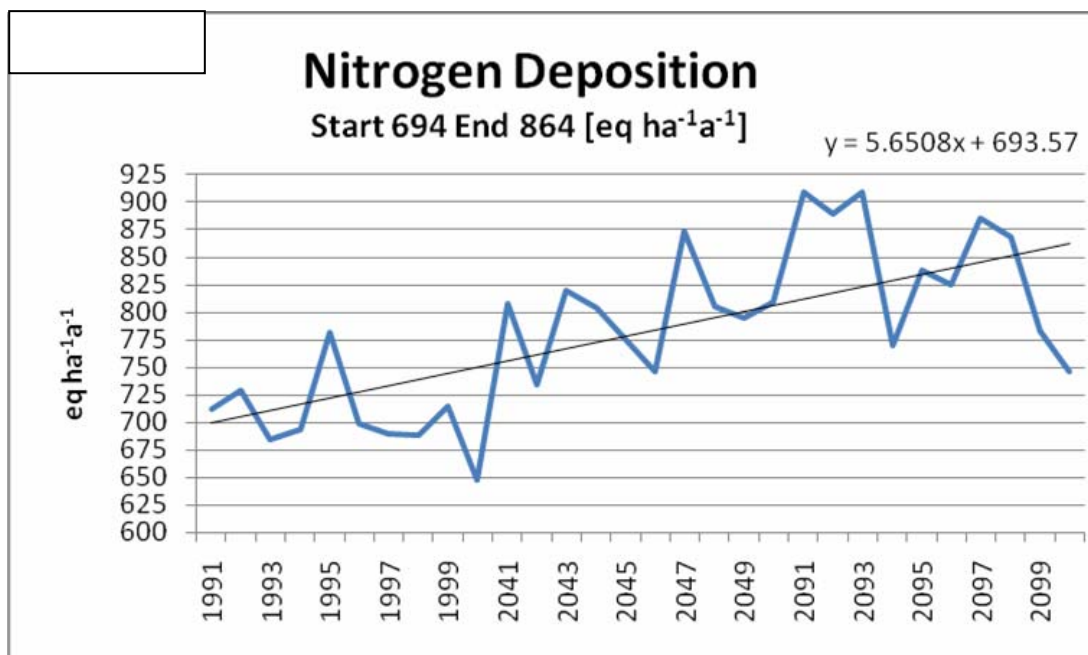


Fig. 4.17 Changes in nitrogen deposition [eq ha⁻¹ a⁻¹] between 1991 and 2100 in Karkonosze domain. Within the entire 1991 - 2100 period a linear continuity was assumed.

As can be observed, the deposition values and trends in both domains are different. Sulphur deposition in Karkonosze domain had significantly lower value in the beginning of analyzed period (369 eq ha⁻¹a⁻¹ in 1991) compared to Kampinos domain (574 eq ha⁻¹a⁻¹). The same can be noted for nitrogen deposition in 1991: 694 eq ha⁻¹a⁻¹ in Karkonosze domain compared to 816 eq ha⁻¹a⁻¹ in Kampinos domain.

In the Karkonosze domain both the sulphur and nitrogen depositions are showing a decreasing trend within the 1991 - 2000 period. The rate of change of the nitrogen deposition is significantly higher than of sulphur deposition. During first future decade (2041-2050) both depositions are growing with a similar rate. In the last decade (2091-2100) the evident downward tendency of sulphur and nitrogen depositions is predicted.

However, the resulting trend of sulphur and nitrogen depositions in the entire analyzed period in Karkonosze domain is an upward one in spite that for two decades it was downward. For Kampinos domain, the increasing trend was predicted as well for nitrogen deposition, on the contrary, sulphur deposition trend was decreasing.

5.2.7 Impacts of climate changes on critical loads

The impact of climate changes on critical loads of acidification and eutrophication was examined by running calculations with changing input data on temperatures and precipitations according to the above presented predictions for the considered time series. To this end a special calculation procedure was prepared to automate the calculations of critical loads and their excedances for every grid cell of the both considered domains.

The Kampinos domain - climate change impacts on Critical Loads

For the control period (1961-2000) the CL_{max}(S) and CL_{nut}(N) trends in the Kampinos domain are nearly even. This could result from a very slight growing trend in temperatures in this period compensated by a slightly decreasing tendency in precipitation values. In both cases the net change might be considered insignificant from practical point of view. For the future decades both critical loads values are growing, with a relatively less rate in the last decade (2071-2100) compared to the previous one (2021-2050). Figure 4.18 shows the critical loads changes in Kampinos domain throughout the considered periods.

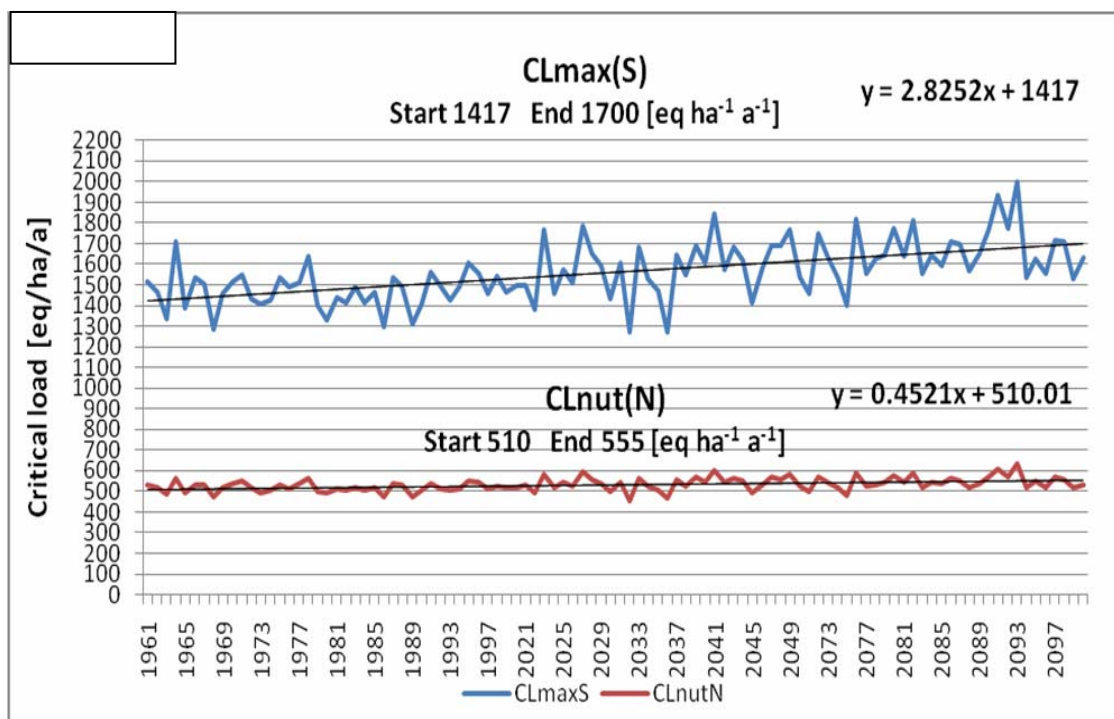


Fig. 4.18 Changes in critical loads ($CL_{max}(S)$ and $CL_{nut}(N)$) [$eq\ ha^{-1}\ a^{-1}$] between 1961 and 2100 in Kampinos domain. Within the entire 1961 - 2100 period a linear continuity was assumed.

The trend of changes of $CL_{max}(S)$ values throughout the entire 1961 - 2100 period is evidently growing and the resulting increase amounts to 283 $eq\ ha^{-1}a^{-1}$. It means that in average the considered ecosystems of the Kampinos domain may resist receiving an equal amount of acid deposition in 2100 with no risk to their structure and functioning.

An upwarding trend is also noted in $CL_{nut}(N)$ values but of a fairly less rate than for $CL_{max}(S)$ values. The main rationale for this less sensitivity to the predicted climate changes is the independency of $CL_{nut}(N)$ values from temperature.

The Karkonosze domain - climate change impacts on Critical Loads

Alike to the Kampinos domain, also for the Karkonosze domain practically no variation in $CL_{max}(S)$ and $CL_{nut}(N)$ values is observed within control period, and the same reasons direct this situation. For the future decades the trend in $CL_{max}(S)$ is growing, driven mainly by the temperature raise predicted for these periods. The forecasted change in $CL_{nut}(N)$ values is almost flat, as the predicted trend in precipitation for that time-slice.

Figure 4.19 shows the critical loads changes ($CL_{max}(S)$ and $CL_{nut}(N)$) in Karkonosze domain throughout the considered periods, assuming a linear continuity:

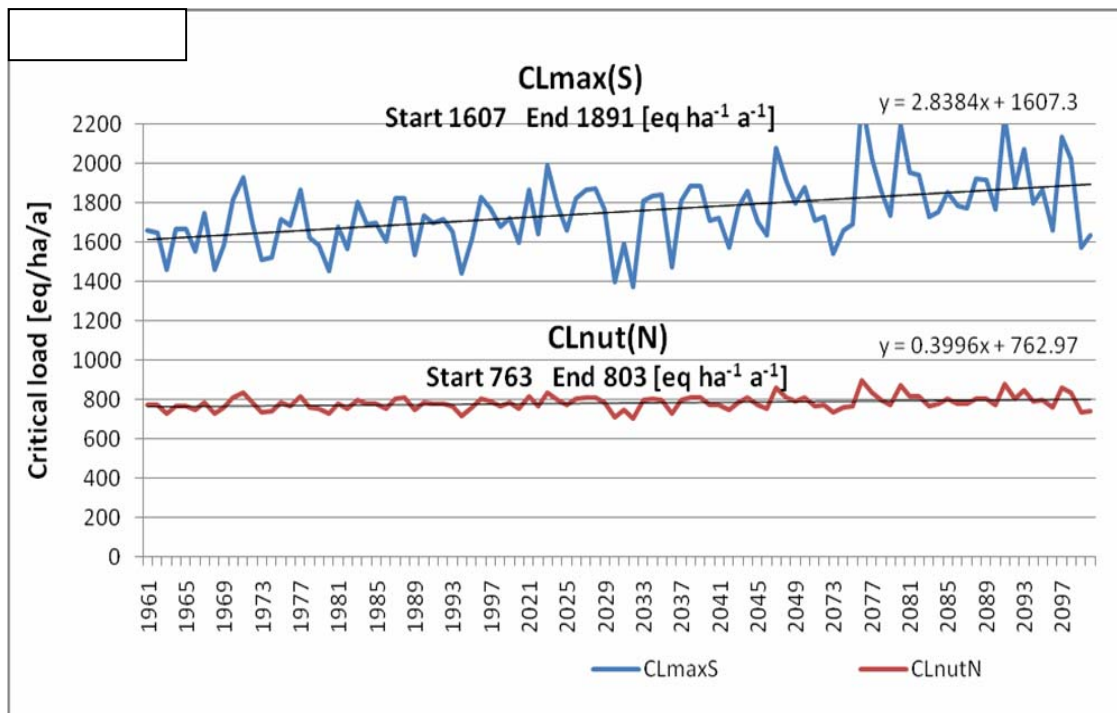


Fig. 4.19 Changes in critical loads ($CL_{max}(S)$ and $CL_{nut}(N)$) [$eq\ ha^{-1}\ a^{-1}$] between 1961 and 2100 in Karkonosze domain. Within the entire 1961 - 2100 period a linear continuity was assumed.

The entire combined period 1961- 2100 shows an upward trend of $CL_{max}(S)$ values with a resulting increase from 1607 $eq\ ha^{-1}a^{-1}$ to 1891 $eq\ ha^{-1}a^{-1}$. It means that the sensitivity to acidification of terrestrial ecosystem residing in the domain of the Karkonosze domain may be less by about 300 $eq\ ha^{-1}a^{-1}$. A similar decrease of vulnerability to acidifying deposition was predicted for Kampinos domain.

As in Kampinos domain, the tendency of changes of $CL_{nut}(N)$ values in the whole considered time span is fairly stable in Karkonosze domain. This has its implications in the only dependence on precipitation of which predicted changes in all the period are not of that dynamic as the temperature variations. However, the significant difference in vulnerability to eutrophying nitrogen in both domains is clear. For Kampinos domain, the $CL_{nut}(N)$ trend line is oscillating around 500 $eq\ ha^{-1}a^{-1}$ while for Karkonosze domain -around 800 $eq\ ha^{-1}a^{-1}$, showing much smaller sensitivity of ecosystems from that area.

5.2.8 Exceedances of critical loads induced by climate changes

The accumulated exceedance of acidity for a given pair of sulphur and nitrogen depositions is defined as the sum of the $Ex(N)$ and $Ex(S)$ deposition reductions required to reach the critical load function by the 'shortest' path. The software especially developed within this project was used to calculate exceedances of critical loads of acidity, based on methodology presented in UBA (2004). Exceedances of critical loads of nutrient nitrogen were calculated in a simple way by subtracting $CL_{nut}(N)$ values from forecasted depositions of nitrogen.

A number of calculation runs were done to derive exceedances of $CL_{max}(S)$ and $CL_{nut}(N)$ values for the three considered decades. For every set of results the trend analysis was done and the spatial distribution of exceedances was mapped.

From the obtained results a general conclusion was drawn that in case of the all three decades and the two domains the exceedance of maximum critical loads of sulphur $CL_{max}(S)$ are low enough not to be subject for any trend analysis. For Kampinos domain the average

exceedance for the decade 1991 - 2000 was the highest, amounting to about 10 eq ha⁻¹a⁻¹. For the next decades the relevant averages are dropping to 5.2 and 3.7 eq ha⁻¹a⁻¹ respectively. For Karkonosze domain, calculated exceedances of CL_{max}(S) equal zero and are not analyzed.

The Kampinos domain – Exceedances of CL_{nut}(N) induced by climate changes

In the period 1991 - 2000 the Ex(CL_{nut}(N)) values got a downward trend decreasing by 107 eq ha⁻¹a⁻¹. This should be assigned to the significant decrease in nitrogen deposition happening than.

Within first from the future decades the trend of exceedances is getting a slightly upwarding tendency. Such a trend development is a consequence of a similar shape of nitrogen deposition trend predicted for the same period. From practical point of view the increase is insignificant, but gives a indication of possible further elevation of critical loads exceedances. For the second future decade the similar tendency is observed. Figure 4.20 shows the changes in exceedances of CL_{nut}(N) values induced by climate changes in Kampinos domain throughout the entire 1991-2100 period, assuming a linear continuity:

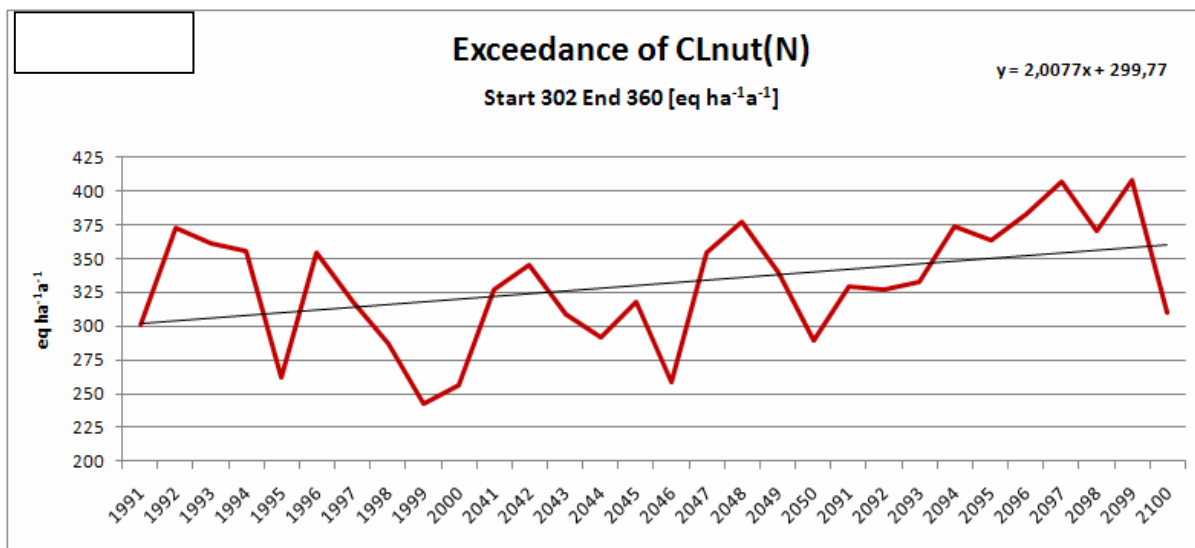


Fig. 4.20 Changes in exceedances of CL_{nut}(N) [eq ha⁻¹ a⁻¹] between 1991 and 2100 in Kampinos domain. Within the entire 1991 - 2100 period a linear continuity was assumed.

The linear trend of the three combined decades is upwarding for predicted exceedances of CL_{nut}(N) values. This has its rationale in the regular increase of the average level of nitrogen deposition values. The resultant trends within separate decades are changing from dropping to upwarding but this effect is covered by the overall increase in nitrogen deposition.

The spatial distribution of exceedances of CL_{nut}(N) in Kampinos domain for three analyzed periods are shown in Figures 4.21-4.23.

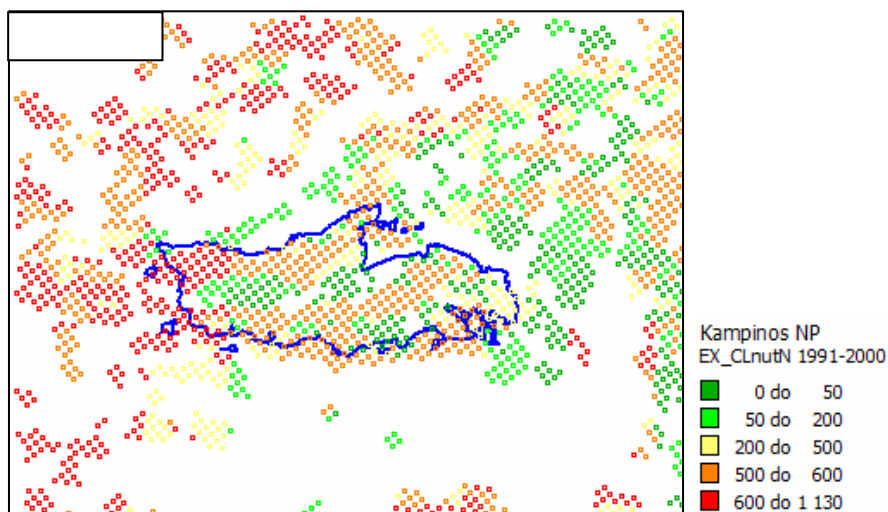


Fig. 4.21 Exceedances of $CL_{nut}(N)$ [$eq\ ha^{-1}\ a^{-1}$] in Kampinos domain for present climate decade (1991-2000).

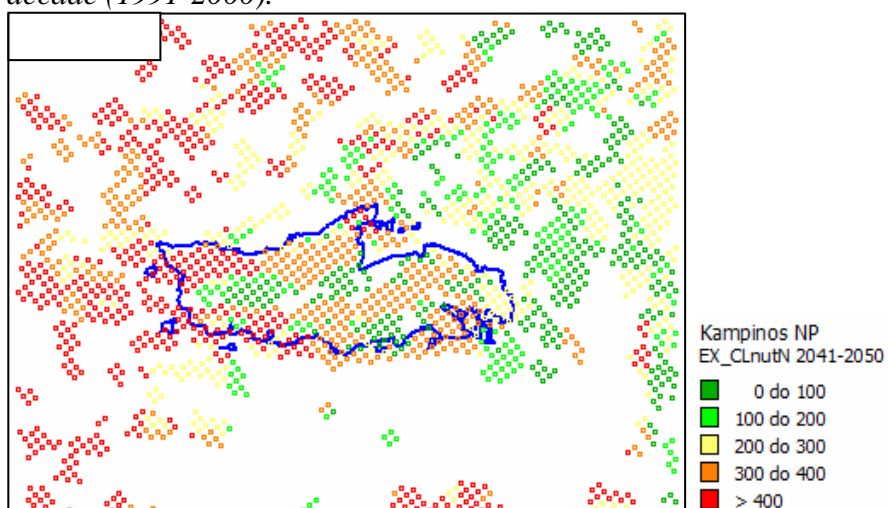


Fig. 4.22 Exceedances of $CL_{nut}(N)$ [$eq\ ha^{-1}\ a^{-1}$] in Kampinos domain for near future decade (2041-2050).

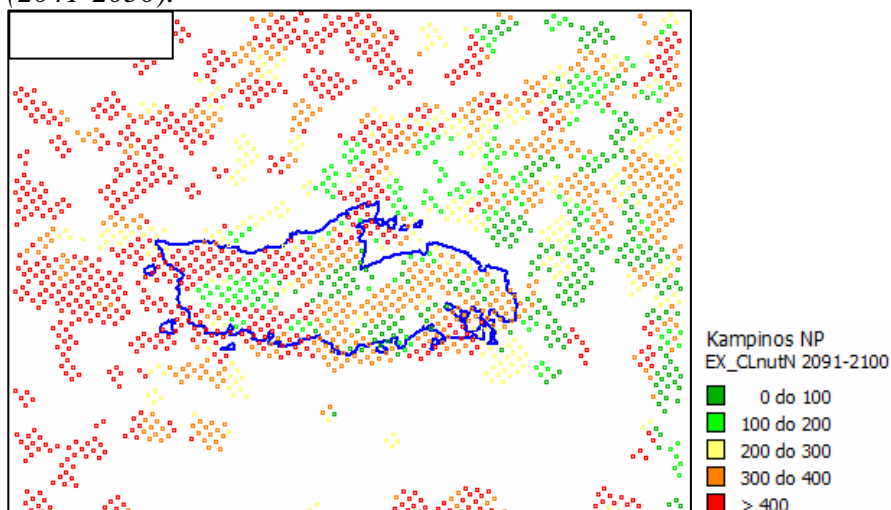


Fig 4.23. Exceedances of $CL_{nut}(N)$ [$eq\ ha^{-1}\ a^{-1}$] in Kampinos domain for far future decade (2091-2100).

The Karkonosze domain – Exceedances of $CL_{nut}(N)$ induced by climate changes

Within extended control period 1991 - 2000 the average level of $CL_{nut}(N)$ exceedance is getting higher and also the tendency of changes turns into slightly increasing as a consequence of the growing trend of nitrogen depositions. During first future decade a further move up in the average exceedance level is predicted in comparison to the previous decade. On the other hand, a quite rapid decrease in nitrogen deposition in the 2091 - 2100 period induces relevant downward trend in the exceedances.

Figure 4.24 shows the changes in exceedances of $CL_{nut}(N)$ values induced by climate changes in Karkonosze domain throughout the entire 1991-2100 period, assuming a linear continuity:

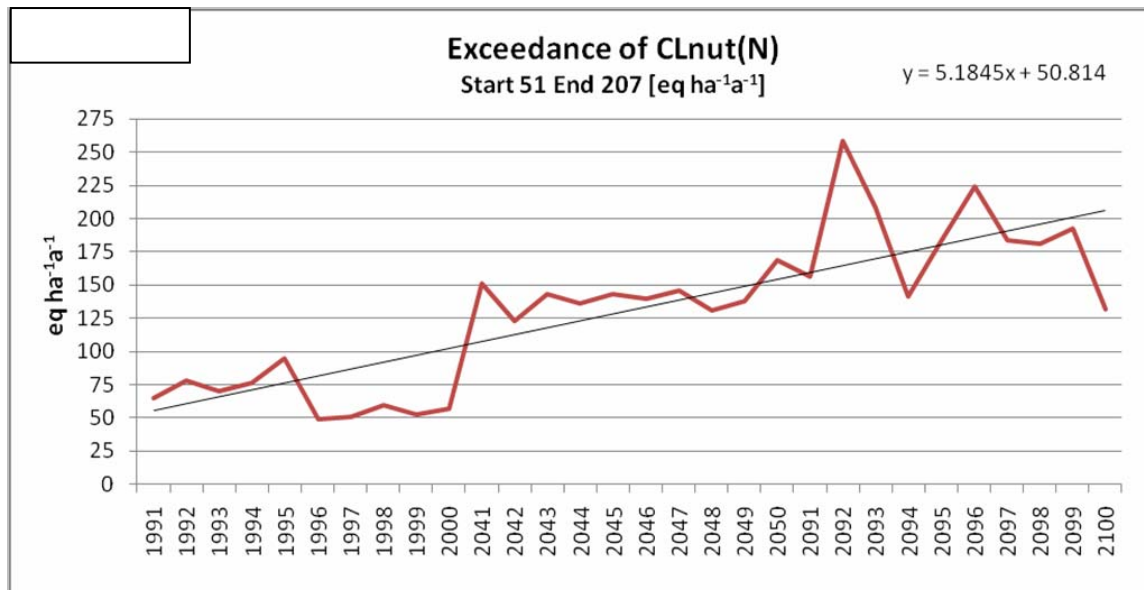


Fig. 4.24 Changes in exceedances of $CL_{nut}(N)$ [$eq\ ha^{-1} a^{-1}$] between 1991 and 2100 in Karkonosze domain. Within the entire 1991 - 2100 period a linear continuity was assumed.

The resulting exceedance trend for the entire analyzed period is increasing. This is due to the systematic increase of the nitrogen deposition level from period to period, regardless from the trends within the three decades.

Again, the differences between both considered domains are clear. For Karkonosze domain a fourfold increase of $CL_{nut}(N)$ exceedances (from 51 to 207 $eq\ ha^{-1}a^{-1}$) is predicted, while for Kampinos domain the predicted increase is relatively small (from 302 to 360 $eq\ ha^{-1}a^{-1}$). On the other hand, the average values of exceedances predicted for Karkonosze domain are much lower than those predicted for Kampinos domain.

The spatial distribution of exceedances of $CL_{nut}(N)$ in Karkonosze domain for three analyzed periods are shown in Figures 4.25-4.27.

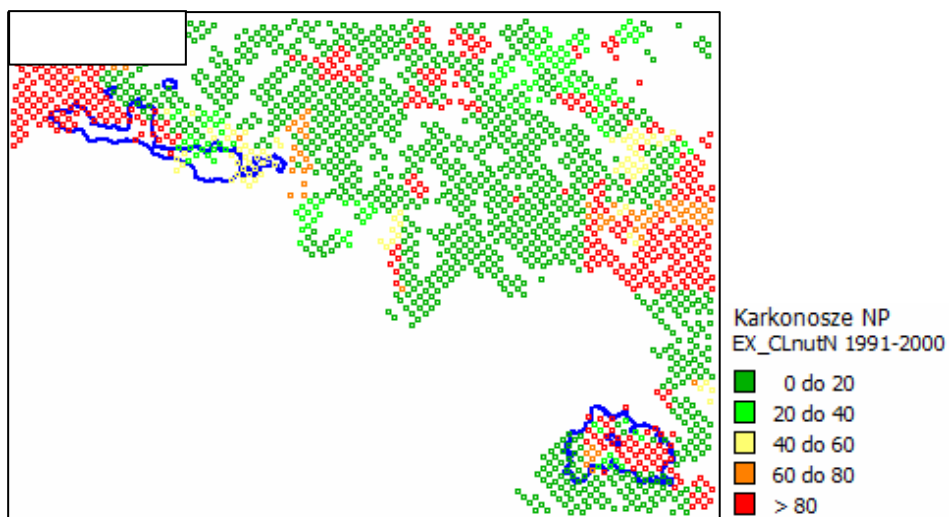


Fig. 4.25 Exceedances of $CL_{nut}(N)$ [$eq\ ha^{-1}\ a^{-1}$] in Karkonosze domain for present climate decade (1991-2000).

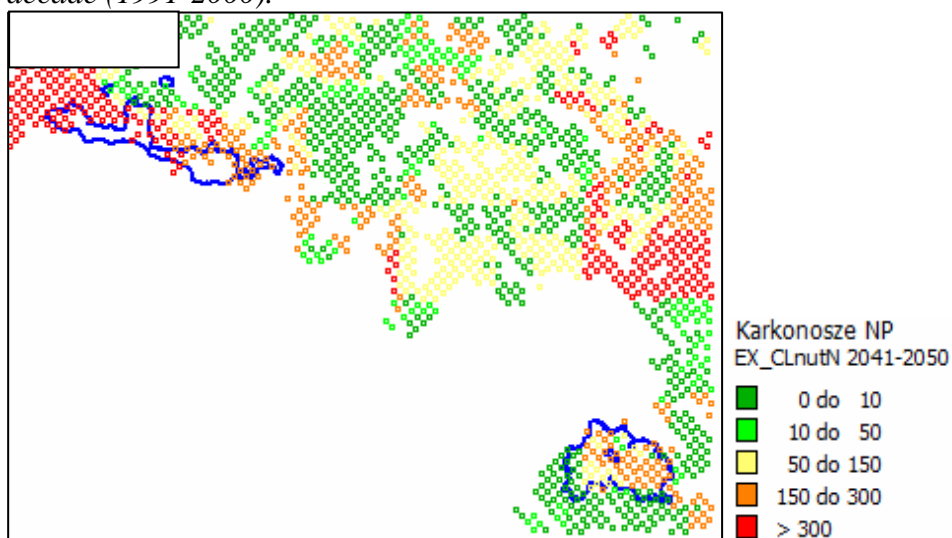


Fig. 4.26 Exceedances of $CL_{nut}(N)$ [$eq\ ha^{-1}\ a^{-1}$] in Karkonosze domain for near future decade (2041-2050).

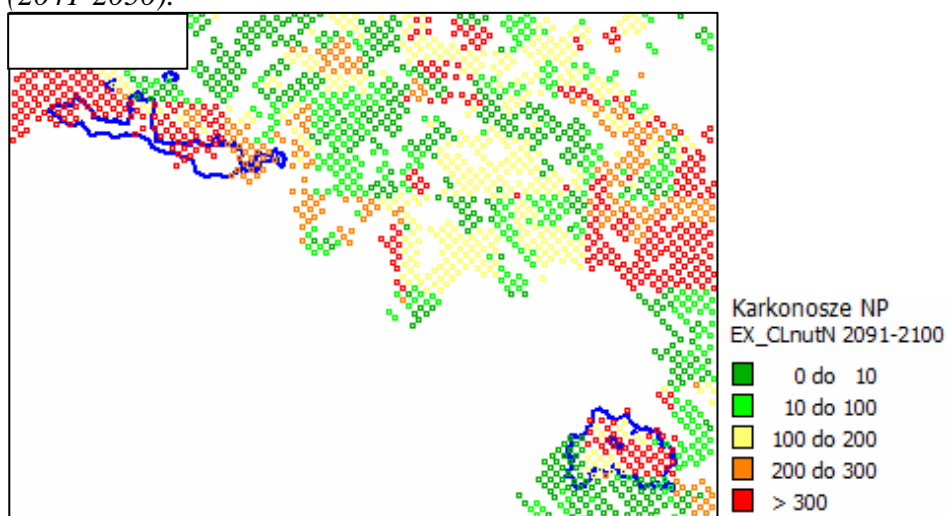


Fig. 4.27 Exceedances of $CL_{nut}(N)$ [$eq\ ha^{-1}\ a^{-1}$] in Karkonosze domain for far future decade (2091-2100).

5.3 Conclusions

From the above presented results, the following conclusions are drawn:

1. Comparing the two considered domains and their National Parks, it is to note that in average the Kampinos National Park with its lower range of $CL_{nut}(N)$ and $CL_{max}(S)$ values is more sensitive to nutrient nitrogen deposition and acidifying sulphur and nitrogen deposition and therefore more vulnerable to eutrophication and acidification than the National Parks from Karkonosze domain: National Park of Stolowe Mountains and Karkonosze National Park.
2. According to the RegCM (CUNI) regional climate simulations for control period (1961-1990) and two future periods (2021-2050 and 2071-2100), with bias correction applied to precipitation data, the following were observed for considered forested domains in Poland:
 - a. the **Karkonosze** domain, situated in the mountain area, is characterized by lower average temperature and higher precipitation sum than **Kampinos** domain situated in lowland area of central Poland. The average temperature during control period oscillates around 8°C in Kampinos domain and around 6.5°C in Karkonosze domain. The average precipitation oscillates around 550 mm a⁻¹ in Kampinos domain and around 780 mm a⁻¹ in Karkonosze domain;
 - b. in the **Kampinos** domain the most intensive climate changes are expected in the period 2021 - 2050. The forecasted resultant raise in temperatures will reach 1.4°C and in precipitation 36 mm a⁻¹. Within the entire period combined from the three particular thirty years periods the estimated increase in temperature amounts to 3.6°C and for precipitation there is a surplus of 68 mm a⁻¹.
 - c. the climate changes for the **Karkonosze** domain can be characterized as follows. Again, the period of the most intensive predicted climate changes is the period 2021 - 2050 during which a similar as for Kampinos domain raise in temperature is expected to happen. For the all combined ninety years period the estimated increase in temperature and precipitation **are bigger** than in Kampinos domain. The estimated increase in temperature equals 3.7°C, and in precipitation 79 mm a⁻¹.
3. The above reported changes in the both considered climatic parameters modified the present critical loads of acidification and eutrophication, represented by $CL_{max}(S)$ and $CL_{nut}(N)$ respectively. In case of the **Kampinos** domain the increase in $CL_{max}(S)$ values will amount to 283 eq ha⁻¹a⁻¹ and for $CL_{nut}(N)$ values the increase will be much lower reaching just 45 eq ha⁻¹a⁻¹.
4. For the same time span, extending from 1961 to 2100 in the **Karkonosze** domain the $CL_{max}(S)$ values are expected to increase also by about 300 eq ha⁻¹a⁻¹ while the $CL_{nut}(N)$ values by 40 eq ha⁻¹a⁻¹.
5. The apparently lower level of changes of nutrient nitrogen critical loads in the both studied areas is resulting from their dependence on precipitation changes only.
6. The above reported increases of critical loads mean, in terms of ecological effects, **an enhancement of tolerance of the terrestrial ecosystems**, residing in the two selected

domains, to acidifying and eutrophying depositions. Thus, the predicted raise in temperature and precipitation result in a protective effect for the considered ecosystems.

7. According to the RegCM (WUT)-CAMx coupled regional climate-air quality simulations for extended control period (1991-2000) and two future decades (2041-2050 and 2091-2100):
 - a. the estimated trend of sulphur and nitrogen depositions in the entire analyzed period in Karkonosze domain is an upward one,
 - b. for Kampinos domain, the increasing trend was predicted as well for nitrogen deposition, on the contrary, sulphur deposition trend was decreasing.
8. No significant changes in the exceedance of maximum critical loads of sulphur have been found, both for the Kampinos and Karkonosze domains within the three considered decades. There are two factors liable for this, on one hand the drop in sulphur deposition in Kampinos domain and small increase in Karkonosze domain and on the other hand a much stronger quantitative increase in $CL_{\max}(S)$ values in the both parks.
9. The development of the resulting exceedances of critical loads of nutrient nitrogen within the studied time span and the both studied areas was noticeably. To this increasing trend, the two 2041 - 2050 and 2091 - 2100 periods contribute with the levels of exceedance significantly elevated against the exceedances noted in the 1991 - 2000 period. The direct reason for this expansion is the constantly growing trend in nitrogen deposition, weakly compensated by the minor changes of critical loads of nutrient nitrogen. However, without this increase of critical loads, their exceedances would be higher.
10. In ecological terms **the effect of climate changes on the ecosystem protection against eutrophication caused by excess deposition of nitrogen is negative** for the structure and functioning of the ecosystems existing in the both domains and National Parks residing within them. The main risk which potentially may result from the permanent nutrient nitrogen critical load exceedance is the loss of biodiversity in the present species constitution of ecosystems.
11. The trends of changes of critical loads and their exceedances induced by climate changes, derived in this study, reflect with a fair approximation the national and European evolution of sulphur and nitrogen deposition effects to ecosystems. The review of the Gothenburg Protocol of the Convention on Long-Range Transboundary Air Pollution revealed that after the Protocol commitment fulfillment after 2010 the exceedance of $CL_{\max}(S)$ will decrease by about 70% in all Europe due to relevant sulphur emission reductions in relation to 1990. For Poland the decrease is of the same level. The main problem that left is the almost 100% coverage of areas with exceeded critical loads of nutrient nitrogen. This a challenge for the upcoming renegotiations of the Gothenburg Protocol. Results of this study should contribute to the scientific effort underpinning the negotiations.

6. REFERENCES

- Abrahamsen P, Hansen S (2000) DAISY: An Open Soil – Plant - Atmosphere System Model. *Environmental Modelling & Software* 15: 313-330
- Audsley E, Pearn KR, Simota C, Cojocaru G (2006) What can scenario modelling tell us about future European scale agricultural land use, and what not?. *Environ Sci Policy*, Berry PM, Dawson TPTP, vol 9: 148–162
- Basra AS (1993) *Stress-induced Gene Expression in Plants*. CRC Press.
- Birkmann J (2006) Measuring vulnerability to promote disasterresilient societies: Conceptual frameworks and definitions. In: *Measuring Vulnerability to Natural Hazards: Towards Disaster Resilient Societies*. Birkmann, J. (Ed.). Tokyo, United Nations University Press. pp. 9–54
- Bogardi JJ (2006) Human security and risk management within integrated river basin management. In: *Towards Integrated River Basin Management*. Casta – Papiernicka, The Slovak Water Research Institute. p. 243.
- Bogardi JJ, Birkmann J (2006) Vulnerability assessment: The first step towards sustainable risk reduction. In: *Disasters and Society – From Hazard Assessment to Risk Reduction*. Malzahn, D., Plapp, T. (Eds.), Karlsruhe, Universität Karlsruhe. pp. 75–82.
- Caballero D, Beltran I (2003) Concepts and ideas of assessing settlement fire vulnerability in the W/UI zone. In: *Forest Fires in the Wildland-Urban Interface and Rural Areas in Europe*. Xanthopoulos G. (Ed.). Athens, Mediterranean Agronomic Institute of Chania. pp. 47–54.
- Di Toppi LS and Pawlik-Skowrońska B (2003) *Abiotic Stresses in Plants*. Springer.
- Dubrovsky M (1997) Creating daily weather series with use of the weather generator. *Environmetrics*, 8, 409-424.
- Dubrovsky M, Nemesova I and Kalvova J (2005) Uncertainties in climate change scenarios for the Czech Republic. *Climate Research*, 29. 139-156
- Ďurský J (1997) Modellierung der Absterbeprozesse in Rein- und Mischbeständen aus Fichte und Buche. *Allg. Forst- und Jagdzeitung*, 168. Jg., H. 6/7, s. 131-134.
- Ďurský J, Pretzsch H, Kahn M (1996) Modellhafte Nachbildung der Mortalität von Fichte und Buche in Einzelbaumsimulatoren. *Jahrestagung 1996 der Sektion Ertragskunde des DVFFA in Neresheim, Tagungsber.*, s. 267-277.
- Eitzinger J, Thaler S, Orlandini S, Nejedlik P, Kazandjiev V, Vucetic V, Sivertsen TH, Mihailovic DT, Lalic B, Tsiros E, Dalezios NR, Susnik A, Kersebaum KC, Holden NM and Matthews R (2008) Agroclimatic indices and simulation models. In: Nejedlik P. and S. Orlandini (eds.): *Survey of agrometrological practices and applications in Europe regarding climate change impacts*. Cost Action 734: *Impact of climate change and variability on European agriculture*. European Science Foundation.
- Fabrika M (2005) *Simulátor biodynamiky lesa SIBYLA, koncepcia, konštrukcia a programové riešenie*. Habilitačná práca. Technická univerzita vo Zvolene, 238 s.
- Fabrika M, Ďurský J (2006) Implementing Tree Growth Models in Slovakia. In: Hasenauer, H., et al.: *Sustainable Forest Management. Growth Models for Europe*. Springer Berlin Heidelberg New York, 398 s, s. 315-341.

- Gadow K (2000) Evaluating risk in forest planning models. *Silva Fennica*, vol. 34(2): 181–191.
- Ghaffari A, Cook HF, Lee HC (2002) Climate change and winter wheat management: A modelling scenario for South-Eastern England. *Clim. Change*, 55: 509–533.
- Halada L, Weisenpacher P, Glasa J (2006) Reconstruction of the forest fire propagation case when people were entrapped by fire. *Forest Ecology and Management*, vol. 234S: p. 127.
- Halaj et al. (1987) Rastové tabuľky hlavných drevín ČSSR. *Príroda Bratislava*, 361 s.
- Halaj J (1957) Matematicko-štatistický prieskum hrúbkovej štruktúry slovenských porastov. *Lesnícky časopis*, III/1, s. 39-74.
- Halaj J (1978) Výškový rast a štruktúra porastov. *Veda Bratislava*, 284 s.
- Halaj J, Řehák J (1979) Vyhotovenie rastových tabuliek hlavných drevín ČSSR. *Lesnícke štúdie*, č.30, 174 p.
- Hall AE (2001) *Crop responses to environment*. CRC Press.
- Hanewinkel M (2002) Comparative economic investigations of even-aged and uneven aged silvicultural systems: a critical analysis of different methods. *Forestry*, vol. 75(4): 473–481.
- Hanewinkel M, Oesten G (1998) Okonomischer Modellvergleich risikobeeinflusster Altersklassen und Plenterwald betriebsklassen. *Allgemeine Forst Zeitschrift für Wald und Umweltvorsorge* 53:427–430.
- Hansen S (2000) DAISY a Flexible Soil – Plant - Atmosphere System Model. Equation Section 1. The Royal Veterinary and Agricultural University, Copenhagen, pp 1-47
- Hasenauer H (1994) Ein Einzelbaumsimulator für ungleichaltrige Fichten-Kieferen- und Buchen-Fichtenmischbestände. *Forstliche Schriftenreihe Universität für Bodenkultur, Wien*, Band 8, 152 s.
- Hathfield JL (1979) Canopy temperatures: the usefulness and reliability of remote measurements. *Agronomy Journal*, 71, 889-892.
- Holécý J (2009) The Paradigm of Risk and Measuring the Vulnerability of Forest by Natural Hazards. In: Střelcová, K., Matyas, C., Kleidon, A., Lapin, M., Matejka, F., Blaženec M, Škvarenina J, Holécý J (2009) *Bioclimatology and Natural Hazards*, Springer, 298 s., ISBN 978-1-4020-8875-9, str. 231-247
- Holling CS, Gunderson LH, Peterson G (2002) Sustainability and panarchies. In: *Panarchy: Understanding Transformations in Human and Natural Systems*. Gunderson, L. H. – Holling, C. S. (Eds.). Washington, D.C., Island Press. pp. 63–102.
- IPCC report (2007)
- Kahn M (1994) Modellierung der Höhenentwicklung ausgewählter Baumarten in Abhängigkeit vom Standort. *Forstliche Forschungsber. München*, Vol. 141, 221 s.
- Kasperson RE, Kasperson JX, Dow K (2001) Vulnerability, equity, and global environmental change. In: *Global environmental risk*. Kasperson, J. X., Kasperson, R. E. (Eds.). Tokyo, United Nations University Press and Earthscan Publications Ltd. 574pp.
- Kennedy P (2007) *A guide to econometrics*, Fifth edition. Blackwell Publishing.
- Khosla R, Westfall D, Reich R, Inman D (2006) Temporal and Spatial Stability of Soil Test Parameters Used in Precision Agriculture. *Communications in Soil Science and Plant Analysis*. 37(15-20): s. 127-136.

- Leamer E (1978) *Specification Searches: Ad Hoc Inferences with Nonexperimental Data*. John Wiley & Sons, Ltd, p. vi.
- Leamer E (1990) Let's take the con out of econometrics, and Sensitivity analysis would help. In C. Granger (ed.), *Modelling Economic Series*. Oxford: Clarendon Press 1990.
- Levitt J (1980) *Responses of plant to environmental stresses*. Academic Press.
- Martell DL (1980) The optimal rotation of a flammable forest stand. *Canadian Journal of Forest Research*, 10: 30–34.
- Nagel J (1996) Anwendungsprogramm zur Bestandesbewertung und zur Prognose der Bestandesentwicklung. *Forst ind Holz*, 3, s.76-78.
- Nakicenovic N, Alcamo J, Davis G, de Vries W, Fenhann J, Gaffin S, Gregory K, Grübler A, Jung T, Kram T, Rovere EL, Michaelis L, Mori S, Morita T, Pepper W, Pitcher H, Price L, Riahi K, Roehrl A, Rogner H, Sankovski A, Schlesinger M, Shukla P, Smith S, Swart R, van Rooijen S, Victor N, Dadi Z (2000) *Special Report on Emission Scenarios*. Cambridge University Press.
- Nováková K (1996) Hydrophysical Properties of Žitný ostrov Soils. *Scientific Papers of the Research Institute of Irrigation, Bratislava*, 22:127–140. (In Slovak)
- Olesen JE, Carter TR, Diaz-Ambrona CH, Fronzek S, Heidmann T, Hickler T, Holt T, Minguéz MI, Morales P, Palutikof J, Quemada M, Ruiz-Ramos M, Rubæk G, Sau F, Smith B, Sykes M (2007) Uncertainties in projected impacts of climate change on European agriculture and ecosystems based on scenarios from regional climate models. *Climatic Change*, 81: 123–143.
- Olesen JE, Jensen T, Petersen J (2000) Sensitivity of field-scale winter wheat production in Denmark to climate variability and climate change. *Climate Research* 15: 221–238.
- Pal JS, Giorgi F, Bi X, Elguindi N, Solmon F, Gao X, Rauscher SA, Francisco R, Zakey A, Winter J, Ashfaq M, Syed FS, Bell JL, Diffenbaugh NS, Karmacharya J, Konare A, Martinez D, da Rocha RP, Sloan LC, Steiner A (2007) Regional climate modeling for the developing world: The ICTP RegCM3 and RegCNET. *B. Am. Meteorol. Soc.* 88, 1395-1409.
- Pannell DJ (1997) Sensitivity analysis of normative economic models: Theoretical framework and practical strategies, *Agricultural Economics* 16: 139-152.
- Pessaraki M (1999) *Handbook of Plant and Crop Stress*. CRC Press.
- Pilkey OH and Pilkey-Jarvis L(2007) *Useless Arithmetic. Why Environmental Scientists Can't Predict the Future*. New York: Columbia University Press.
- Pretzsch H (1992) Konzeption und Konstruktion von Wuchsmodellen für Rein- und Mischbestände. *Forstliche Forschungsberichte München*, Nr.115, 332 s.
- Pretzsch H (1993) Analyse und Reproduktion räumlicher Bestandesstrukturen. Versuche mit dem Strukturgenerator STRUGEN, *Schriften aus der Forstlichen Fakultät der Universität Göttingen und der Niedersächsischen Forstlichen Versuchsanstalt*, Bd. 114, 87 p.
- Pretzsch H, Kahn M (1998) Konzeption und Konstruktion des Wuchsmodells SILVA 2.2 - Methodische Grundlagen. *Abschlußbericht Projekt W 28, Teil 2*, München, 277 p.
- Pukkala T, Miina J (1997) A method for stochastic multiobjective optimization of stand management. *Forest and Ecology Management*. 98, s.189-203.
- Ravetz JR (2007) *No-Nonsense Guide to Science*, New Internationalist Publications Ltd.

- Reineke LH (1933) Perfecting a stand density index for even-aged forests. *Journal of Agricultural Research*, 46 (7), s. 627-638.
- Saltelli A, Ratto M, Andres T, Campolongo F, Cariboni J, Gatelli D, Saisana M and Tarantola S (2008) *Global Sensitivity Analysis. The Primer*, John Wiley & Sons.
- Shrestha A (2004) *Cropping Systems: Trends and Advances*. Haworth Press.
- Sisak L, Pulkrab K (2001) Damaging factors and their influence on forestry in the Czech Republic. pp. 125–132. In Proc. IUFRO Division 4 Conference “The Economics of Natural Hazards in Forestry”, June 7–10, Solsona, Catalonia, Spain, Italy, Padua University Press. 164pp.
- Skvarenina J, Krizova E, Tomlain J (2004) Impact of the climate change on the water balance of altitudinal vegetation stages in Slovakia. *Ekol'ogia (Bratislava)*, vol. 23, Supplement 2/2004: 13–19.
- Sloboda B, Pfreundt J (1989) Tree and stand growth. A system analytical spatial model with consequences for test planning for thinning and single tree development. In: *Proceedings: Artificial intelligence and growth models for forest management decision*. School of forestry and Wildlife Resources, Virginia Polytechnic Institute and State University, Blacksburg, Virginia, s.119- 153.
- Šmelko Š, Pánek, F, Zanvit B (1987) Matematická formulácia systému jednotných výškových kriviek rovnovekých porastov SSR. *Acta Facultatis forestalis Zvolen*, XIX, p. 151-174.
- Sterba H (1995) Prognaus – ein absandsunabhängiger Wachstumssimulator für ungleichaltrige Mischbestände. *DVFF – Sektion Ertragskunde, Joachimstahl*, s.173-183.
- Takáč J (2002) Využitie matematického modelovania na hodnotenie procesov v poľnohospodárskej krajine. In: *Zborník referátov z konferencie: Pôda a rastlina*. Phytopedon (Bratislava), *Journal of Soil Science, Supplement 2002/1, Gemini, Bratislava*, 227 – 231.
- Taleb NN (2007) *The Black Swan: The Impact of the Highly Improbable*, Random House.
- Thywissen K (2006) Core terminology of disaster reduction: A comparative glossary. In: *Measuring Vulnerability to Natural Hazards: Towards Disaster Resilient Societies*. Birkmann, J. (Ed.). Tokyo, United Nations University Press. pp. 9–54.
- Trnka M, Dubrovský M, Semerádová D, Žalud Z (2004a) Projections of uncertainties in climate change scenarios into expected winter wheat yields. *Theoretical and Applied Climatology*, 77: 229–249
- Trnka M, Dubrovský M, Žalud Z (2004b) Climate change impact and adaptation strategies in spring barley production in the Czech Republic, *Climate Change.*, vol. 64, s. 227-255.
- Trnka M, Hlavinka P, Dubrovský M, Thaler S, Eitzinger J, Semerádová D, Rischbeck P, Žalud Z, Formayer H (2008) Regional differences in the climate change impacts on the rainfed cereal production in the Central Europe-consequences, uncertainties and adaptation options. *Climate Change (v tisku)*.
- UBA (2004) *Manual on Methodologies and Criteria for Modelling and mapping critical Loads and Levels and Air Pollution Effects, Risks and Trends*, Umweltbundesamt, Berlin.
- Van Ittersum MK, Howden SM, Assng S (2003) Sensitivity of productivity and deep drainage of wheat cropping systems in a Mediterranean environment to changes in CO₂, temperature and precipitation. *Agric. Ecosyst. Environ.*, 97: 255–273.
- Van Wagner CE (1978) Age class distribution and the forest fire cycle. *Canadian Journal of Forest Research*, vol. 8: 220–227.

Vierling E (1991) The roles of heat shock proteins in plants. *Annu. Rev. Plant Physiology Plant Mol. Biol.* 42, 579-620.

Weber DJ, Andersen WR, Hess S, Hansen DJ and Gunasekaran M (1977) Ribulose-1, 5-biosphosphate carboxylase from plants adapted to extreme environments. *Plant and Cell Physiology*, 18, 693-699.

Žalud Z, Dubrovský M (2002) Modelling climate change impacts on maize growth and development. *Theoretical and Applied Climatology*, 72, Issue 1–2: 85–102.

Zimmermann HJ, Zysno P (1980) Latent connectives in human decision making. *Fuzzy Sets and Systems*, H.4, s. 37-51.